IMMUNOCHEMICAL DETECTION OF MUTAGENIC LESIONS IN DNA

by Thomas Barlow

A thesis presented for the degree of Doctor of Philosophy

University of Edinburgh

1995

To Anne, Danny, Sharon, Leon, Leon and Jordan

ACKNOWLEDGEMENTS

I would first and foremost like to thank my supervisor, Professor Tom Brown for his advice, help, enthusiasm and encouragement for the last four years.

I wish to acknowledge the BBSRC for this earmarked studentship.

Thanks also to OSWEL Research Products Ltd. and members of the research group past and present in particular Duncan Graham, Dave Lough and John McClean. I would also like to thank Lisa McIver, Doctor Scott Webster and Doctor Bob Baxter.

I would like to thank Doctor Paul Aston for his supervision of my industrial secondment with Shell Research Ltd.. Thanks also to Lathan Ball, Eric Hitchings, Tony Crane, Doctor Euan Booth and Doctor Bill Watson. All live animal experiments were conducted by Doctor Paul Aston.

^{1}H and ^{13}C NMR spectra were recorded by John Miller and Wesley Kerr, ^{31}P NMR spectra were recorded by Duncan Graham and FAB-mass spectra were recorded by Alan Taylor all of Edinburgh University. ^{31}P NMR spectra of oligonucleotides were recorded by Andrew Lane of the National Institute of Medical Research, London.

Love and tears to (in alphabetical order) Craig, Eric, Gaynor, Gill, Kathryn, Mel, Mike and Raymond for being misfortunate enough to live with me.

Special thanks and love to Dianne.

ABREVIATIONS

A	Adenosine.
Ab	Antibody.
Ag	Antigen.
alkG	2-Amino-6-oxo-N^7-ethoxy-3-β-D-ribofuranosyl purine.
AP	Alkaline phosphatase.
APC	Antigen presenting cell.
BCIP	5-Bromo-4-chloro-3-indoyl phosphate.
BSA	Bovine serum albumin.
C	Cytidine.
CAA	Chloroacetaldehyde.
CEO	Chloroethylene oxide.
CγG	Chicken gamma globulin.
C_H	Constant region on the heavy chain of an antibody molecule.
C_L	Constant region on the light chain of an antibody molecule.
CZE	Capillary zone electrophoresis.
dA	2'-Deoxyadenosine.
DAB	3,3'-Diaminobenzidine.
dC	2'-Deoxycytidine.
DCM	Dichloromethane.
dG	2'-Deoxyguanosine.
DMSO	Dimethyl sulphoxide.
DMTr	4,4'-Dimethoxytrityl.
DNP	2,4-Dinitrophenyl.
dsDNA	double stranded DNA.
εA	Etheno-2'-deoxyadenosine.
εC	Etheno-2'-deoxycytidine.

εC/AP	Etheno-2'-deoxycytidine conjugated to alkaline phosphatase.
ecp	3'-Monophosphate of etheno-2'-deoxycytidine.
E. coli	*Escherichia coli.*
EDTA	Ethylenediamine tetraacetic acid.
εG_1	Etheno-2'-deoxyguanosine (angular structure).
εG_2	Etheno-2'-deoxyguanosine (linear structure).
ELISA	Enzyme linked immunosorbent assay.
ether	Diethyl ether.
FAB	Fast atom bombardment.
Fab	Antibody binding fragment.
Fc	Antibody fragment which carries antibody effector functions.
FPLC	Fast protein liquid chromatography.
G	Guanosine.
G	Relative centrifugal force (only in the experimental sections).
HAT	Hypoxanthine, aminopterin and thymidine.
HGPRT	Hypoxanthine guanine phosphoribosyl transferase.
Hchain	Antibody heavy chain.
HPLC	High performance liquid chromatography.
HRP	Horse radish peroxidase.
IC_{50}	Concentration of inhibitor that gives 50% inhibition of binding.
Ig	Immunoglobulin.
IL	Interleukin.
K_A	Antibody affinity.
k_a	Rate constant of association.
k_d	Rate constant of dissociation.
Lchain	Antibody light chain.
MES	*N*-Morpholinoethanesulphonic acid.
MHC	Major histocompatibility complex.
mRNA	Messenger RNA.
MPD	Methylpentanediol.

NBD	7-Nitrobenzo-2-oxa-1,3-diazole.
NBT	Nitro blue tetrazolium.
NAP	Nucleic acid purification columns.
OD	Optical density.
oeG	N^7-Hydroxyethyl guanosine.
PBS	Phosphate buffered saline.
pecp	3',5'-Bisphosphate of etheno-2'-deoxycytidine.
PEG	Polyethylene glycol.
pNPP	*Para*-nitrophenyl phosphate.
pI	Isoelectric point.
PVC	Polyvinyl chloride.
RIA	Radioimmunoassay.
roalkG	Imidazole ring opened alkG.
SDS	Sodium dodecyl sulphate.
ssDNA	Single stranded DNA.
dT	2'-deoxythymidine.
TEA	Triethylamine.
TEMED	*N',N',N',N'*-Tetramethylethylenediamine.
THF	Tetrahydrofuran.
Tm	Melting temperature.
TMB	3,3',4,4'-Tetramethylbenzidine.
V_L	Variable region on the light chain of an antibody molecule.
V_H	Variable region on the heavy chain of an antibody molecule.
U	Uridine.

ABSTRACT

Vinyl chloride, a widely used industrial precursor, is an established chemical carcinogen. It is metabolically activated to forms which alkylate DNA, producing a range of nucleic acid adducts. Resultant mutagenesis occurs almost exclusively at cytosines which are converted into the exocyclic lesion, 3,N^4-ethenodeoxycytidine (εC).

A monoclonal antibody which specifically recognises εC has been developed. The specificity and affinity of this antibody has been determined by ELISA. Immunoaffinity gels have been prepared and an immunoenrichment procedure developed to detect and identify εC from normal nucleotides at very low abundance. Immunopurified samples of εC have been quantified by CZE on addition of a standard spike with a detection sensitivity of 1 εC in 10^8 normal nucleotides. Kinetic studies using this detection system found production of εC to be greater in single stranded DNA than in double stranded DNA when incubated with a metabolite of vinyl chloride.

Oligonucleotides incorporating εC have been synthesised and used in thermodynamic and structural studies investigating the base-pairing effect of εC in double stranded DNA. εC was found to have a detrimental effect on duplex stability although the overall duplex structure was found to be undistorted.

Oligonucleotides labelled with the dansyl group have been synthesised for use as gene probes. A monoclonal antibody with affinity to dansyl was developed to immunochemically detect this reporter group. Femtomole quantities of labelled probe were detected with this system.

CONTENTS

CHAPTER ONE

Immunochemical, Thermodynamic and Structural Studies on the Mutagenic Lesion 3, N^4-ethenodeoxycytidine

INTRODUCTION

Cancer and Carcinogenesis

Cancer is a dense, distorted, conglomeration of cells or tumour. Tumours develop from a single cell that has been freed from the normal constraints of cellular growth and proceeds to multiply without limits. If the growth is local and remains within the initial area, the tumour is said to be benign. However, tumours can become malignant by propagating outwards to multiple sites in the surrounding tissues and also to distant organs. Commonly death is due to this metastatis disrupting the functions of vital organs leading to irreversible damage[1].

As cell growth is central to tumour formation it follows that cells that multiply are more prone to become cancerous. Indeed, mature nerve cells do not multiply and are rarely sites of primary tumour formation. Conversely, cells in the skin, gut and bone marrow multiply continuously and often are the sites of initial tumours. Cells in the liver, thyroid and other glands multiply discontinuously and only in response to certain stimulii and are less commonly sites of initial tumour growth[1].

Two steps are required for the metamorphosis of a normal cell into one capable of tumour development. In an initiation step an agent affects a persistent but dormant cellular change and, after a period of latency, in a promotion step an additional agent induces uncontrolled cell propagation and tumour growth. UV light and some viruses and chemicals are recognised as initiation agents. Hormones, steroids and growth factors are promotors.

The determinants which control cell number are cell division and cell death. These two factors provide the basis for the principal concepts which describe the carcinogenic modes of action of initiators and promotors at the cellular level:

1) It is suggested that both initiators and promoters act on the reserve cell population known as stem cells. Stem cells are only stimulated to develop into growing, tissue specific cells under certain conditions. This perhaps accounts for the latent period in cancer development. These agents may modify the process of differentiation when stem cells move from dividing cells to non-invading, functioning cells by removing their controls on division, thus initiating tumourigenesis[2].

2) *Necrosis* and *apoptosis* describe the two processes of cellular death. *Necrosis* represents death by external agents which severely injure the cell. *Apoptosis*, or programmable cell death is an internally controlled mechanism whereby the cell commits suicide in response to a mild injury. Both initiators and promotors may trigger both forms of cell death but it has been suggested that they may have a more subtle inhibitory effect on *apoptotic* cell death. It is known that the p53 tumour suppressor gene monitors DNA damage and will induce *apoptosis* in irreparably damaged cells. If however, the p53 gene is damaged by the action of an initiator or promoting agent *apoptosis* is eliminated from the cell. Such a defect in programmable cell death may then lead to tumourigenesis[3].

As has been suggested, the origins of cancer may lie in initiators and promotors irreversibly changing heritable cellular characteristics at the molecular level. To effect such heritable changes, genetic modifications need to be made. This is the basic premise of the "Somatic Theory of Carcinogenesis" which states that initiators primarily interact with DeoxyriboNucleic Acid (DNA), the genetic macromolecule that stores the library of information for cellular growth and function[4].

DNA

DNA is a linear co-polymer composed of four monomeric, nucleoside subunits. The nucleosides are deoxyribose pentose sugar groups bearing β-*N*-glycosyl bonds to heterocycles. In DNA the heterocycles are commonly the pyrimidines: cytosine and thymidine, and the purines: adenine and guanine. These nucleosides: deoxycytidine (dC), thymidine (T), deoxyadenosine (dA) and deoxyguanosine (dG) are coupled together by phosphodiester linkages forming strands of nucleic acid (figure 1).

The overall tertiary, polymeric structure of DNA was determined by Watson and Crick to be a right handed double helix where two strands of nucleic acid run antiparallel to each other[5]. Watson and Crick proposed that forces holding the double helix together were generated from interstrand hydrogen bonds between heterocyclic base-pairings. Due to steric restrictions purines could only pair with pyrimidines. The base pairings were deduced from the probable tautomeric forms of the heterocycles. Adenine pairs with thymine generating two hydrogen bonds and guanine pairs with

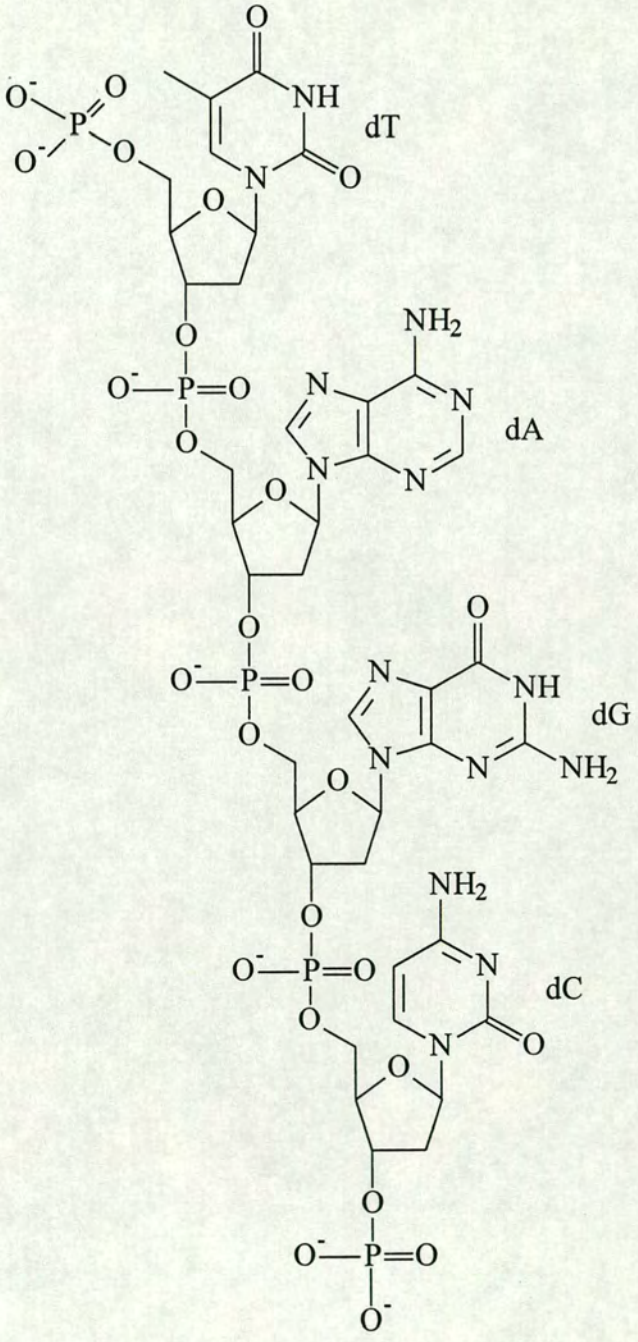

Figure 1: Deoxyribonucleic Acid

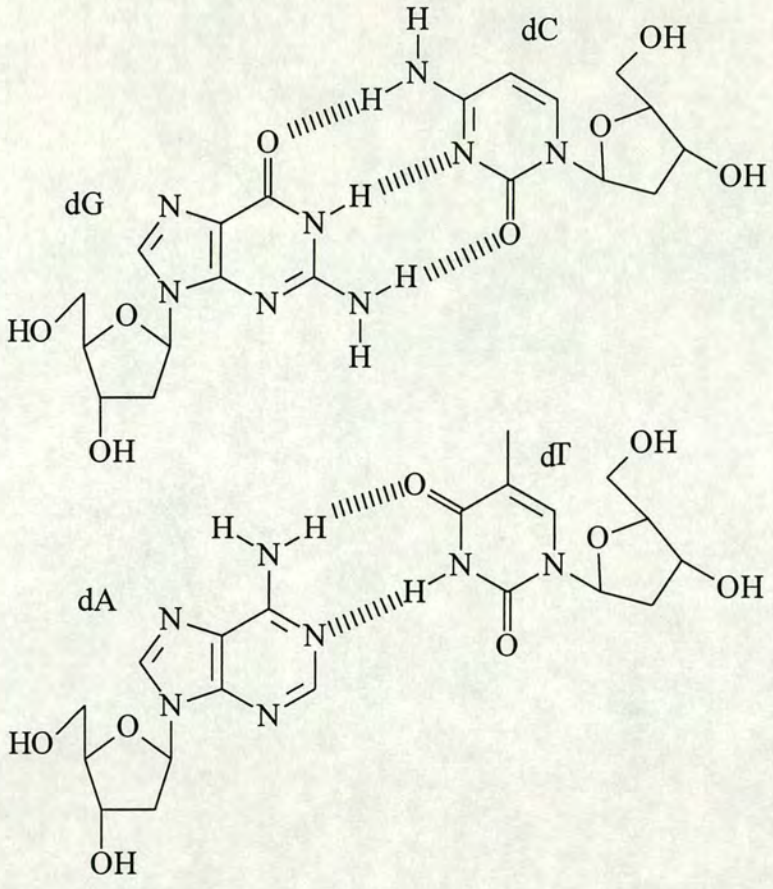

Figure 2: Watson-Crick Base-Pairings

cytosine generating three hydrogen bonds (figure 2)[6]. This was confirmed in an observation made by Chargaff: the molar proportions of dA to T and dG to dC were approximately equal irrespective of the source of DNA[7]. This proposed model has now become established and it is known that the structure is stabilised not only by hydrogen bonds but also by π-orbital base-stacking, van der Waals and hydrophobic/hydrophilic interactions within the double helix[8].

The implications of the specific base-pairings led Watson and Crick to propose mechanisms whereby DNA could carry and store genetic information. They intuitively saw that as one strand is the complement of the other, the exact order of bases in one strand could be interpreted from knowing the base sequence of the other. This concept became the cornerstone of the "Central Dogma of Molecular Biology" which suggested DNA's role as a template that could be read and copied. The central dogma of molecular biology models the directional flow of genetic information and indicates the transfer pathways involved (figure 3)[9]. What follows is an account of the

current knowledge of the processes involved in these transfer pathways and their role in molecular carcinogenesis[10-12].

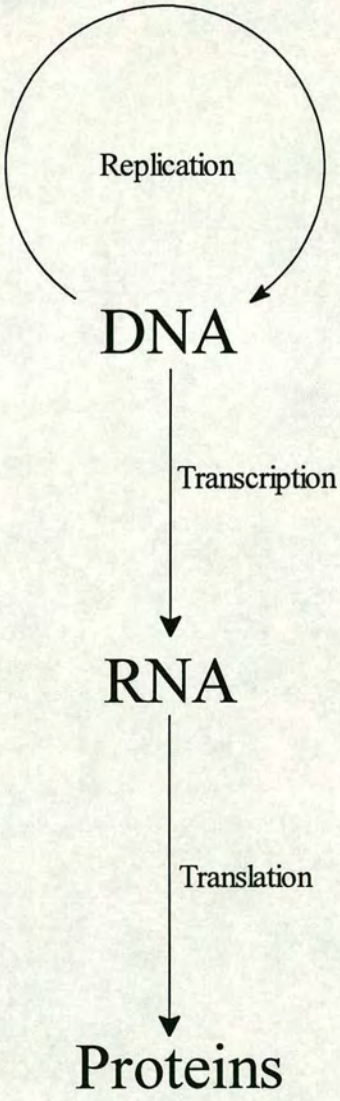

Figure 3: The Transfer Pathways in the Central Dogma of Molecular Biology

The DNA bases represent the four letters of the genetic code: A, T, C and G. These letters are organised within a specific reading frame as triplets or codons thus 64 (4^3) combinations are possible. Each codon represents an amino acid and a gene is the series of codons encoding the amino acid sequence of a protein. The precise order of amino acids determines how the protein will fold and hence operate. Thus the sequence of nucleotides in DNA ultimately contols protein structure and function. There are 20 amino acids and although codons are specific for one amino acid they are degenerate as some amino acids are associated with more than one codon.

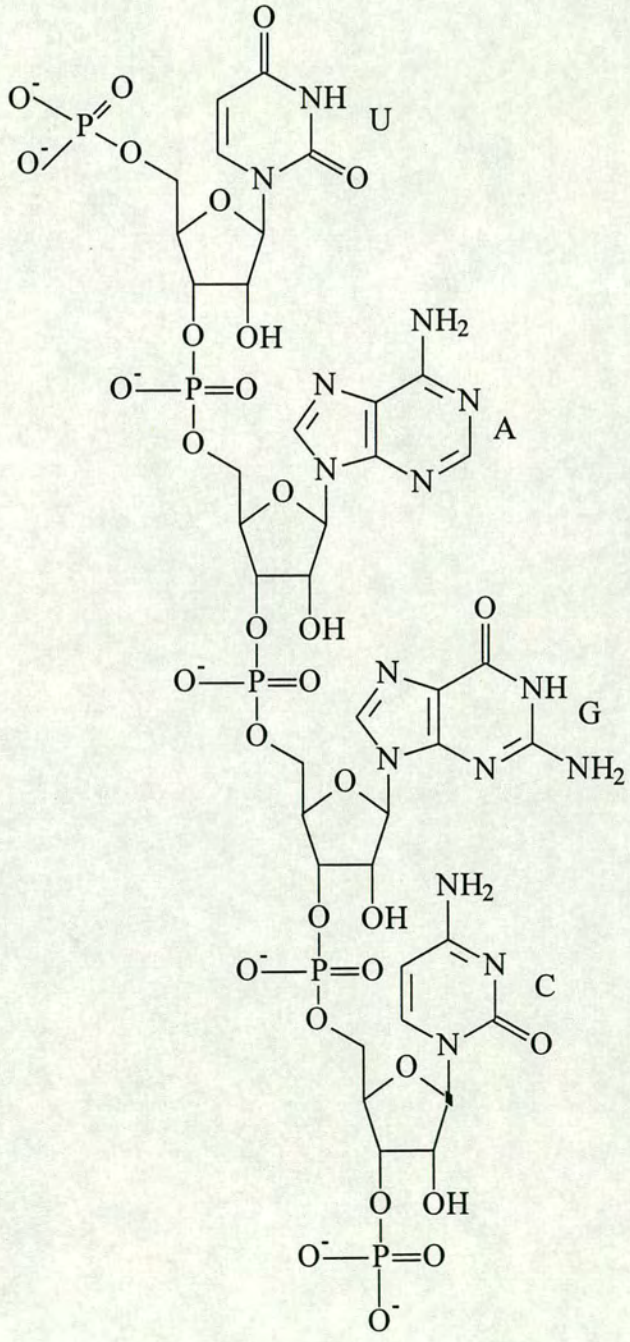

Figure 4: Ribonucleic Acid

There is an intermediary step in the process of translating the four letter DNA code into the 20 letter protein-amino acid code. This involves RiboNucleic Acid (RNA). Enzymes unravel the double helix and using one strand as a template, synthesise the complementary sequence with the four ribonucleotides: adenosine (A), cytidine (C), guanosine (G) and uridine (U), uridine replaces T in RNA (figure 4). This process known as transcription, creates a new template called messenger RNA (mRNA) which is translated distant from DNA at ribosomes into amino acid sequences which are folded into proteins.

Gene expression is controlled by regulatory proteins that bind to regions of DNA that promote mRNA synthesis. These proteins can therefore repress synthesis of the gene product. Repressor proteins are also gene products capable of being repressed. Thus expression of a single gene can be subject to a complex system of interacting feedback mechanisms (figure 5).

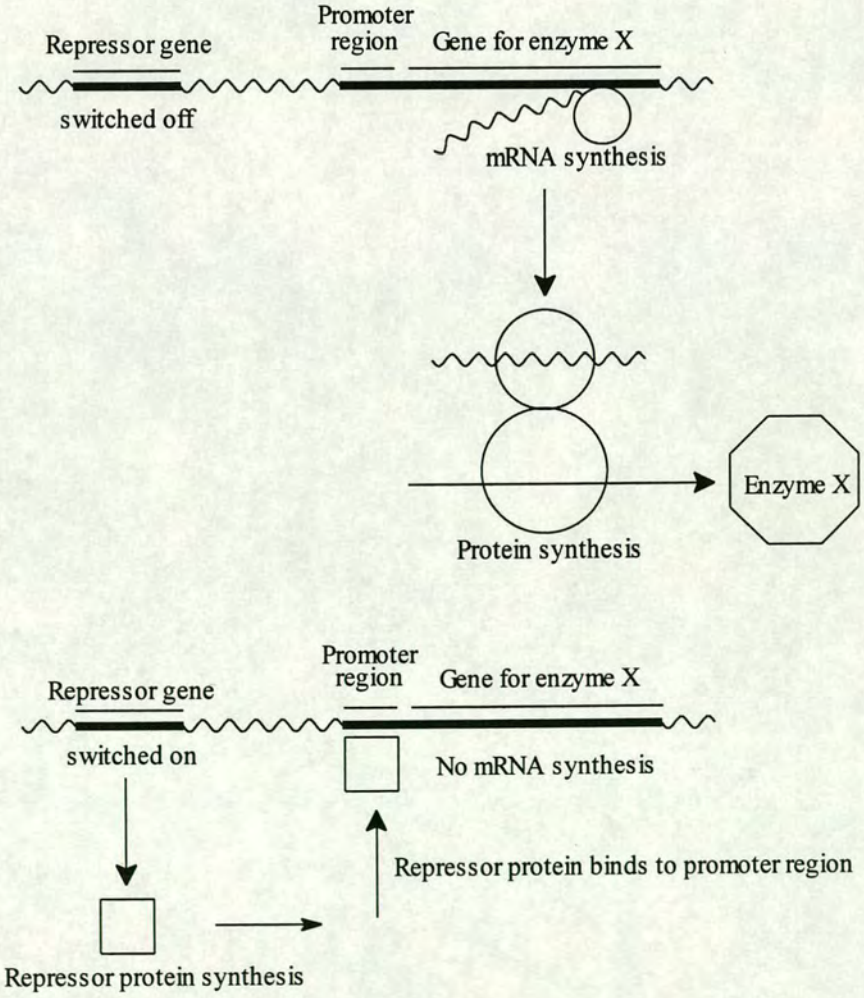

Figure 5: Gene Expression and Repression

Before cells can divide and multiply they must undergo mitosis which duplicates the cellular nucleus. A requirement for mitosis is replication of DNA. To preserve the integrity of genetic information replication must be extremely precise. However, the entire human genetic database or genome consists of approximately $3x10^9$ base-pairs. The speedy duplication of such a large amount of material with high fidelity is a huge undertaking and it is inevitable that mistakes occur. The replicative process has been well studied in the bacterial strain, *Escherichia coli* (*E. coli*) which has a smaller genome of approximately $5x10^6$ base-pairs. The replication rate in *E. coli* is 250-1000 nucleotides *per* second yet, despite this high copying velocity, mispaired bases occur only once in every 10^9 to 10^{10} nucleotides ie. one error every 10^3 to 10^4 copies.

A large battery of enzymes is responsible for this achievement. DNA polymerases are the enzymes that synthesise DNA. They insert nucleotides using Watson-Crick base-pairings between opposing bases along the template strand. However, other base-pairings are thermodynamically and sterically feasible. This would potentially result in an error rate of one in 10^4 to 10^5 nucleotides but polymerases have an inbuilt error-checking capability which recognises such mismatches, inhibiting further chain elongation until the aberrant nucleotide has been removed and the correct base inserted. This ability to correct mistakes results in one erroneous base every 10^6 to 10^8 nucleotides. The fidelity of DNA replication is further increased 10^2 to 10^3 fold by mismatch repair enzymes. These enzymes proof-read DNA and recognise mismatched bases causing excision of the DNA strand section containing the mispaired base and resynthesis of that segment in the daughter strand. Once a newly synthesised DNA strand has been proof-read it is methylated at the N^6-postion on deoxyadenosines (in mammalian DNA the C^5-postion on deoxycytosines is methylated) enabling mismatch repair enzymes to distinguish between parent and daughter strands.

The Molecular Basis of Carcinogenesis

The structural integrity of DNA is crucial to cellular function. However, despite this, DNA is in a state of constant flux. DNA is chemically reactive and can undergo a variety of reactions which change the covalent structure. Any structural

modification can potentially lead to alterations in the genetic code and how it is read. Such changes are termed mutations and there are three broad classes of mutation:

1) point mutations,

2) frame shift mutations,

3) large scale rearrangement mutations.

Point mutations are single base changes in the genetic code. During replication they occur either as transitions where a purine is replaced by another purine or a pyrimidine is replaced by another pyrimidine or transversions where purine is replaced by pyrimidine or *vice versa*. Of the three types of mutational event, point mutations have the least effect as only one codon is changed *per* point mutation. They may even be "silent" due to the degeneracy of the genetic code when the altered codon still codes for the same amino acid.

Frame shift mutations occur when bases are added or removed. This results in a complete change in the way the gene is read as it alters the reading frame. This type of mutation can have a devastating effect on amino acid sequence and hence protein structure usually resulting in a "nonsense protein".

Large sequences of DNA can be deleted, inverted or transfered from one genomic region to another. Such large scale rearrangements can affect a number of genes.

Mutations can result in carcinogenesis when the gene responsible for a biological process is partially or completely defective. Many genes have specific regions or "hot spots" that are susceptible to mutational events. Mutational agents often have their own, widely different spectrum of hot spots within a gene. After a mutation the faulty gene products either operate as normal, operate with decreased efficiency, cease to operate at all or have an altered function. The consequences of this are entirely dependent on the nature of the protein involved. Usually the result is detrimental to the survival of the cell and leads to cell death. However, it can on occasion promote cellular growth and carcinogenesis.

The origins of frame shift and large scale rearrangement mutations are speculative and more is known about point mutations. Point mutations occur when non-Watson-Crick base-pairing has escaped the error checking and proof reading phases of replication or as the result of DNA damage.

DNA is damaged by endogenous or exogeneous genotoxic agents. Endogenous DNA damage arises from normal cellular, environmental conditions and metabolic processes. Commonly, dC and dA are deaminated, dG and dA depurinated and dC and T depyrimidated by hydrolysis in the aqueous medium. In addition, highly reactive chemical species can be released during cellular metabolism which can oxidise and alkylate DNA generating modified adducts. Exogeneous genotoxins include radiation, viral cells and a wide spectrum of chemicals. To cope with such continual change in their DNA, cells have developed a large range of repair systems to limit spontaneous or induced damage and maintain the genetic code.

Chemicals possess carcinogenic properties by covalently binding to or reacting with DNA thus creating mutagenic lesions. Ultimate carcinogens are those chemicals which act directly with DNA. Some chemicals, known as precarcinogens, require transformation into an activated form. This can occur spontaneously but often requires activation *via* an enzymatic pathway and can involve a number of intermediate steps. DNA is a nucleophilic target and therefore ultimate carcinogens are often electrophiles.

Vinyl Chloride

Vinyl chloride is an important industrial precursor, used in huge quantities for the manufacture of polyvinyl chloride (PVC) and other polymers. During the early 1970s toxicological experiments investigating the long term effects of this chemical in mammals reported tumour formation in rats exposed to vinyl chloride contaminated air[13]. Subsequent studies found vinyl chloride also induced cancer when administered to mice and hamsters[14,15]. By the mid-1970s a high incidence of liver angiosarcoma (blood vessel derived tumours) among workers involved in vinyl chloride manufacture was noted and reported[16]. Thereafter, two epidemiological studies revealed an increased incidence of malignant tumours of the skin, lung, colon and thyroid in industrially exposed employees[17,18]. It was also noted that the frequency of chromosomal aberrations was higher in these workers compared to unexposed people[19,20].

The mutagenic properties of vinyl chloride were examined in bacterial systems. It was found to induce a high spontaneous mutation rate in *E. coli*[21],

Schizosaccharomyces pombe and *Saccharomyces cerevisiae*[22] but only in systems supplemented with microsomal enzyme activity. The requirement for microsomal enzyme activity suggested that vinyl chloride was not a direct mutagen but a precarcinogen that required prior metabolic activation before any mutagenic effect could be observed. The mono-oxygenase enzymes in microsomes were presumed to be responsible for this metabolic activtion in vinyl chloride induced mutagenesis. *In vitro* studies using radiolabelled vinyl chloride revealed high levels of covalent binding of the putative metabolic product to cellular proteins with substantially lower levels of binding to DNA. This observation was rationalised by a proposed mechanism whereby vinyl chloride was metabolically activated by cytochrome P_{450} mediated monooxygenases present in microsomes to form the reactive metabolite chloroethylene oxide (CEO). CEO then spontaneously rearranges to a less reactive compound, chloroacetaldehyde (CAA) (figure 6). CAA was thought to be responsible for the predominant protein adduction and CEO to be solely responsible for DNA binding[23].

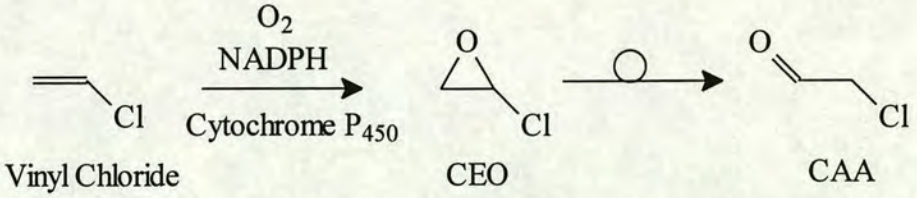

Figure 6: Metabolic Activation of Vinyl Chloride to CEO and CAA

The presence of both compounds was established when vinyl chloride was passed through mouse liver microsomes in the presence of oxygen and both volatile metabolites, CEO and CAA were trapped by reaction with 4-(4-nitrobenzyl) pyridine[24]. The half-life of CEO due to rearrangement into CAA was calculated at 1.6 minutes in aqueous solution from kinetic experiments[23]. Vinyl chloride metabolism has since been found to be entirely dependent on cytochrome P_{450} oxidation and as such obeys first order kinetics before enzyme saturation occurs at high dose levels[25,26]. Tumour formation has been directly correlated to the concentration of vinyl chloride exposed to rats at first order kinetic levels[27].

Evidence for the identity of the ultimate carcinogen was provided by feeding experiments to probe the *in vivo* modes of action of CEO and CAA. 2,2'-Bis(2-chloroethyl) ether and chloroethanol are also metabolised to form CAA but by

pathways other than *via* a CEO intermediate. 2,2'-dichlorodiethyl ether is oxidised by cytochrome P_{450} to CAA and chloroethanol which is in turn metabolised to CAA by alcohol dehydrogenase. When groups of rats were exposed to 2,2'-dichlorodiethyl ether, chloroethanol and vinyl chloride only the last group developed tumours. On analysis of the rat livers only those rats administered with vinyl chloride showed significant DNA binding[28]. In corroberation with these findings CEO was found to be mutagenic in *Salmonella typhimurium*[29] and carcinogenic in mice[30]. Contrary to this conclusion subsequent tests found CAA to be mutagenic in strains of *Salmonella*[31] and *Aspergillus nidulans*[32] and carcinogenic in mice[33]. It is now presumed that both CEO and CAA alkylate DNA *in vivo* but to different extents and with a different pattern of DNA adducts. CAA is further metabolised combining with glutathione *via* glutathione transferase before urinary excretion[16] (figure 7).

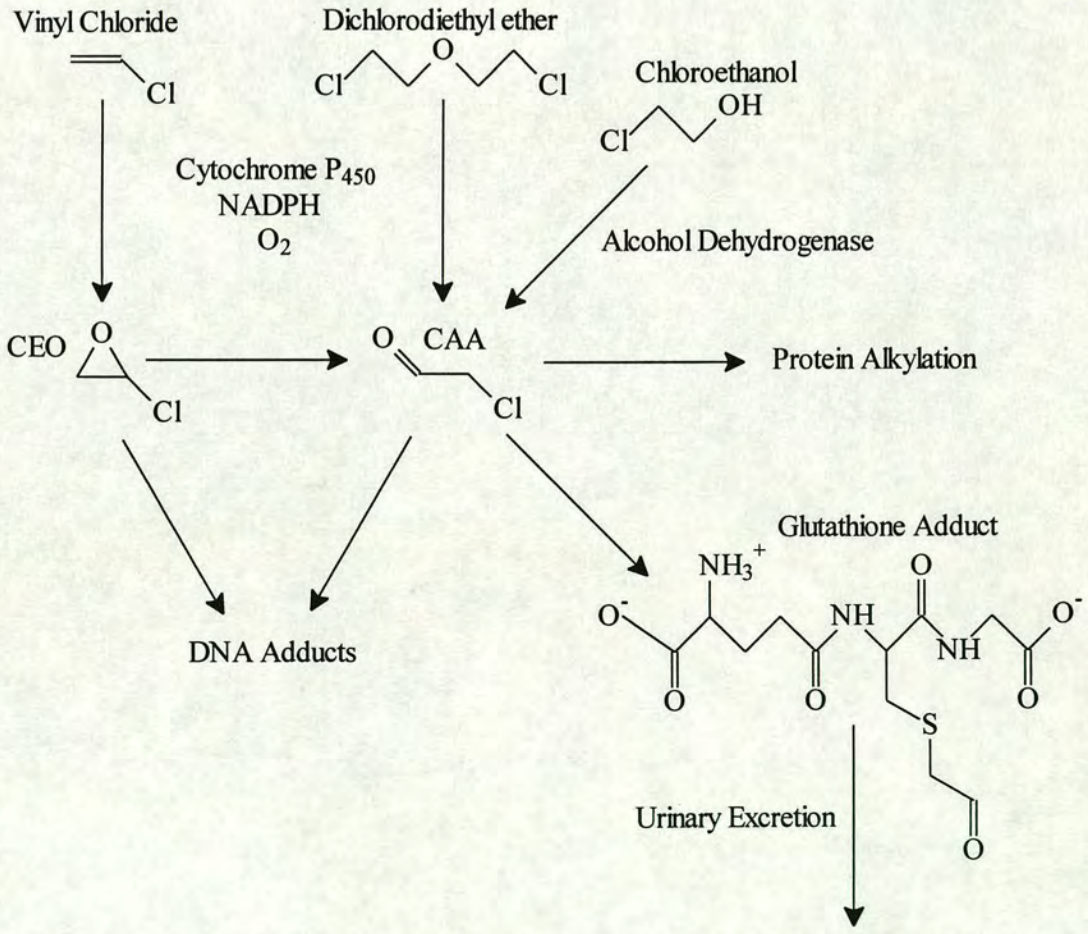

Figure 7: The Metabolism of Vinyl Chloride, Bis(2-chloroethyl) ether and Chloroethanol

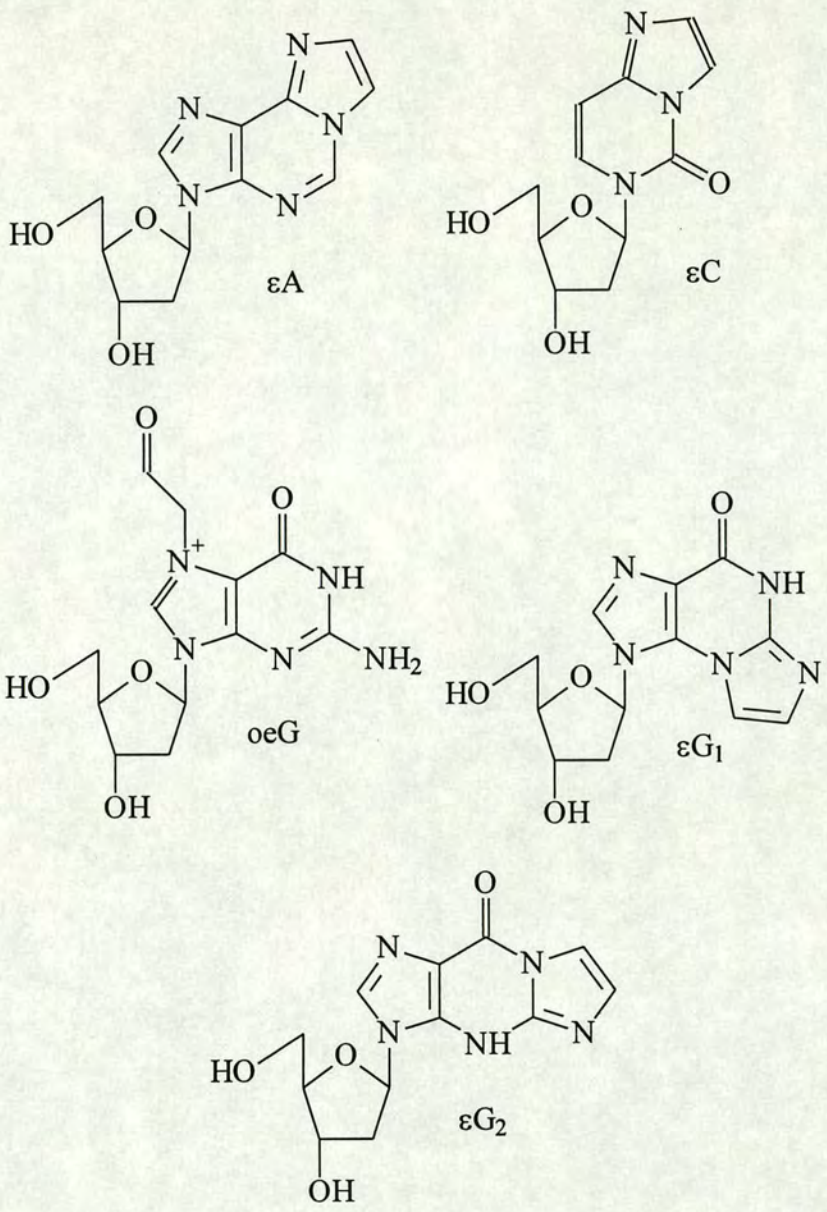

Figure 8: Vinyl Chloride, CEO and CAA Induced DNA Adducts

The identity of the alkylated DNA adducts formed from vinyl chloride exposure was established both by *in vivo* and *in vitro* experiments using radiolabelled vinyl chloride. 1,N^6-ethenodeoxyadenosine (εA), 3,N^4-ethenodeoxycytidine (εC) and N^7-(2-oxoethyl) deoxyguanosine (oeG) were readily formed upon *in vitro* incubation of DNA and rat liver microsomes with ^{14}C-labelled vinyl chloride[34]. However, only oeG was formed under non-denaturing conditions and in far greater abundance relative to the etheno adducts. When ^{14}C-labelled vinyl chloride was administered to rats only oeG was detected at low dose levels but at higher doses εA, εC and a further adduct were detected. This was identified as N^2,3-ethenodeoxyguanosine (εG_1)[34].

When DNA and RNA were incubated with CAA *in vitro* εA, εC, oeG, εG_1 and a fifth adduct assigned as 1,N^2-ethenodeoxyguanosine (εG_2) were formed[34] (figure 8).

Inter-strand crosslinking was also found between dA residues in poly d(AT) duplexes treated with CAA[34]. Although this would have significant biological effects crosslinking has not been observed in any *in vivo* experiments.

In vitro experiments had suggested that the formation of the etheno adducts is specific to single stranded regions of DNA. The amino and imino groups involved in formation of the etheno bridge are involved in hydrogen bonding interactions within double stranded DNA. They are therefore electronically deactivated and sterically protected within the double helix. It is also been observed that such chemical modifications are sensitive to intrastrand base-stacking interactions. Formation of oeG is due to alkylation by CEO and is observed in both single and double stranded regions of DNA. This is a result of the accessibility of the N^7 position of dG in the major groove of duplex DNA[35].

The specific mechanism of DNA alkylation by CEO and CAA to form the etheno adducts was elucidated from direct observation of reaction intermediates by FTNMR and GCMS (figure 9). Initially nucleophilic attack by the imino nitrogen displaces chloride from the alkylating agent in a concerted process. This is of S_N2 type during reaction with CAA but the less hindered epoxide carbon is probably attacked in CEO with chloride displacement. This is followed by nucleophilic attack from the exocyclic amino group in close proximity to form a cyclic hydrate intermediate. These are isolateable compounds under physiological conditions with half-lives of 1.4 and 13 hours for the hydrated etheno forms of dA and dC respectively. The energetically-favourable planar, resonance-stabilised ring system formed by loss of water pushes the reaction forward to the formation of the etheno bridge system. Evidence that nucleophilic attack is by the imine nitrogen first then the amine nitrogen was provided from experiments involving the analogue N^3-methyl cytidine which was unreactive towards CEO and CAA under ambient conditions[35,36].

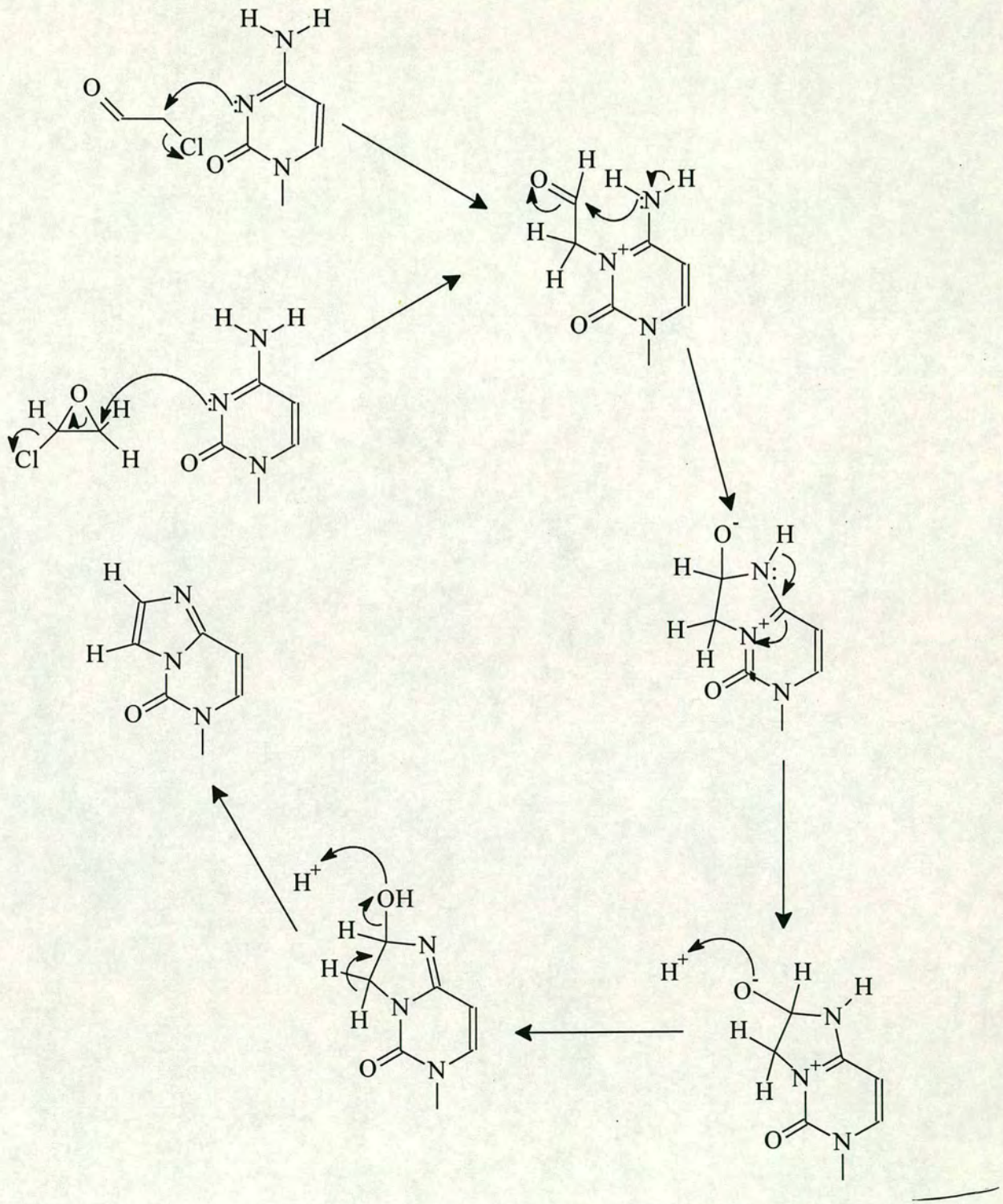

Figure 9: The Mechanism of CEO and CAA Alkylation of DNA to Form Etheno Adducts

Vinyl chloride is not the only source of these adducts. Vinyl bromide is recognised to behave similarly to vinyl chloride as it is metabolised to bromoethylene oxide and bromoacetaldehyde[26]. The industrial chemicals 1,2-dichloroethane and chloroethanol are both metabolised in mammals to chloroacetic acid *via* CAA[31]. CAA

is also an industrially used chemical and has been identified as a contaminant in drinking water due to chlorination of humic substances[33]. Vinyl carbamate epoxide, a structurally similar compound to CEO is produced by mammalian metabolism of the industrial polymer materials ethylcarbamate (urethane) and vinyl carbamate (figure 10). This compound was found to be a highly potent mutagen and carcinogen, forming the same spectrum of DNA adducts as vinyl chloride[37]. It is thought that these adducts are also formed endogenously as well as by exogeneous chemicals. εA, εC and εG_1 have been identified in the livers, lungs and kidneys of animals unexposed to exogeneous sources[38]. In these cases the DNA reactive species are presumed to be by-products originating from lipid peroxidation processes. These are known to produce highly reactive alkenes and aldehydes which can react with DNA directly[39] or be enzymatically activated first[40].

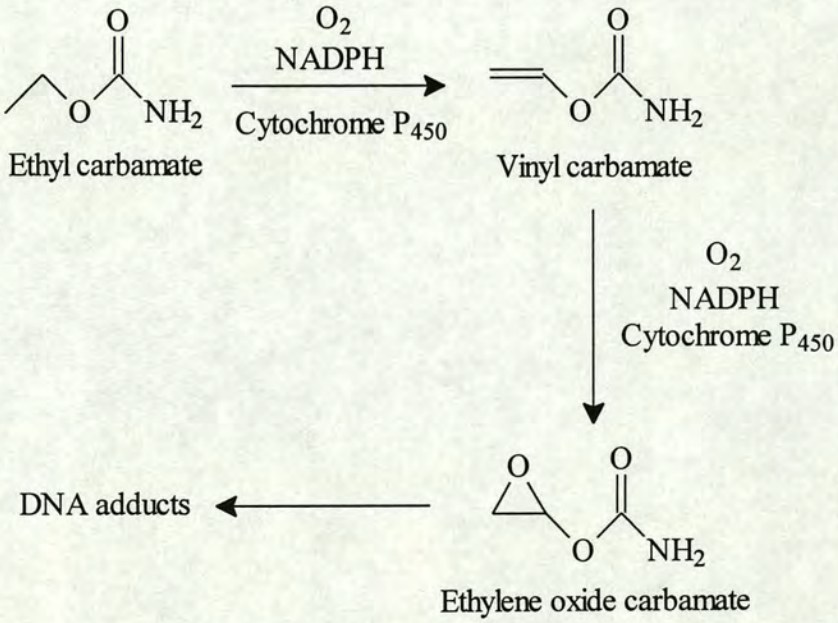

Figure 10: The Metabolic Activation of Ethyl Carbamate and Vinyl Carbamate

The Molecular Biological Consequences of CEO and CAA Modified DNA

CEO and CAA are known to inhibit DNA synthesis in mammalian cells. The inhibitory effect is not directed at nucleotide biosynthesis but directly on the DNA replication machinery as DNA alkylation by these chemicals disrupts DNA polymerase and other enzymes[41]. This has been directly attributed to the DNA adducts formed and their properties have been studied.

1) **εA:** The etheno bridge in εA blocks both the hydrogen bonding sites of dA. These sites are crucial to Watson-Crick base-pairing of dA with T. Their unavailability will affect transcription and replication. Therefore εA is potentially a promutagenic lesion.

It has been demonstrated that εA does possess a miscoding effect on *in vitro* RNA and DNA synthesis. Poly dA templates modified with CAA were shown to induce errors in transcription by *E. coli* DNA dependant RNA polymerase. This enzyme incorporated a range of nucleotides opposite εA in the newly synthesised strand with insertion of A favoured to the biologically correct U[42]. C was also a minor incorporation product[42]. Studies using similarly treated poly dA templates showed the replicative fidelity of *E. coli* DNA polymerase I was also corrupted. This enzyme incorporated dG opposite εA in the complementary strand but with poor miscoding efficiency with only one mispair occuring in every 60-550 εA adducts[43,44]. This represents a dA.dT to dC.dG type of transvertion point mutation. These studies also reported a significant reduction in the rate of primer elongation along the modified template with stops occuring at εA residues. Paradoxically *in vivo* mutagenesis by εA has never been established. It is proposed that error-free bypass of εA by polymerase results from an unknown, favoured configuration of εA templating for T reducing the mutagenic efficiency[45].

Structural and thermodynamic studies have not supported this hypothesis. Results from NMR studies on εA containing duplexes have found that although T can be incorporated opposite εA with little disruption of the double helix, no inter-base hydrogen bonding is formed[46] (figure 11). This makes it extremely unlikely that εA can template for T. The converse is true for base-pairing between εA and dG which can form two hydrogen bonds when εA is rotated into a *syn*-configuration[47] (figure 11). This is supported by a crystal structure which also shows dG pairing with εA in a *syn*-configuration and thermodynamic data which indicate the εA.dG base-pairing to be the most stable base-pairing possible[48].

The lack of *in vivo* evidence for εA coding for dG possibly indicates that this mutagenic lesion is a substrate for a repair enzyme which can effectively remove εA prior to replication.

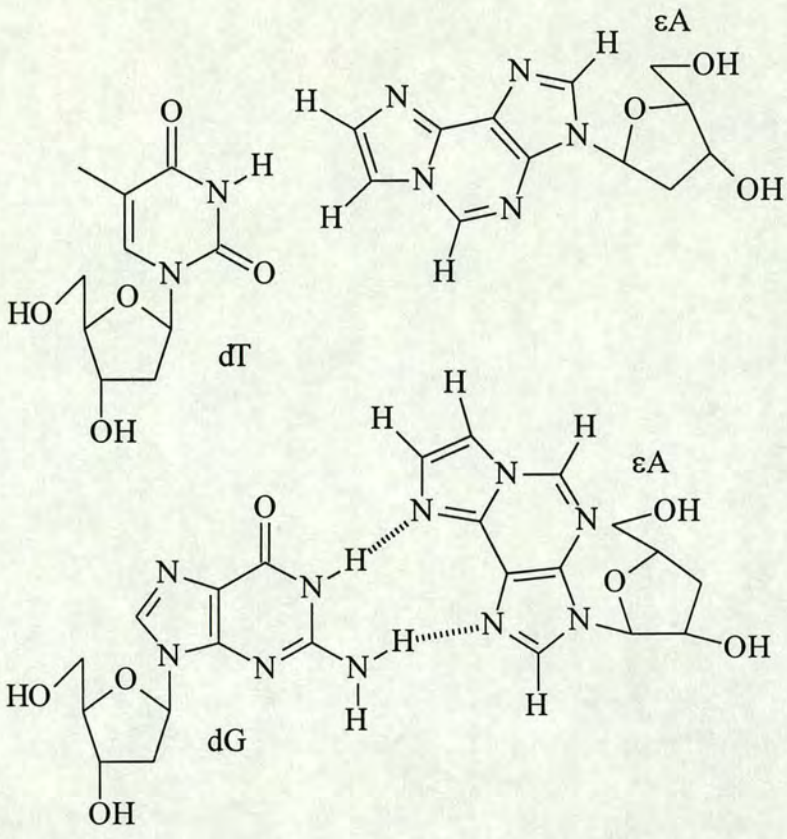

Figure 11: T(*anti*):εA(*anti*) and dG(*anti*):εA(*syn*) Base-Pairings

2) εC: The etheno bridge in εC blocks two of the three hydrogen bonding sites of dC. In this way the genetically correct base-pairing of εC with dG is destabilised which could possibly induce errors in transcriptional and replicative processes. Therefore εC is also a potential promutagnic lesion.

εC does demonstrate miscoding properties on *in vitro* RNA and DNA synthesis. CAA modification of poly dC templates can cause *E. coli*[42] and calf thymus[49] DNA dependent RNA polymerases to transcribe with ambiguity. These enzymes incorporate U or A opposite εC during transcription. This base-pairing ambiguity is also demonstrated during replication. Errors are induced on *E. coli* DNA polymerase I by CAA modified poly dC[43] and poly d(CG)[44] templates. Both dA and T are incorporated opposite εC, with incorporation of dA being slightly favoured. A higher miscoding efficiency is observed relative to εA as one εC.dA mispair occurs every 30 εC and every 80 εC for a εC.T mispair[44].

Due to the ambiguous coding nature of εC it has been described as a non-instructural mutagenic lesion as it allows replication past the lesion site but does not direct incorporation of a specific base. A more detailed study of the miscoding

properties examined the base incorporation and primer extension at a site specific εC by *E. coli* DNA polymerase I Klenow fragment[50]. Klenow fragment is *E. coli* DNA polymerase I minus 5'-to-3' exonuclease activity. However, the enzyme used in this mutagenesis study was also devoid of the 3'-to-5' exonuclease proof reading capability. It revealed that although misinsertion of dA opposite εC is favoured over T, chain extension occurs more readily when T is paired with εC. In this way εC can be responsible for both dC.dG to dT.dA transition and dC.dG to dA.dT transversion point mutations.

In vivo studies using DNA which was treated *in vitro* with CAA and transfected into *E. coli* suggested that mutagenesis occurs almost exclusively at dCs. Of the mutations targeted at dCs 80% were dC to dT transitions and 20% were dC to dA transversions[45]. This indicates that although εC is an non-instructional lesion it has some miscoding bias where dA is preferentially inserted in 4 out of every 5 misinsertion events attributable to εC. This observation has not yet been rationalised but it may be that insertion of either base is sequence dependent.

It is commonly believed that other non-instructional lesions such as abasic sites and bulky lesions cause polymerases preferentially to insert dA opposite the lesion site. In this respect εC lesions follow this "adenine rule". The mechanism for the "adenine rule" whereby dA is preferentially inserted is thought to include SOS functions. SOS functions are induced by events that halt normal polymerase replication and bulky DNA lesions are known to cause such stops in replication. To continue DNA synthesis past the lesion site, SOS functions provide a mechanism for base-pairing at the lesion and translesional synthesis. The base-pairing is often insertion of dA and is therefore error prone. However, when cells transfected with CAA modified templates were irradiated with UV light, which also induces SOS functions, no change in the specificity of base mutations at dC was observed. As an alteration in mutations would be expected on UV irradiation it was concluded that unlike all other known non-instructional lesions εC mutagenesis is independent of SOS functions[51]. Further experimental evidence supporting this view was obtained by using the mutant *E. coli* strains, $recA^+$ and $recA^-$. They were transfected with a oligonucleotide template bearing a site specific εC and mutagenesis in progeny plaques examined at this position. The recA gene product is an integral protein in SOS

mechanisms for error prone repair and as such is required for mutagenesis at "classical" non-instructional lesions. It was found that neither the survival nor the mutational efficiency in either $recA^+$ or $recA^-$ cells was significantly different. The conclusion from these findings is that εC represents a previously undiscovered class of mutagenic lesion that is non-instructional but allows DNA synthesis at and past the lesion site without invoking SOS responses[52]. The mutagenic frequency was measured at the site specific εC in both cell strains and found to be approximately 30% which represents a high mutational efficiency[52].

Base-pairings for both the εC.dA and εC.T mismatches have been proposed that include hydrogen bond formation[53] (figure 12). However, no structural information to support these models has been reported.

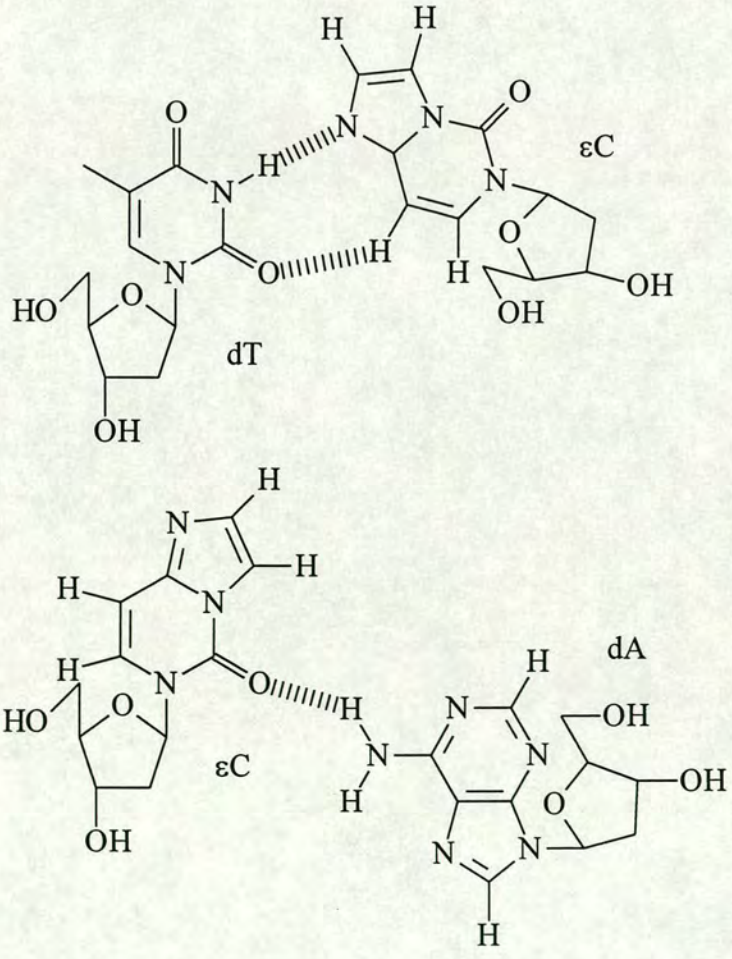

Figure 12: Proposed T(*anti*):εC(*anti*) and εC(*anti*):dA(*syn*) Base Pairings

3) oeG: The N^7 position of dG takes no part in normal Watson-Crick base pairing and therefore oeG would be expected to retain base-pairing capabilities with dC. The additional alkyl group may however, inhibit the binding of DNA regulatory

proteins. Promutagenic properties for oeG have been proposed based on an expected hemiacetal isomer of oeG. This isomer, in equilibrium with dG could code analogously to dA and therefore base-pair with T (figure 13). Although this model is plausible no evidence for any *in vitro* miscoding properties has been demonstrated in experiments using poly d(GC) templates treated with CEO and *E. coli* DNA polymerase I[54].

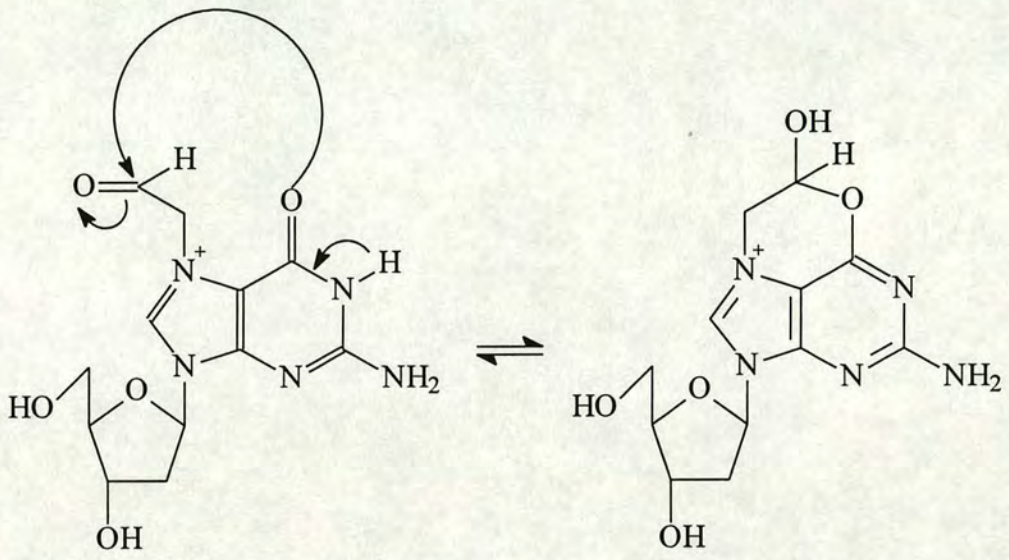

Figure 13: Proposed Isomerisation of oeG

4) εG_1 and εG_2: Of the two ethenodeoxyguanosine adducts found on *in vitro* treatment of DNA with CAA, only εG_1 has been found *in vivo*. εG_1 has been found to be mutagenic in both *in vitro* and *in vivo* assays. Unlike εC it induces monospecific base changes. *In vitro* experiments demonstrated εG_1 miscoding for T with a mutagenic frequency of 20% during reverse transcription of RNA templates treated with CAA[55]. Consistent with this report were *in vivo* assays in *E. coli* that illustrated site specific εG_1 lesions producing dG to dA transitions with a mutagenic frequency of 13%[56].

Enzymatic Repair of Etheno Adducts

To maintain the integrity of their genomic DNA, cells have developed enzymes to repair the DNA lesions produced by DNA damaging agents. Studies on DNA repair mechanisms have classified DNA repair into three broad categories[57]:

1) Incision-excision repair: Enzymes nick phosphodiester bonds to produce breaks in the strand containing the lesion. The segment of oligonucleotide containing

the lesion is then removed along from the cleavage site. Enzymes resume DNA synthesis and the double strand is reconstructed and ligated.

2) DNA *N*-glycosylase repair: Aberrant DNA bases are recognised by enzymes and removed by cleavage of the *N*-glycosyl bond to leave apurinic or apyrimidinic sites. These are then repaired by the incision-excision mechanism.

3) Transferase repair: The original identity of the DNA base is restored after removal of the adduct functionality by an enzyme.

To determine whether DNA repair systems mediate mutagenesis induced by etheno adducts the metabolism of vinyl chloride adducts was examined. Rats were exposed to vinyl chloride for a five day period and the levels of DNA adducts present in the liver, lungs and kidney measured at 3, 7 and 14 days post-exposure. It was found that all the vinyl chloride induced adducts were highly persistent in these tissues and half lives of oeG and εG_1 were calculated at 62 hours and 30 days respectively while εC and εA were even more persistent[58]. These results seem to indicate that no effective repair system for the removal of these adducts, particularly the etheno bases exists.

Contrary to this evidence were *in vitro* experiments which demonstrated that when CAA modified DNA was treated with rat brain tumour cell-free homogenates ethenoguanine and ethenoadenine were released[59]. This indicated the presence of specific *N*-glycosylases which could cleave these adducts from DNA. Subsequently it was found that ethenoguanine could be released from CAA treated DNA by the 3-methyladenine DNA glycosylase II repair enzyme isolated from *E. coli*. The specific enzyme activity for ethenoguanine release was 20 fold lower than that of 3-methyladenine but was at levels that would still effectively mediate εG_1 induced mutagenesis[60]. It has also been discovered that a human *N*-methylpurine DNA glycosylase cloned into *E. coli* has a 10 fold substrate preference for εA relative to 3-methyladenosine which was originally thought to be the primary enzymatic substrate[61]. The substrate specificity of this enzyme was explored further and was found to release all the etheno adducts induced by vinyl chloride. The rate of adduct release by this glycosylase was substrate dependent with release of εA and εC occuring at similar rates while εG_1 was released 5 times slower[62].

The existence of such repair capacities in cells obviously mediates the mutagenic effects of these etheno adducts. The evolution of such repair enzymes also supports the proposal that these adducts are formed endogenously as well as by exogeneous chemicals.

Antibodies

Antibodies have been used as biochemical tools to monitor the formation and metabolism of DNA adducts.

Antibodies are a class of serum proteins that are induced by the host's immune defence mechanism on recognition of a foreign body. In general, antibodies are symmetrical molecules comprised of four peptides. Two identical glycosylated heavy chains of 50,000 to 70,000 Daltons and two identical non-glycosylated light chains of approximately 25,000 Daltons. These peptides are held together covalently by disulphide bridges and also by coulombic interactions between amino acid residues (figure 14).

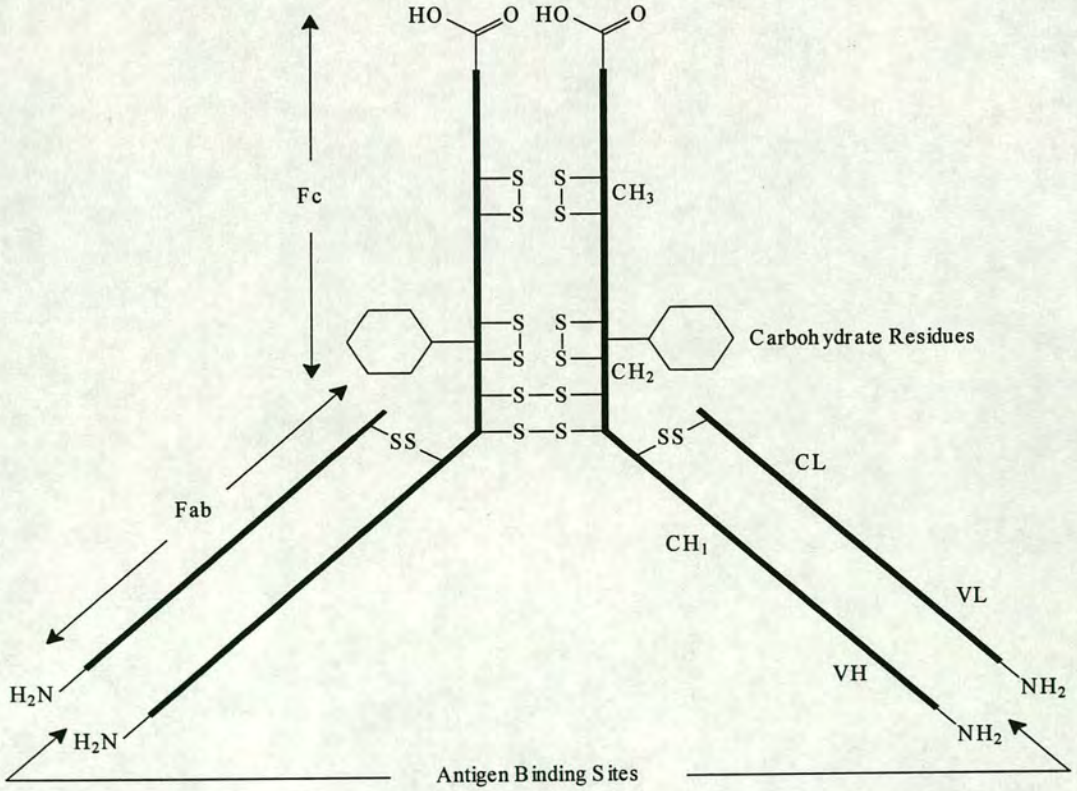

Figure 14: Diagramatic Representation of an IgG Antibody Molecule

Antibodies are grouped into 5 main classes which distinguish their structural and biological properties: IgA, IgD, IgE, IgG and IgM. The IgG class is the

predominant serum isotype and is subdivided into 4 subclasses in mice: IgG_1, IgG_{2a}, IgG_{2b} and IgG_3. Both the light and heavy chains are made up of homology units of approximately 110 amino acid residues which are folded into regions called domains. The class and subclass of an antibody can be determined by examination of the amino acid sequences of the light and heavy chain domains. Both have sections of amino acid sequence homology known as constant regions. These show little variation in antibody molecules of the same class and subclass. They are designated C_L and C_{Hx} for the light and heavy chains respectively where x=1 to 3 for the heavy chain domain number. There are also light and heavy chain domains of considerable sequence variability designated V_L and V_H. These domains create the antigen binding sites.

Antibody molecules can be pictorially represented as "Y" shaped molecules with the antigen binding sites at the ends of the "arms". These arms are known as the Fab regions and the "body" which provides the antibody effector functions is known as the Fc region (figure 14).

The binding between antibody and antigen is created by coulombic forces including electrostatic, van der Waals and hydrophobic interactions as well as hydrogen bonding. Binding specificity and affinity directly result from the structural and electrostatic complementarity of the antigen and antigen binding site. Antigen binding sites are extremely specific. However, cross-reaction can occur if antigens are structurally related. Antibody-antigen affinities typically range from 10^5 to 10^{10} M^{-1} and are dependent on the rates of association and dissociation between antibody and antigen according to the equation:

$$K_A = k_a/k_d = [\text{Ab.Ag}]/[\text{Ab}].[\text{Ag}]$$

where K_A is the antibody (Ab) affinity to the antigen (Ag),

k_a is the rate of association,

k_d is the rate of dissociation,

[Ab.Ag] is the concentration of antibody-antigen complex,

[Ab] is the concentration of free antibody,

[Ag] is the concentration of free antigen at equilibrium. The rate of association is limited by solution diffusion but also the time spent by the antigenic determinant or binding region in the conformation recognised by the antibody. The rate of

dissociation is dependent on the strength of the bonds formed between the antibody and antigen[63].

Immunoaffinity Chromatography

The specificity of antibodies has been exploited to isolate biological material. Immunoaffinity chromatography uses the specific but reversible binding between an antigen and an antibody bound to a solid phase support[64]. The method can be used to purify natural substances from contaminating constituents in biological samples but also to concentrate dilute solutions of these molecules[65].

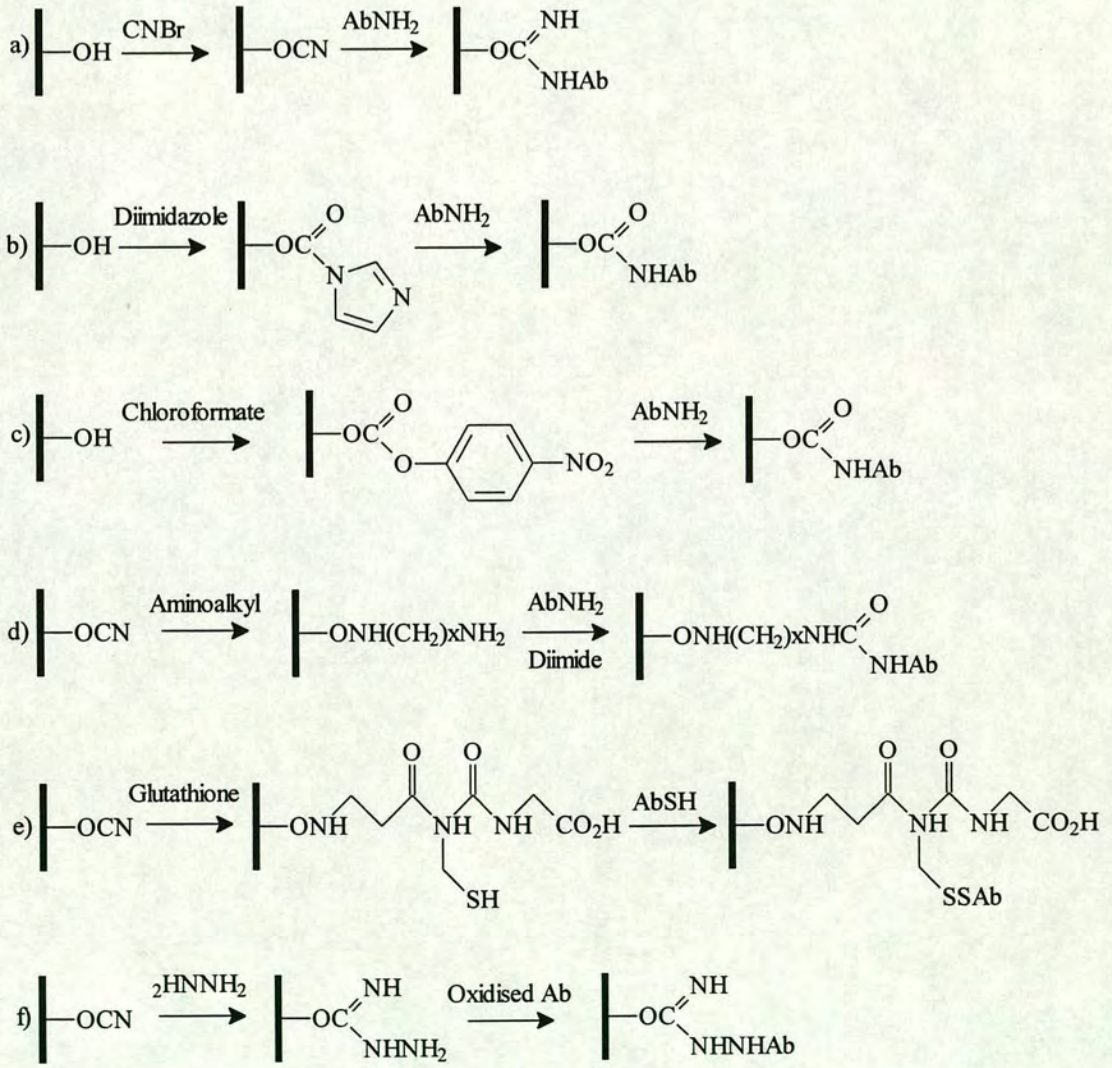

Figure 15: Solid Phase Coupling Chemistries: a) Cyanogen Bromide, b) Carbodiimide, c) Chloroformate, d) Haloaminoalkyl, e) Glutathione and f) Hydrazide Activated Agarose

The immobilisation support is usually agarose based but many different coupling chemistries have been used for antibody attachment to the solid phase. The agarose based solid support provides hydroxyl groups which are functionalised to become reactive with the amino acid residues on the antibody. The antibody can also be functionalised often by oxidation of vicinal diol groups on the carbohydrate residues (figure 15)[64-67].

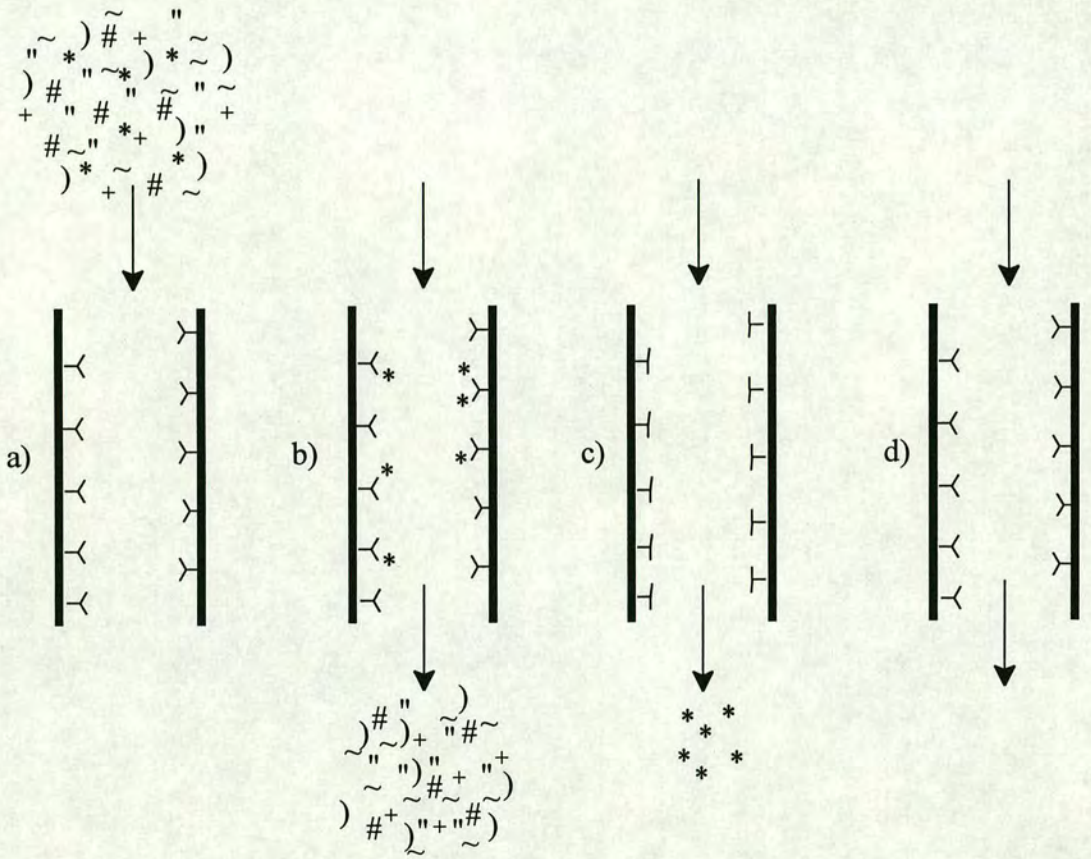

Figure 16: Immunoaffinity Chromatography Stages: a) Loading, b) Washing, c) Eluting and d) Regenerating

The principal stages involved in immunoaffinity chromatography are:

1) Loading: the crude sample is applied to the column and the desired product allowed to bind to the immobilised antibodies.

2) Washing: the column is washed to remove the contaminating impurities.

3) Eluting: the desired product is eluted from the column with a buffer that reduces the antibody affinity to the antigen.

4) Regeneration: the column is prepared for further use, removing the elution buffer by washing[64] (figure 16). The sample and washing buffers used are usually around physiological pH and salt concentration. However, many different eluting conditions have been used. After removal of any contaminating substances the desired product must be desorbed. This must break the antibody-antigen interactions but leave the antibody sufficiently intact to enable reuse of the column. Elution buffers can reduce the antigen-antibody interactions by a number of different mechanisms:

1) Antibody denaturing: high concentrations of guanidine.HCl or urea or extremes of pH will denature antibodies.

2) Disruption of hydrogen bonding and coulombic interactions: chaotrophic ions disrupt hydrogen bonds. They can be arranged in order of chaotrophicity: $Cl^- < I^- < ClO_4^- < CF_3CO_2^- < SCN^- < CCl_3CO_2^-$.

3) Disruption of hydrophobic interactions: organic solvents such as acetonitrile, methanol, ethanol, dioxane and ethylene glycol have been used in aqueous solutions to reduce buffer polarity and hence hydrophobic interactions.

Immunoaffinity chromatography has been widely used for the successful isolation and concentration of many biological materials such as proteins, peptides, nucleic acids, cofactors, steroids, hormones and cells.

Antibodies to Carcinogen-DNA Adducts

As antibodies had been successfully raised to naturally occurring nucleosides and nucleic acids[69] immunological methods have been employed in the detection and analysis of carcinogen-DNA adducts. Initially antibodies were raised to the bulkier DNA adducts such as N^2-[10-(7β,8α-trihydroxy-7,8,9,10-tetrahydrobenzo[a]pyrene)yl]dG (figure 17a), 2-(7-dG)-2,3-dihydro-3-hydroxyalfatoxin B_1 (figure 17b) and 3-[*N*-(dG-N^2-yl)]acetamidofluorene (figure 17c). The antibodies were used in immunoassays for the detection and quantification of small amounts of DNA components modified by carcinogens[70].

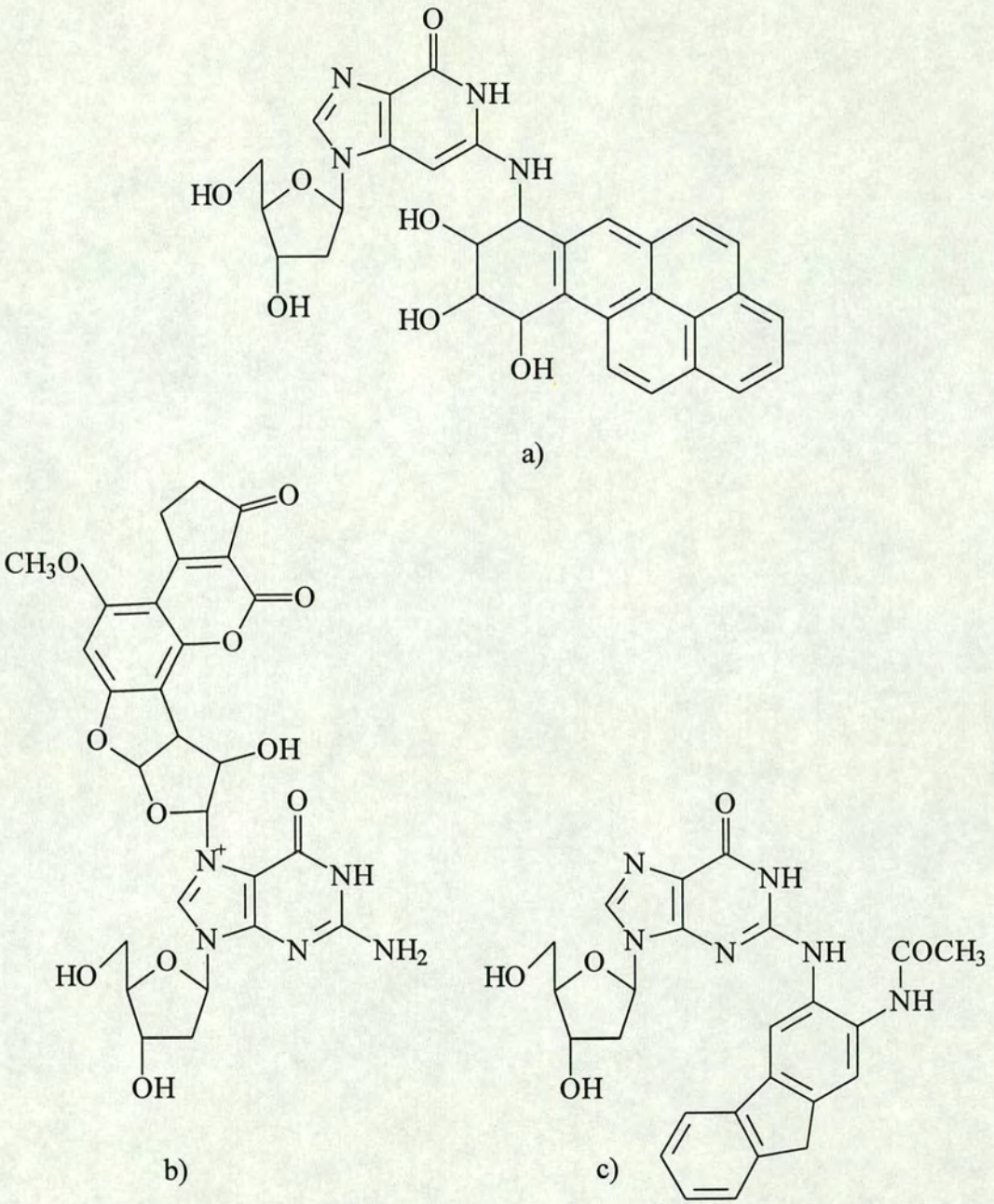

Figure 17: Bulky DNA Adducts

Later it was found that nucleosides structurally altered with even very small alkyl modifications such as methyl (figure 18a) or ethyl (figure 18b) groups could be recognised by antibodies even in the presence of large excesses of unmodified nucleosides[71]. These antibodies have been used to detect carcinogen-DNA adducts directly using immunological techniques such as radioimmunoassay (RIA),

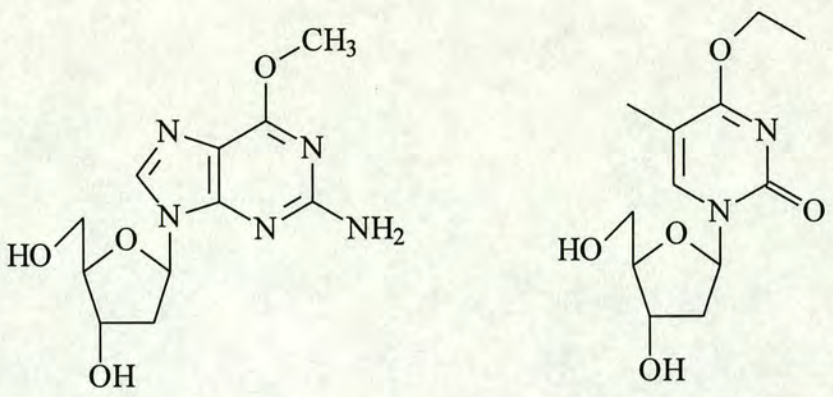

a) b)

Figure 18: Small DNA Adducts

enzyme linked immunosorbent assay (ELISA), immunoslot-blots and immunoelectromicroscopy or to clean-up and concentrate carcinogen-DNA adduct samples prior to analysis[71]. Detection limits vary but it has been possible to detect as little as attomole concentrations of carcinogen-DNA adducts[72].

Biomonitoring of Etheno Adduct Levels

In model studies exposing rats to vinyl chloride, tumour incidence correlated well with etheno adduct level[73]. Methods of etheno adduct detection have been investigated to effectively monitor the formation of these adducts in biological samples. This could facilitate the creation of effective risk assessment models for human exposure to the chemicals that induce these adducts and the potential for carcinogenesis. Due to the extremely low levels of DNA adducts present *in vivo*, highly sensitive analytical techniques must be employed.

Many methods to achieve effective biomonitoring have been reported with varying degrees of sensitivity of adduct detection. Initially rats were exposed to [1,2-^{14}C] labelled vinyl chloride. The liver DNA was extracted, enzymatically hydrolysed and the adducts separated by HPLC before scintillation counting to quantify the adduct levels[73]. The fluorescent properties of the etheno bases especially εA and εG have been used in on-line fluorescent detection of HPLC eluents[74]. The sensitivity of detection using this method was highest for εA, detecting levels of 1 picomole. Higher detection limits of 0.1 picomole[75] were obtained using a two step HPLC purification and ^{32}P postlabelling system. Monoclonal antibodies have been raised to both εA and εC. Significant levels of cross-reactivity to other etheno adducts and unmodified

nucleosides was reported. The antibodies were used to detect these adducts with sensitivities of 980 femtomoles and 800 femtomoles respectively using competitive ELISA[76]. More specific monoclonal antibodies to εA and εC have been raised and were used in competitive RIA with a detection sensitivity of 187 femtomoles for both adducts[77]. These antibodies have also been used to detect etheno adducts in DNA hydrolysates from the liver, lung and brain of rats exposed to vinyl chloride. After HPLC purification the molar ratios detected were 0.6×10^{-7} to 1.3×10^{-7} for εA/dA and 1.95×10^{-7} to 4.92×10^{-7} for εC/dC[78]. The levels of all the vinyl chloride induced adducts were measured in DNA hydrolysates from the liver, lung and kidney of rats exposed to vinyl chloride. oeG was measured by on line fluorescence HPLC, εG by isotope dilution mass spectrometry using [$^{13}C_4$] εG as an internal standard and εA and εC by HPLC followed by competitive RIA. The same spectrum of adducts was found in all three organs with oeG representing 98% of all adducts. Levels of εC and εG each accounted for 1% of the total adduct number of adducts while εA was present at lower concentrations[79]. Monoclonal antibodies to εC and εA have also been used in immunoaffinity chromatography to isolate and concentrate these adducts in the presence of other nucleotides. Used in conjunction with ^{32}P post labelling the detection limits for this system were 50 attomoles of each etheno adduct[80] or 4 etheno adducts *per* 10^9 parent deoxynucleotides[75]. This technique has also been used to analyse liver DNA from untreated rats with detection limits of 0.5×10^{-9} etheno adducts *per* parent deoxynucleotides[81]. This study found low but unspecified concentrations of both εA and εC in these tissues indicating endogenous production of these adducts.

AIMS OF THE PROJECT

Quantitative determination of DNA adducts is essential for effective assessment of the risks associated with exposure to chemical carcinogens. DNA adducts are present at levels below one adduct in 10^7 nucleotides. Selective enrichment of adducts from the biological milieu is required to facilitate their detection at these low abundances.

The primary aim of this project is to develop a system to enrich and quantify low levels of εC from the large excesses of nucleotides present in biological samples using immunochemical methods.

The mutagenic properties of εC have been described. However, the molecular basis of this mutagenicity is not understood. The secondary aim of this project is to investigate the base-pairing properties of εC by thermodynamic and structural methods to rationalise the mutagenicity of εC.

RESULTS AND DISCUSSION

Preparation of εC Conjugated Protein

Nucleic acids are natural products common to all cells and as such have low immunogenic potential. To induce the immune system into producing an immune response to nucleic acids researchers have covalently and electrostatically bound them to carrier proteins[82,83]. Nucleosides also require protein conjugation as they escape detection by the immune system due to their small size. Numerous methods have been employed to bind nucleosides to carrier proteins. This involves the introduction of a reactive functionality onto the nucleoside which is capable of reacting with amino acid residues on the protein[84].

Previous work to produce monoclonal antibodies to etheno adducts[76,77] used the ribose sugar analogue of εC for protein conjugation (figure 19). The vicinal diol group was oxidised with periodate to open the sugar ring to form aldehyde groups. These react with lysine residues on the protein and the resulting aldimine system is stabilised by reduction with borohydride to form a morpholino ring system.

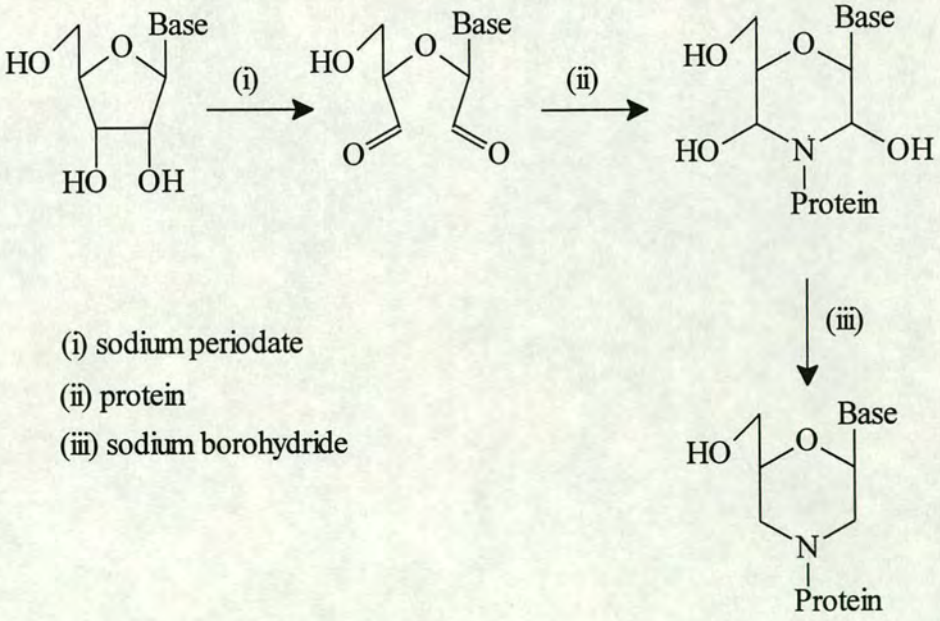

Figure 19: Protein Conjugation to a Nucleic Acid Riboside

A different approach was used in our work. A spacer arm with a carboxy terminus was introduced onto the 3'-hydroxyl group of deoxyribose εC. The

carboxylic acid moiety was then the point of reaction for subsequent amide bond formation with lysine residues on the carrier protein. This method is advantageous as it preserves the deoxyribose ring and thus the immunogenic determinant is more closely related to the antigen. In addition, previous research into immunogenic carrier protein conjugates found that antibodies of greater antigenic specificity are produced when the antigen is located distally from the carrier protein by the introduction of a spacer arm[85].

The preparation of the εC conjugated protein involved a five step synthesis (figure 20). εC was synthesised by a procedure modified from that of Srivastava *et al*[86]. Bromoacetaldehyde buffered to pH 4.5 was added to a similarly buffered solution of dC as the reaction is kinetically favoured at this pH. Before functionalisation of the 3' hydroxyl group the 5' hydroxyl was selectively protected by addition of a 4,4'-*O*-dimethoxytrityl functionality by the method of Srivastava *et al*[86]. Succinic anhydride was used to introduce a five bond spacer arm with a carboxy terminus onto the 3' ribose sugar position. The labile dimethoxytrityl group was removed on addition of mild acid and due to the resulting high hydrophilicity the product was purified by reverse phase HPLC. Conjugation to the carrier protein was achieved *via* an activated ester of the carboxyl group formed by addition of a carbodiimide in the presence of the protein. Two protein conjugates were prepared from the proteins bovine serum albumin (BSA) and chicken gamma globulin (CγG).

The proteins were examined for εC conjugation by analysis of the UV absorbances of free protein, protein conjugate and εC in the region of 240 to 300nm. Comparison of the profiles revealed significant "εC-like" absorbance in the protein conjugates (figure 21a and figure 21b). The εC conjugated BSA was characterised further by determining the number of εC residues *per* protein molecule using the method of Habeeb[87]. This technique labels free primary amino groups with trinitrobenzene sulphonic acid. Free lysine residues on the free protein and conjugate were labelled in this way and their numbers estimated spectrophotometrically by their absorbtion at 335nm. The free protein was calculated to bear 60 surface lysine residues which is in close agreement to the 61 reported by Habeeb.

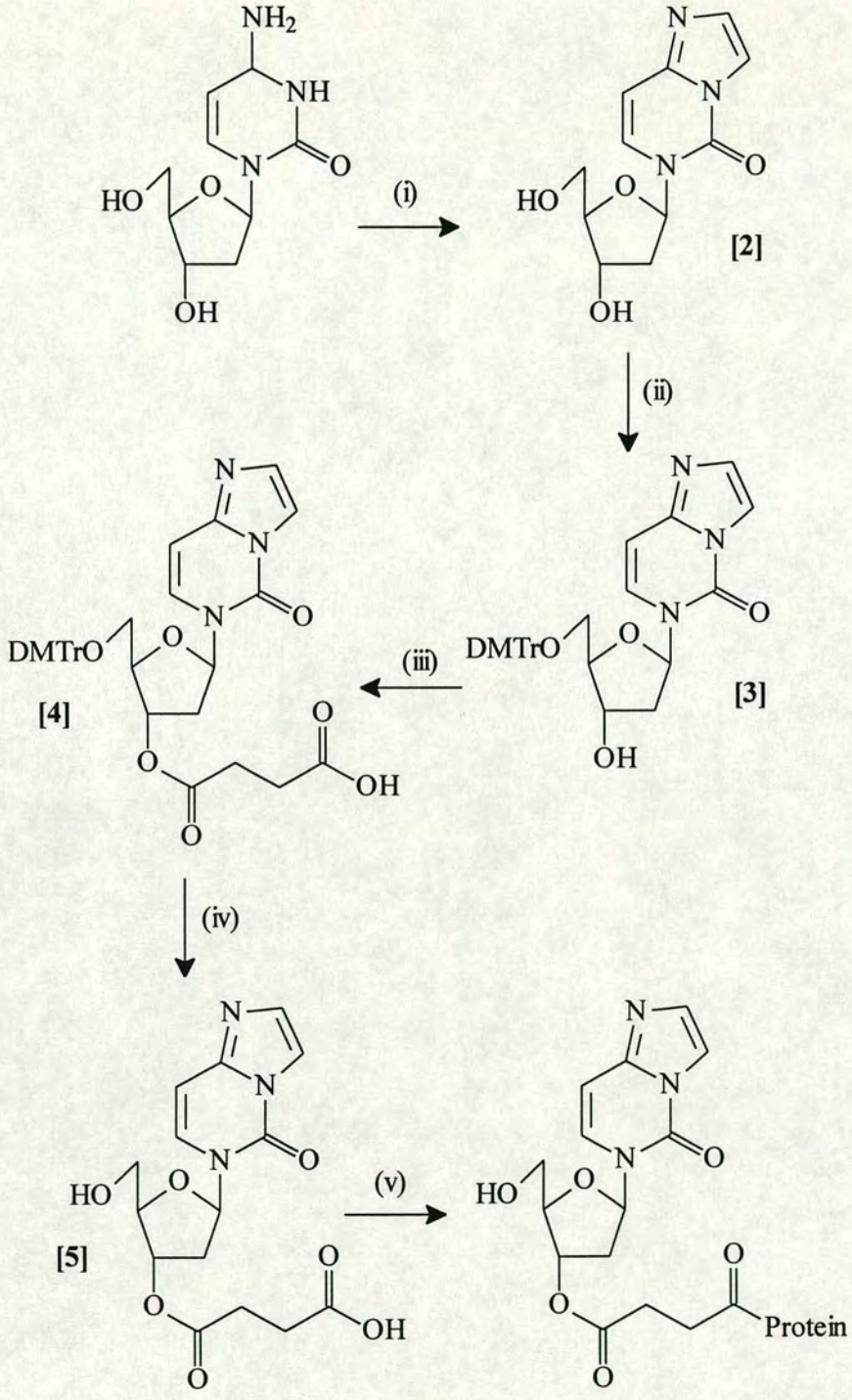

(i) bromoacetaldehyde
(ii) dimethoxytrityl chloride
(iii) succinic anhydride
(iv) HCl
(v) ethyl(dimethylaminopropyl) carbodiimide and protein

Figure 20: The Conjugation of εC to Proteins

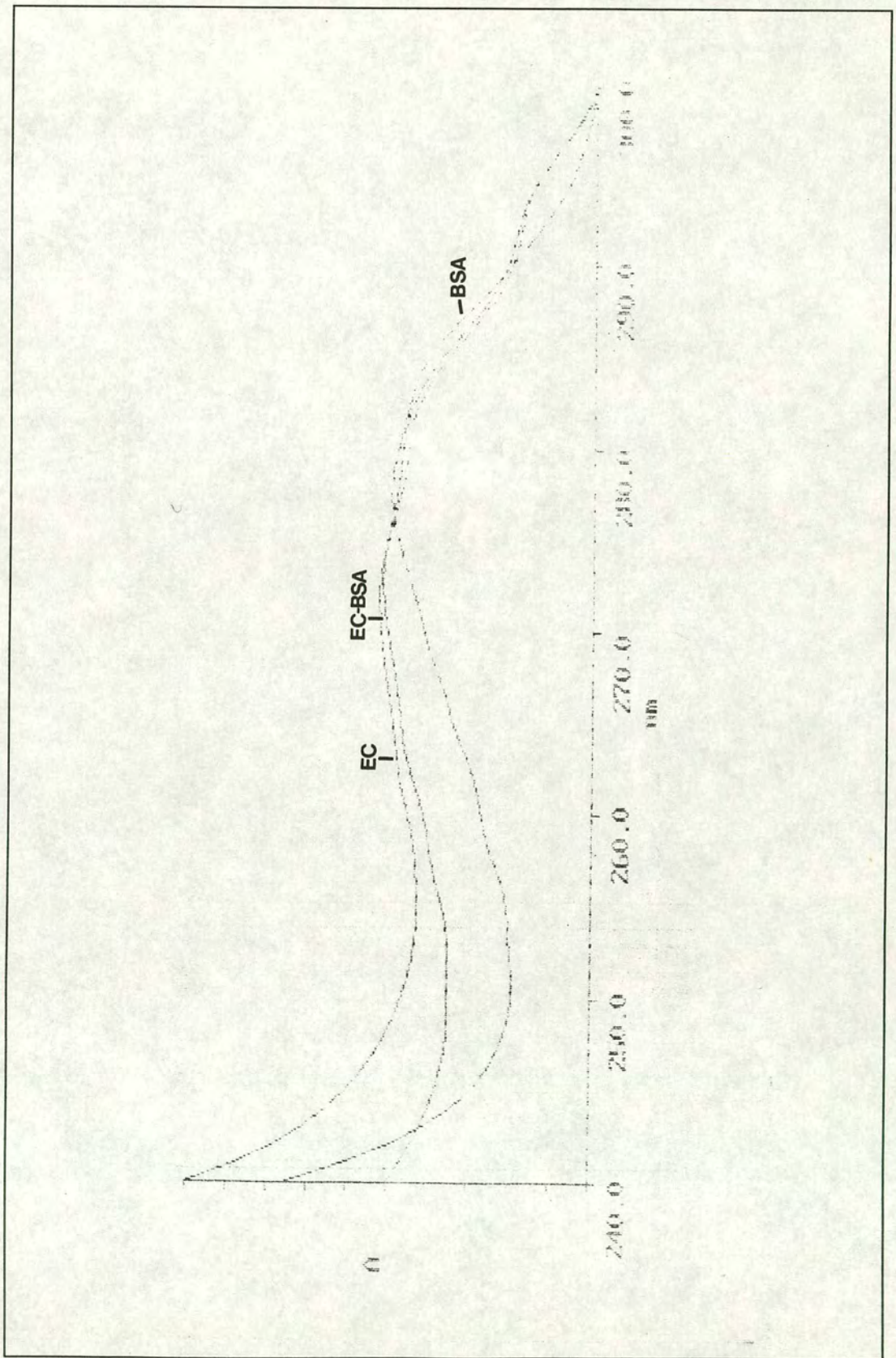

Figure 21a: UV Scans of εC, BSA and εC Conjugated to BSA

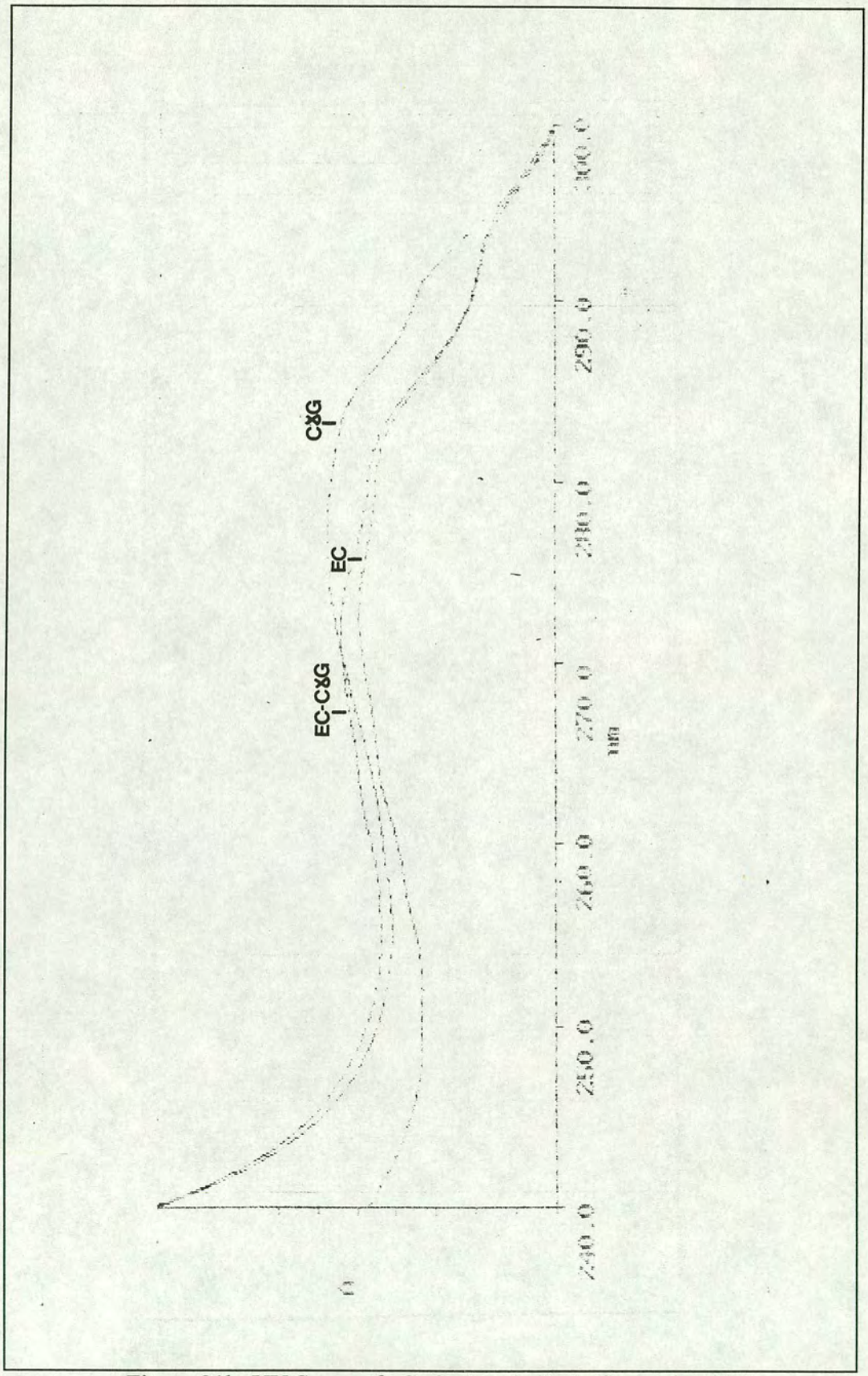

Figure 21b: UV Scans of εC, CγG and εC Conjugated to CγG

The εC conjugated BSA was calculated to have 35 free lysines. The average ratio of εC to carrier protein was therefore approximately 25:1.

The conjugates were sent to Shell Research Ltd. laboratories for the production of anti-εC monoclonal antibody secreting cell lines. The εC conjugated BSA was used in murine immunisations and the εC conjugated CγG was used to screen and select the resulting hybridoma cell lines and also in subsequent antibody characterisation. The methods and procedures used were similar to those outlined in Chapter 2.

Initial Characterisation of the Antibody Secreting Cell Line

Two mice were immunised at Shell. Preliminary experiments examined the most promising hybridoma cell line for reactivity to εC. The dot-blot method of analysis was used.

Oligonucleotides bearing site specific εC residues (Oligos A and B) as well as an unmodified oligonucleotide (Oligo C) were synthesised by automated solid phase DNA synthesis using phosphoramidite chemistry (table 1). The εC nucleoside was

Oligonucleotide	Sequence
Oligo A	TCT TAG CAG εCTC ATG ATC TG
Oligo B	εCCT TAG CAG CTC ATG ATC TG
Oligo C	TCT TAG CAG CTC ATG ATC TG

Table 1

prepared by the method of Srivastava *et al*[86] with the addition of dimethoxytrityl onto the 5' hydroxyl and a phosphoramidite group onto the 3' hydroxyl positions (figure 22).

It has been reported that the εA ring opens at the C^2 position of the pyrimidine heterocycle when exposed to aqueous base[87] (figure 23). This has consequences in automated DNA synthesis as the final deprotection and resin cleavage step uses concentrated ammonia at 60°C. In order to determine whether the structurally similar ring system in εC undergoes this reaction εC was subjected to concentrated ammonia at 70°C for 16 hours.

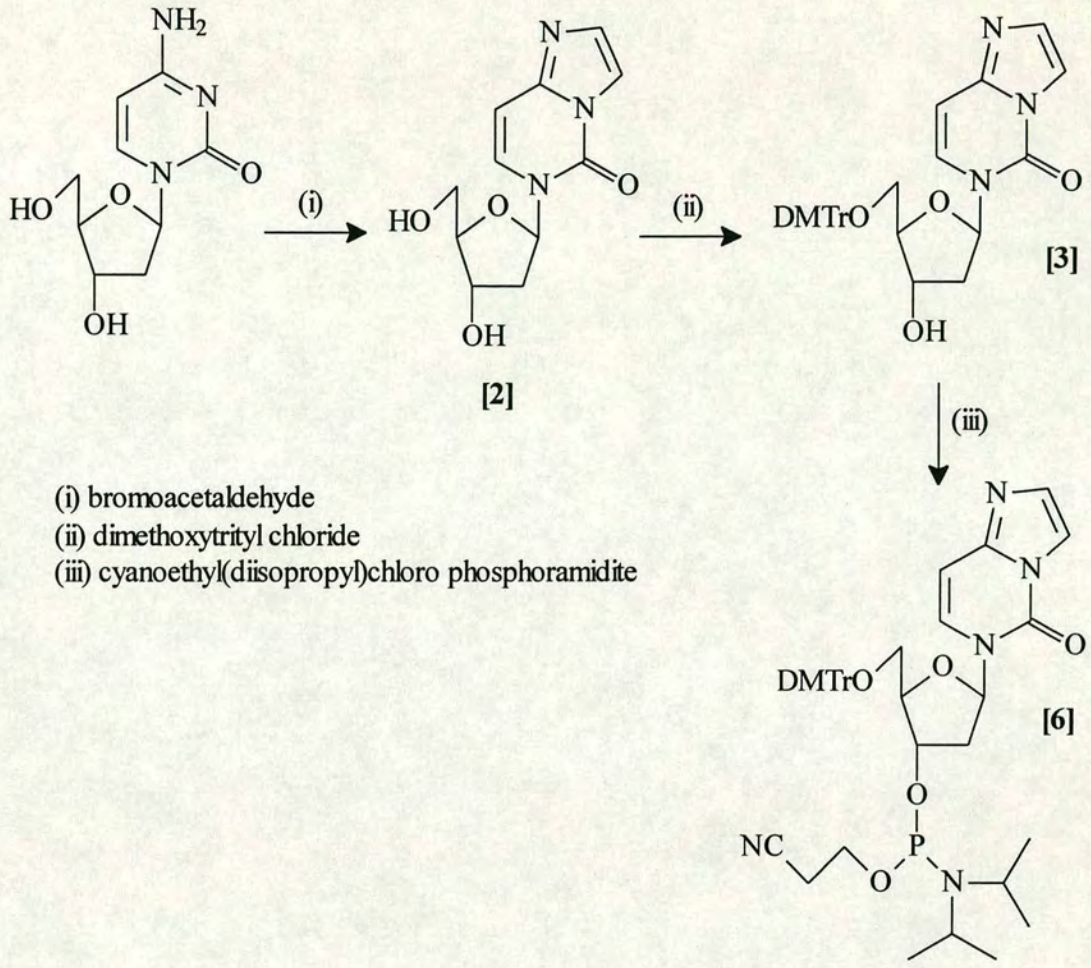

Figure 22: The Synthesis of εC Phosphoramidite

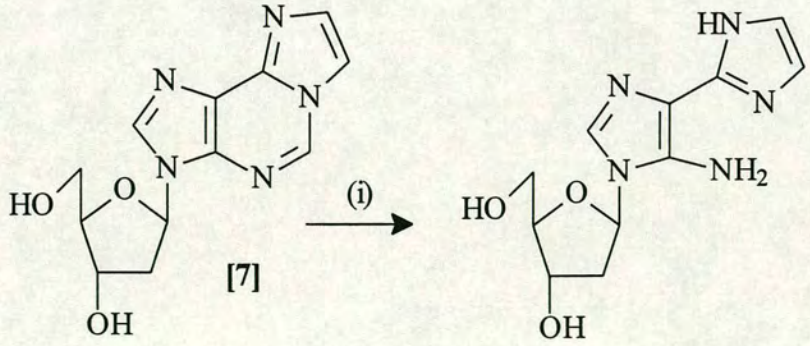

(i) NaOH

Figure 23: The Reaction of εA with Nucleophilic Base

^{1}H NMR and TLC revealed that εC was stable under these conditions. After DNA synthesis the oligonucleotides were purified by reverse phase HPLC. The base

composition was confirmed by digesting small quantities of the oligonucleotides to produce nucleosides using the enzymes snake venom phosphodiesterase II and alkaline phosphatase. The enzyme digests were analysed by reverse phase HPLC (figure 24) and the εC peak identified by coinjection of an εC standard.

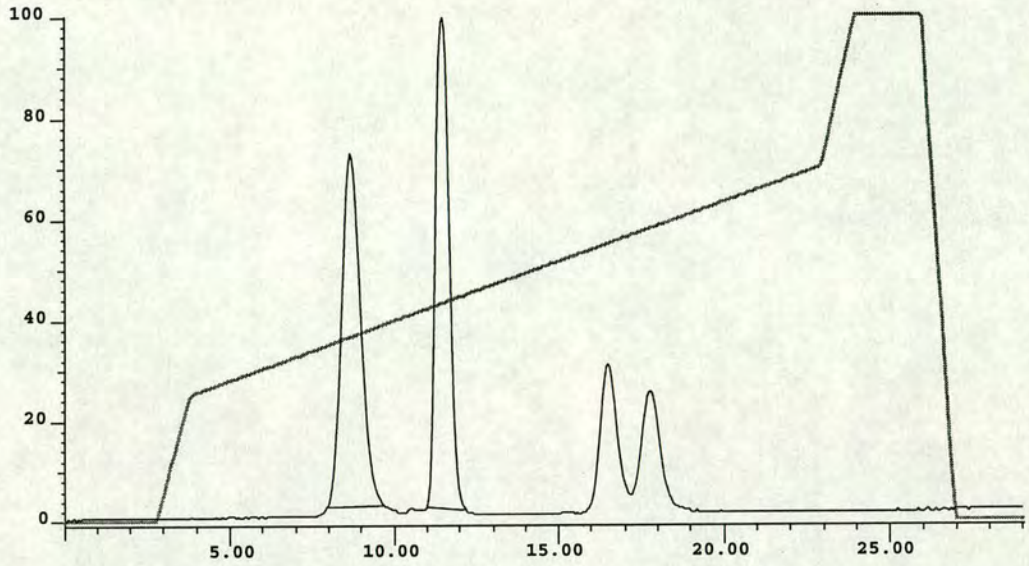

Figure 24: Enzyme digest

The oligonucleotides were applied in known concentrations to nylon membranes and covalently fixed by UV irradiation. The membranes were soaked in undiluted hybridoma culture medium and antibodies binding to the membrane were detected by anti-mouse immunoglobulin HRP conjugate and DAB (figure 25). Antibodies binding to the membrane were visualised in the regions fixed with Oligos A and B down to a lower concentration of 500 attomoles. No binding to Oligo C was detected at an upper concentration of 50 picomoles. It was concluded that the difference in antibody binding shown between Oligos A and B was due to the increased steric hindrance encountered by the antibody binding site to a centrally positioned εC. No such steric hindrance is encountered at the 5' end of the oligonucleotide.

The level of sensitivity exhibited by the antibody in this preliminary dot-blot examination indicated an antibody of high selectivity and affinity to εC and the characterisation of this hybridoma cell line was continued.

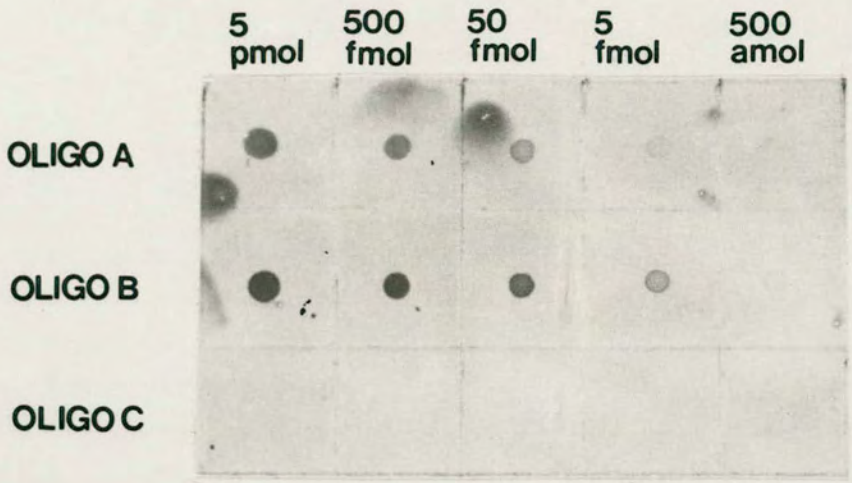

Figure 25: Comparison of Immunoreactivity of Oligo A, Oligo B and Oligo C

Antibody Purification

The cell line was cultured to produce large volumes of cell culture medium. This was partially purified and concentrated by salt fractionation, taking a 50% ammonium sulphate cut which precipitated the antibody along with other proteins. This was purified further by one of the following methods:

1) anion exchange HPLC,

2) strong cation exchange HPLC,

3) Protein-A affinity chromatography.

The purification efficiency of each method was compared in terms of protein yield but most critically in terms of purity and titre using the same sample of cell culture medium (table 2). The yield was determined spectrophotometrically assuming that an antibody solution of $1mg.ml^{-1}$ absorbs 1.4 OD at 280nm. This "rule of thumb" was used throughout to calculate the concentration of antibody solutions. The purity of antibody solutions was determined by analytical SDS-PAGE.

Method	Yield μg protein/ml culture medium	Purity	Titre
Anion Excange HPLC	23	unpure	1/3500
Cation Exchange HPLC	26	unpure	1/3000
Protein-A Affinity Chromatography	17	pure	1/9000

Table 2

Gels were run under reducing conditions with β-mercaptoethanol which cleaves disulphide bonds. This breaks interpeptide bonds within antibodies. The molecule was therefore visualised as two distinct bands. One band at approximately 49,000 Daltons and the other at 25,000 Daltons corresponding to the heavy and light chains respectively (figure 26). Antibody titre was determined using ELISA by titrating dilutions from $1mg.ml^{-1}$ of antibody using plates coated with εC conjugated to CγG. This provided a measure of antibody activity (figure 27).

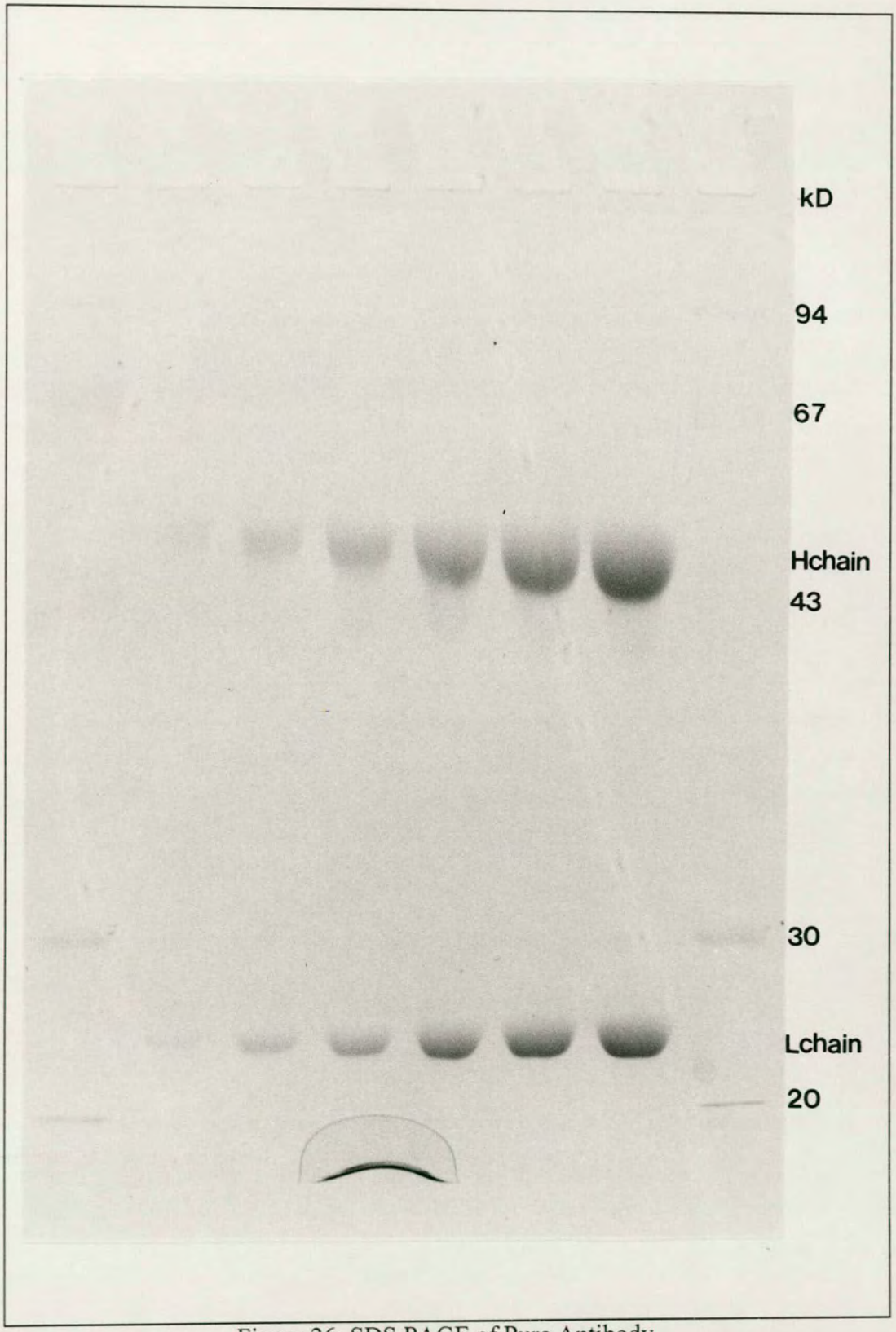

Figure 26: SDS PAGE of Pure Antibody

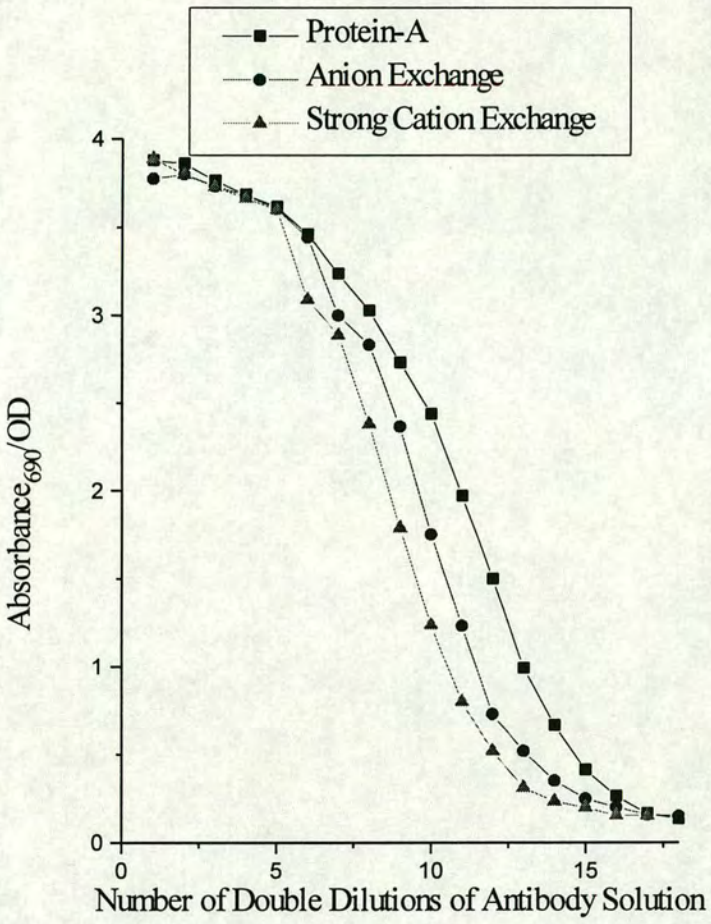

Figure 27: Comparison of Antibody Purification Methods

Protein-A affinity chromatography proved to be the best purification technique. Protein-A is a protein isolated from the cell wall of the bacterial strain, *Staphlococcus aureus*[88]. It selectively binds antibody molecules at the Fc region. This method provided pure antibody of high titre. The ion exchange HPLC methods provided large amounts of protein but this was of a heterogeneous nature and these antibody samples were also less active.

Antibody samples were stored at 4°C or -20°C with no obvious deterioration in performance. Samples were also freeze dried but this proved counter productive as the protein was insoluble on attempted rehydration.

Antibody Characterisation

Subsequent to obtaining large amounts of pure protein the antibody characterisation was continued to determine whether it would be suitable for an immunoaffinity chromatography application. The following criteria were used:

1) antibody isotype,

2) reactivity to εC,

3) affinity to εC,

4) cross-reactivity with normal nucleosides,

5) cross-reactivity with other vinyl chloride induced DNA adducts.

1) Antibody Isotype: The antibody isotype was established using an antibody isotyping kit with class and subclass specific anti-mouse immunoglobulin HRP conjugates in an ELISA. The antibody was found to be of the IgG isotype and subclass 2b.

2) Reactivity to εC: εC and Oligos A and B were tested in competitive ELISA to determine their ability to inhibit antibody binding to plates coated with εC conjugated CγG. All three compounds inhibited antibody binding (figure 28) and IC_{50} values were calculated (table 3).

Inhibitor	**IC_{50}/nM**
εC	3
Oligo A	50
Oligo B	7

Table 3

Differences in antibody reactivity between the three compounds can be correlated with antigen availability to the antibody binding site. The antigen in Oligo A due to central positioning in the oligonucleotide is the most sterically inhibited followed by Oligo B and then εC.

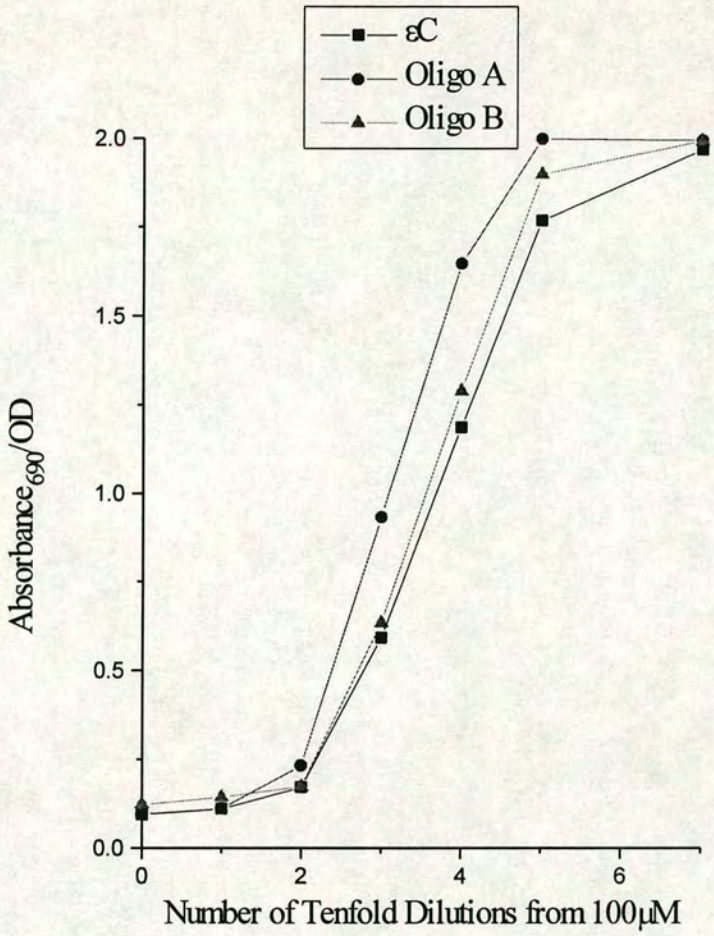

Figure 28: Comparison of the Immunoreactivities of εC, Oligo A and Oligo B

3) Affinity to εC: To obtain a more accurate measure of antibody affinity, known quantities of labelled εC were titrated by ELISA on antibody coated plates in a Scatchard experiment[89]. Scatchard analysis utilises the equation:

$$[Ab_b]/[Ab_f] = K_a[Ag_t] - K_a[Ab_b]$$

where: Ab_b is the concentration of antibody binding antigen,

Ab_f is the concentration of antibody not binding antigen,

K_a is the antibody affinity,

Ag_t is the total concentration of antigen.

Plotting $[Ab_b]/[Ab_f]$ against $[Ab_b]$ gives a straight line of gradient $-K_a$ and intercept Ag_t and so if $[Ab_b]$ and $[Ab_f]$ are known K_a can be experimentally determined.

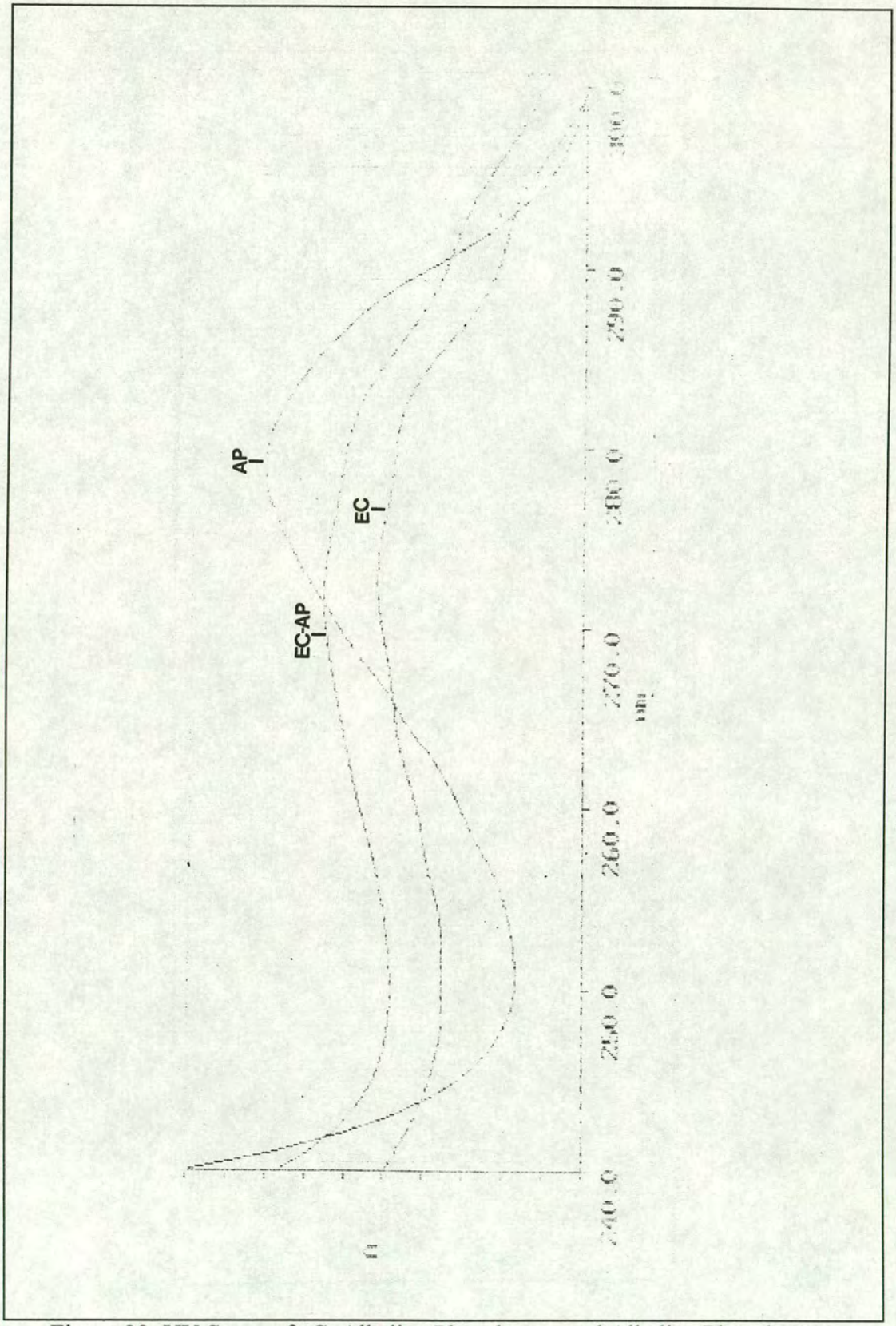

Figure 29: UV Scans of εC, Alkaline Phosphatase and Alkaline Phosphatase Labelled εC

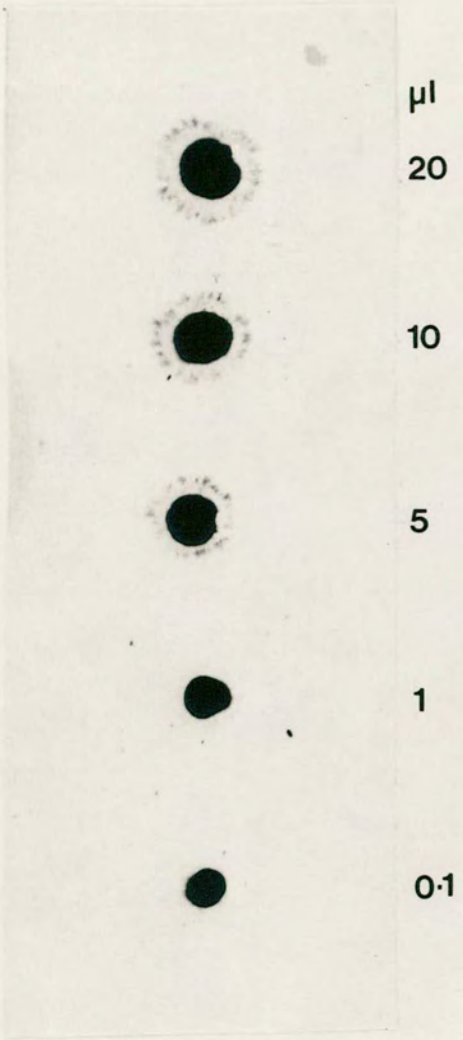

Figure 30: Dot Blot of Immunoreactivity of Alkaline Phosphatase Labelled εC

The antibody was used in the solid phase to simulate the conditions encountered in immunoaffinity chromatography. εC was labelled with the enzyme, alkaline phosphatase. The labelling procedure was similar to that used to prepare the εC conjugated BSA. The reaction time was shortened to 10 minutes to ensure low conjugation levels and to preserve the enzyme activity. Successful conjugation was determined by examination of the respective UV scans of εC, alkaline phosphatase and the reaction product (figure 29). Dot-blots showing strong positive signals were also obtained when the alkaline phosphatase labelled with εC was fixed to nitrocellulose membrane and incubated with the antibody and anti-mouse immunoglobulin HRP conjugate and DAB (figure 30).

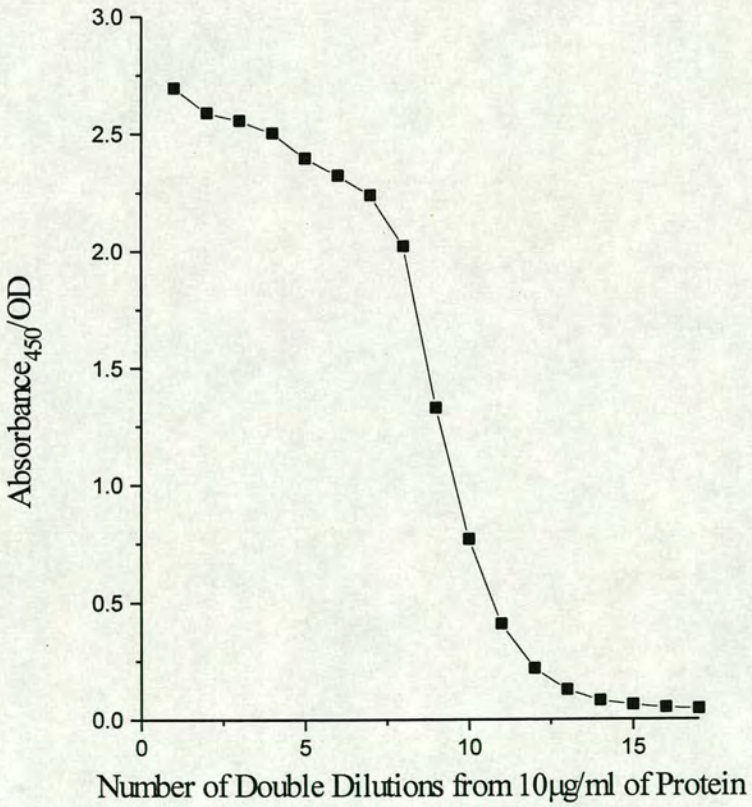

Figure 31: Titration of Alkaline Phosphatase Labelled εC

The alkaline phosphatase labelled εC was titrated on antibody coated plates (figure 31). The concentrations that gave the linear response in the curve were used in the Scatchard experiment. These concentrations were determined in terms of the protein rather than the antigen as it was assumed that the size of an alkaline phosphatase molecule (140,000 Daltons) would preclude multiple antigen binding to one antibody. The titration was repeated using these concentrations alongside standards of these concentrations. This gave readings for the concentration of antigen bound and the total concentration of antigen. The Scatchard calculation gave a plot indicating an antibody affinity of $1.8 \times 10^8\ M^{-1}$ in the solid phase (figure 32).

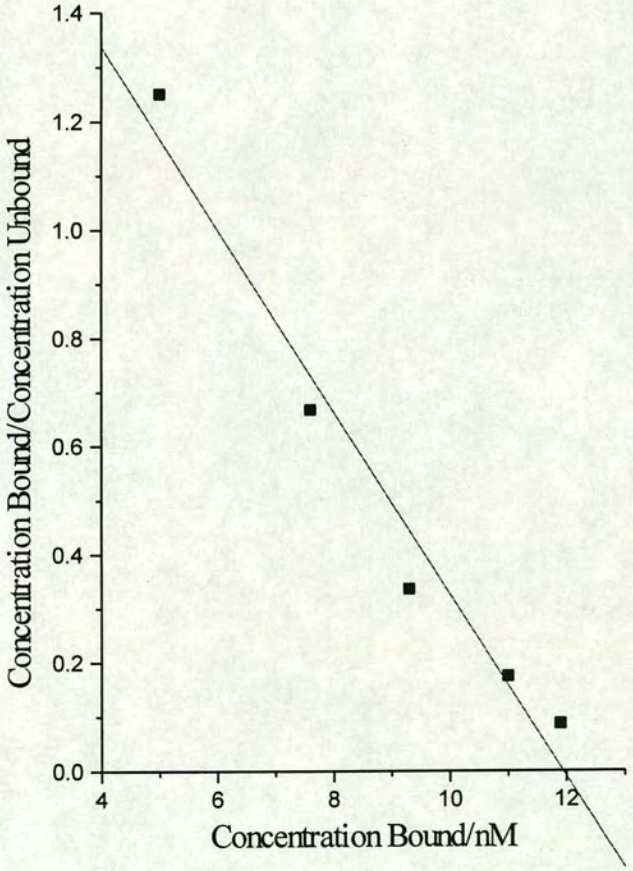

Figure 32: Scatchard Plot

4) Cross-reactivity with Normal Nucleosides: The nucleosides: dA, dC, dG, T and U were tested as inhibitors to antibody binding in competitive ELISA (table 4). The

Inhibitor	Upper Concentration Used/mM	% Inhibition
dA	4.3	0
dC	19.9	0
dG	2.3	0
T	14.7	13
U	50.0	40

Table 4

antibody was found to be completely unreactive to dA, dC and dG upto the limits of compound solubility. T and U were found to exhibit some antibody binding at just below saturation concentrations. This slight cross-reactivity of the antibody between the compounds εC, T and U can be rationalised by examination of their structures (figure 33). All three bear similarities in size, shape and electrostatic charge distribution. All have pyrimidine heterocycles with trigonally coordinated nitrogens at the N^1 and N^3 positions and a C^5 to C^6 double bond. The ring systems are also substituted at the C^2 and C^4 positions by double bonds to heteroatoms.

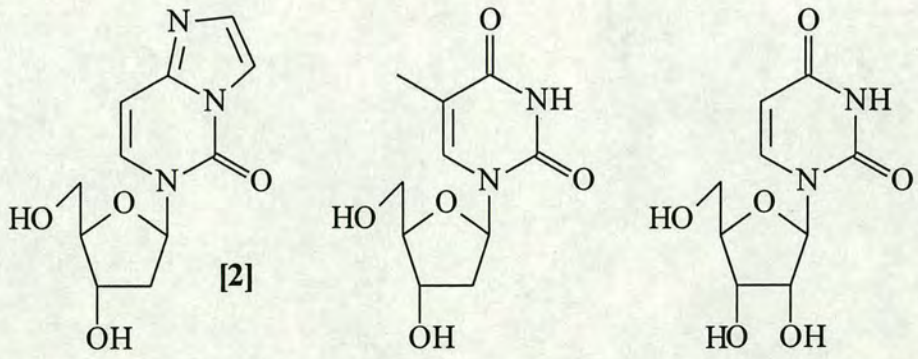

Figure 33: The Structural and Electrostatic Similarities of a) εC, b) T and c) U

5) Cross-reactivity with Other Vinyl Chloride Induced Adducts: The antibody was also examined for any class specific properties which would enable it to bind other vinyl chloride induced DNA adducts. The nucleosides, εA, εG_2, and an analogue of oeG plus the imidazole ring opened form were synthesised.

εA was synthesised from dA by a method modified from the procedure of Srivastava *et al*[86] using bromoacetaldehyde (figure 34) As with the synthesis of εC the reaction was buffered to pH 4.5. This is the pH where the reaction proceeds most quickly. However, it was imperative that the pH remain above 4.0 as the starting material and particularly the product can depurinate in strongly acidic conditions.

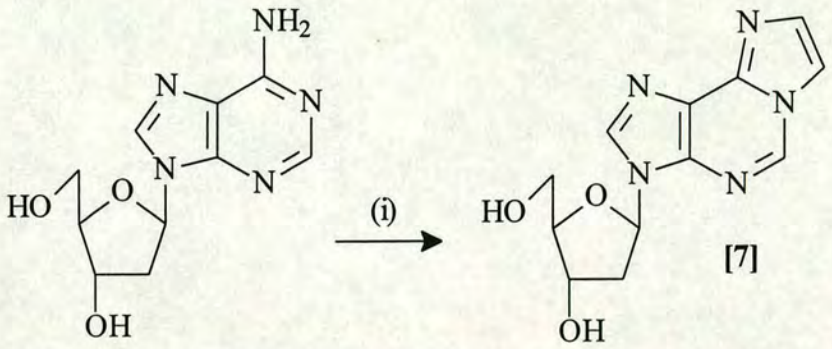

(i) bromoacetaldehyde

Figure 34: The Synthesis of εA

εG_2 was synthesised from G in three steps by a method modified from the procedure of Boryski[90] (figure 35). Here guanosine was used as the starting material as the ribose sugar is less susceptible to depurination relative to the deoxyribose sugar[91]. To increase the solubility of guanosine in organic solvents it was selectively protected at the 3' and 5' ribose hydroxyls to give a cyclic silyl derivative. This was alkylated at the N^1 position with bromoacetaldehyde diethylacetal. Subsequent imidazole ring closure was achieved upon the addition of methanolic acid which also freed the 3' and 5' ribose hydroxyls.

The synthesis of oeG required CEO which was commercially unavailable and required specialised equipment to prepare. Therefore a structurally similar analogue, 2-amino-6-oxo-N^7-ethoxy-3-β-D-ribofuranosyl purine (alkG) was synthesised by the method of Roe *et al*[92] (figure 36). dG alkylated at the N^7 postion is known to open the imidazole ring under physiological conditions[93] (although an imidazole ring opened adduct has never been identified as the result of reaction with CEO *in vivo* or

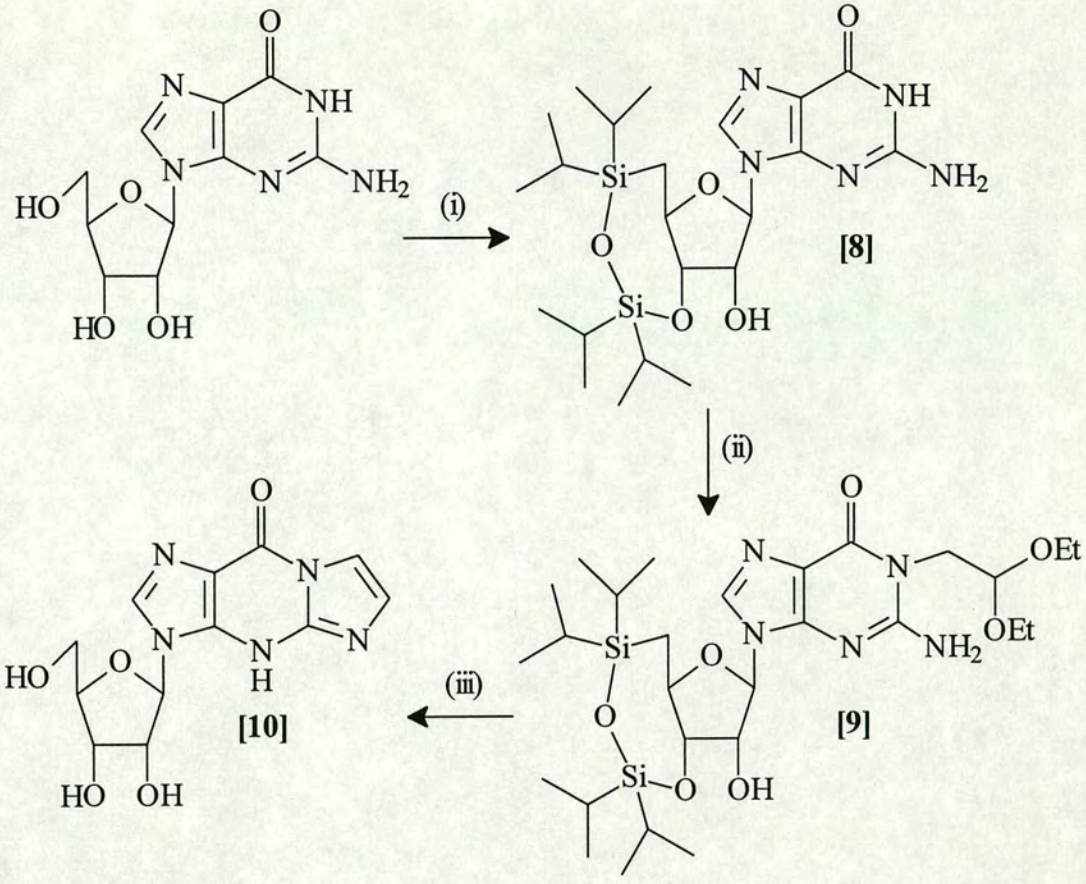

(i) tetraisopropyldisiloxy chloride
(ii) bromoacetaldehyde diethyl acetal
(iii) HCl

Figure 35: The Synthesis of εG_2

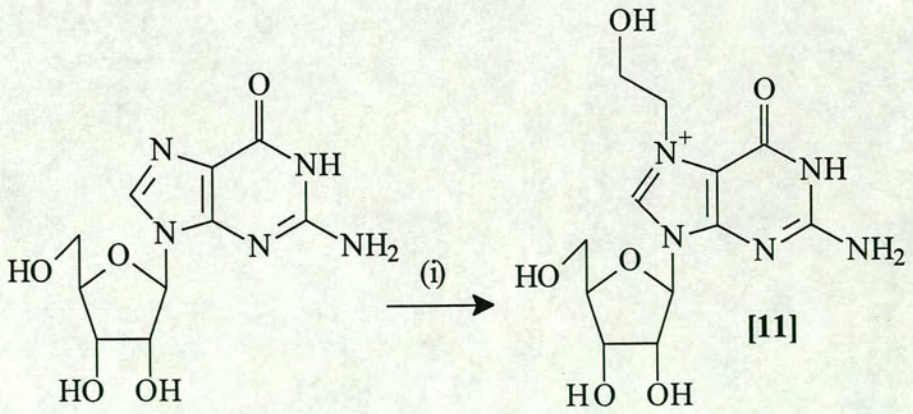

(i) ethylene oxide

Figure 36: The Synthesis of alkG

in vitro). The ring opened compound (roalkG) was synthesised by addition of nucleophilic base (figure 37).

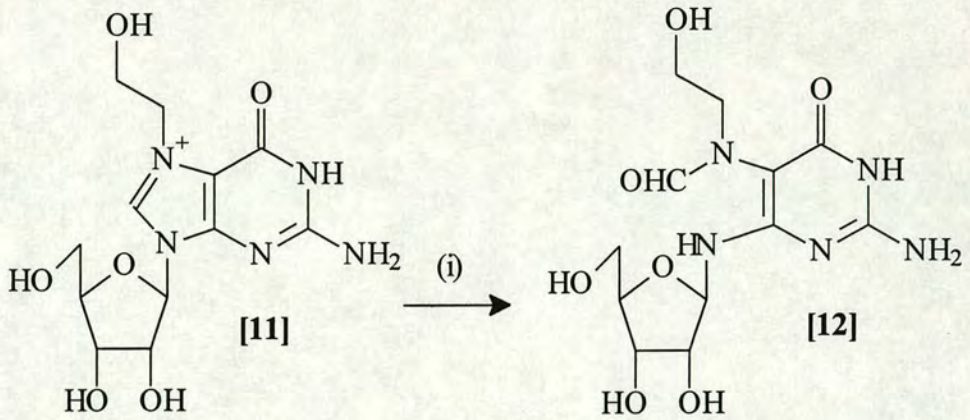

(i) NH_4OH

Figure 37: The Synthesis of roalkG

The antibody was unreactive in competitive ELISA experiments to all of the compounds synthesised even at saturation levels (table 5). This was slightly surprising as εA and εG_2 were predicted to show some reactivity due to close similarities to εC in structure and electrostatic charge distribution (figure 38). These compounds all bear the same imidazole ring and in εC and εG_2 this is fused to a pyrimidine ring with an oxo substituent. The lack of cross-reactivity possibly indicates that the antibody binding site is too small to accommadate these bulkier DNA adducts although other properties of antibody binding such as dipole moments, hydrophobicity, polarity and H-bonding may account for this observation.

Inhibitor	Upper Concentration Used/mM	% Inhibition
εA	2	0
εG_2	2	0
alkG	48	0
roalkG	12	0

Table 5

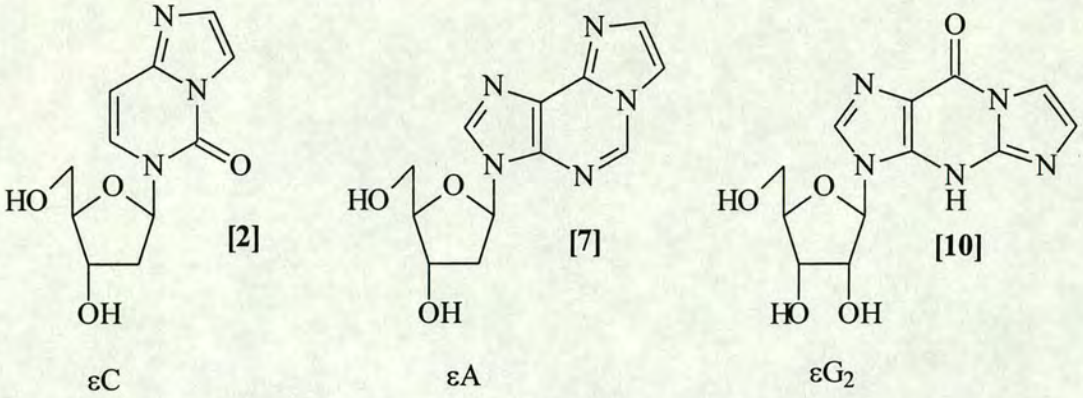

Figure 38: The Structural and Electrostatic Similarities of εC, εA and εG_2

Summary

The results indicate an antibody of high affinity to εC. This affinity is also maintained when the antibody is bound to a solid phase. This is crucial to the proposed utilisation of the antibody in an immunoaffinity column. The antibody was also found to be extremely specific for εC although binding to T was also observed at very high concentrations of that nucleoside. This low level of cross-reactivity does have serious implications for the purification of εC in the presence of large excesses of nucleotides. The results indicate that inhibition of εC binding by T will occur at greater than 20×10^6 fold excesses of nucleosides (assuming equimolar quantities of all four nucleosides). When attempting to purify low levels of εC from human cells which contain 3×10^9 nucleotides, serious problems of T inhibiting εC binding could be encountered. However, this problem cannot be readily circumvented as cross-reactivity between two similar compounds cannot be avoided.

Immunoaffinity Column Construction

The chemical methods used to covalently couple antibodies to a solid phase are dependent on the availability of sites on the antibody that can be alkylated. These electrophilic or nucleophilic centres can be protonated and their availability is therefore pH dependent. One property of a protein that indicates the propensity to protonation at a particular pH is the isoelectric point (pI).

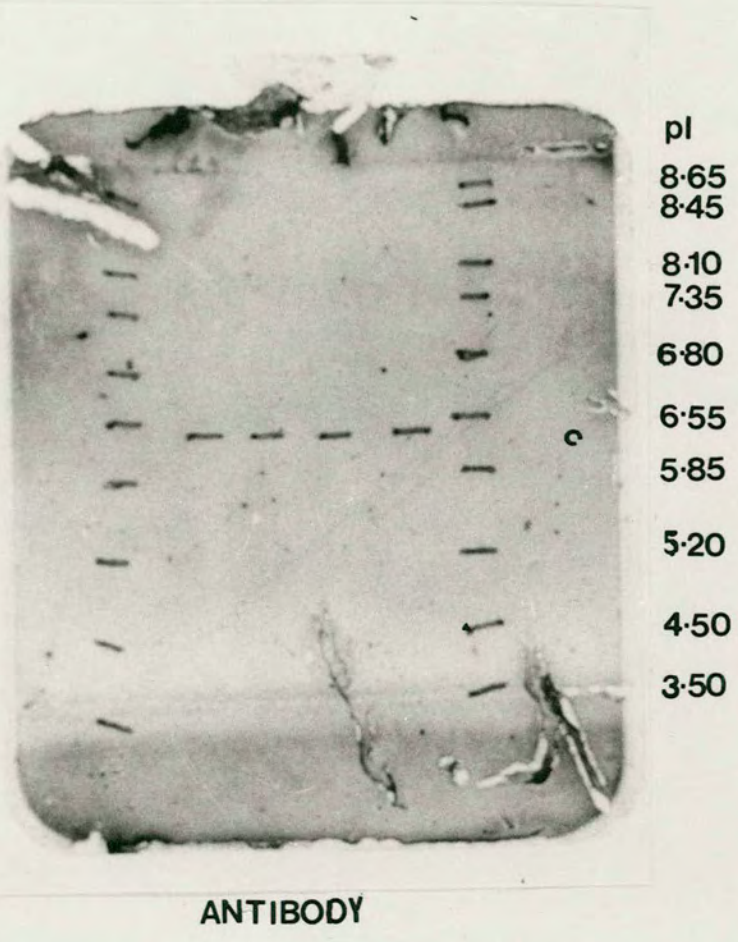

Figure 39: Isoelectric Focusing Gel

The pI of the antibody was determined by an isoelectric focusing gel to be in the range of pH 5.85 to 6.55 (figure 39). This indicates that within these pHs the antibody has zero overall electric charge but at higher pHs more acidic residues will become deprotonated and at lower pHs more basic residues will become protonated. Many common coupling chemistries use lysine residues as alkylation points and therefore solid phase antibody coupling using these methods is favoured at pHs above the pI.

The antibody proved to be very sensitive to covalent solid phase coupling and a number of different coupling chemistries were tried before a successful immunoaffinity column was produced (table 7).

Coupling Method	**Coupling Efficiency/%**	**Column Immunoreactivity**
CNBr agarose	89	inactive
Aldehyde agarose	72	inactive
Protein-A HiTrap	13	inactive
Protein-A agarose (method 1)	98	inactive
Protein-A agarose (method 2)	94	inactive
Hydrazide agarose	37	active

Table 7

Initially, cyanogen bromide activated agarose was used (figure 40). However, despite a high coupling efficiency the antibody was inactive and no antigen could be bound to the column.

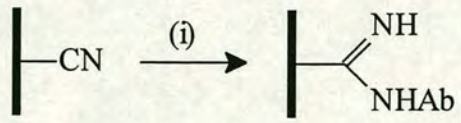

(i) antibody

Figure 40: Antibody Coupling to Cyanogen Bromide Activated Agarose

It was thought that the cyanogen bromide method was too harsh and antibody coupling was attempted using aldehyde activated agarose. This milder method uses aldehyde groups on the support to form Schiff's bases with lysine residues on the antibody which can then be stabilised by reduction with cyanoborohydride (figure 41).

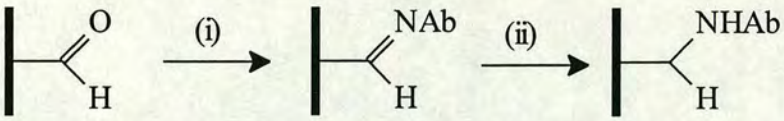

(i) antibody
(ii) sodium cyanoborohydride

Figure 41: Antibody Coupling to Aldehyde Activayted Agarose

Prior to using this coupling method the antibody was incubated in the presence of sodium cyanoborohydride and titrated by ELISA against untreated antibody to determine whether the reductant could be detrimental to antibody activity. The reductant was found to have no effect and the antibody remained active. Again a high coupling efficiency was achieved using this method but the column proved ineffective in binding the antigen.

A strategy involving the binding of the antibody to Protein-A coupled agarose followed by chemical crosslinking to create a permanent antibody-Protein-A complex was attempted. It was thought that this could provide the antibody with additional stability in the solid phase.

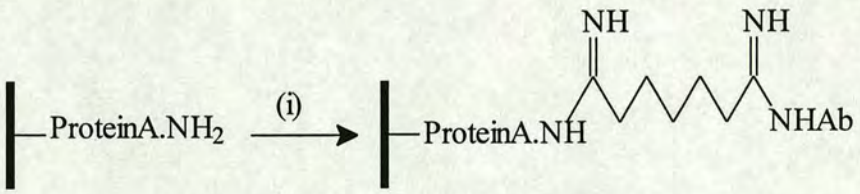

(i) antibody; dimethylpimelimidate

Figure 42: Antibody Coupling to Protein-A Agarose

Initially, commercially available HiTrap columns (Pharmacia) were used. HiTraps contain Protein-A bound to agarose housed in compact columns which allow buffer and sample addition by syringe. Dimethyl pimelimidate was the crosslinking agent used to create the permanent antibody bound matrix (figure 42). After coupling, little antibody was found bound to the matrix. As the antibody is known to bind to Protein-A this was attributed to the high back pressures encountered when using the column and incomplete mixing of antibody and crosslinker in the column. To circumvent this problem the coupling was attempted

using unpacked Protein-A agarose in a gravity column. Successful antibody binding was obtained and very high coupling efficiencies were achieved. However, no antigen binding was observed. The crosslinking agent was examined for detrimental effects on antibody acivity. ELISA revealed that the activity was drastically reduced when the antibody was incubated with the crosslinker relative to unexposed antibody (figure 43). This experiment indicated that the antibody was extremely sensitive to

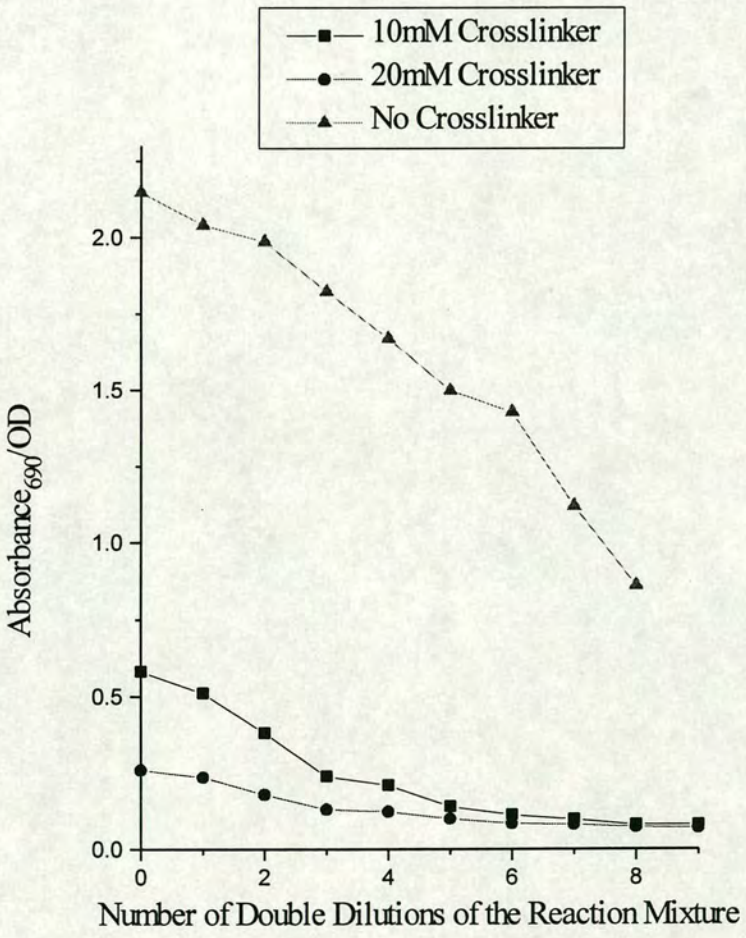

Figure 43: Comparison of Immunoreactivity Before and After Reaction with Crosslinker

electrophilic reagents. All the previous coupling chemistries used also alkylated the antibody at nucleophilic centres. To verify this further the antibody was acetylated using carbodiimide and acetic acid buffered to pH 6 (figure 44) after which it was found by ELISA titration to be deactivated with respect to unacetylated antibody

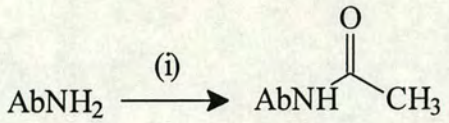

(i)CH_3CO_2H; ethyl (dimethylaminopropyl) carbodiimide

Figure 44: The Aceylation of the Antibody

(figure 45). The coupling method was modified by "preactivating" the Protein-A agarose with crosslinker to reduce the exposure time to the antibody. This also successfully coupled the antibody but the matrix would not bind any antigen.

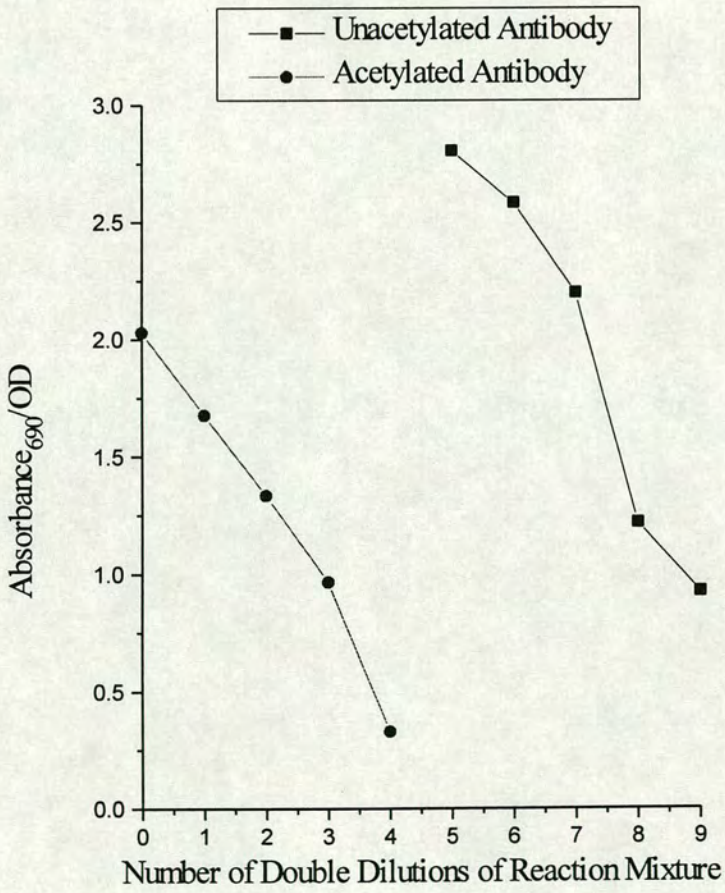

Figure 45: Comparison of the Immunoreactivities of Unacetylated and Acetylated Antibody

It was assumed that the antibody binding site was dependent on amino acid residues which are very susceptible to alkylation.

An alternative, site directed approach to solid phase coupling was attempted. This utilised carbohydrate residues as points of alkylation. These are situated on the Fc region and are therefore remote from the antibody binding sites. The carbohydrate residues provided vicinal diol groups which were oxidised to aldehydes with periodate. These provided electrophilic points for reaction by a solid support activated with nucleophiles. This approach was therefore orthogonal to the methods used previously. Hydrazide activated agarose was used (figure 46) and although the coupling efficiency was reduced relative to some of the previous methods a column was produced capable of antigen binding.

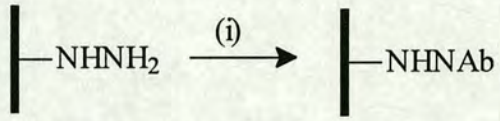

(i) antibody

Figure 46: Antibody Coupling to Hydrazide Activated Agarose

Immunoaffinity Column Operation

The optimal conditions to release the antigen bound to the column were determined by the following criteria:

1) efficiency of antigen release,

2) ease of eluting buffer removal,

3) column reuse.

ELISA was used to measure antibody binding in the presence of agents that disrupt the interactions between antibody and antigen. This revealed a number of possible eluting conditions (table 8).

Of these conditions, organic solvents showed promise as they are easily removed by evaporation to give pure antigen. Evaporation of the other solvent systems would leave salt residues. Subsequent desalting would be impractical as gel filtration methods are only effective for high molecular weight antigens.

Type of Eluent	Eluent	% Binding
Physiological	PBS/T	100
Organic solvent	40% methanol	55
	60% methanol	46
	80% methanol	33
	100% methanol	12
	40% ethanol	52
	60% ethanol	38
	80% ethanol	23
	100% ethanol	9
Salts	1M sodium sulphate	94
	1M sodium chloride	55
	1M sodium iodide	45
	3M sodium sulphate	57
	3M sodium chloride	30
	3M sodium iodide	5
pH	0.1M glycine.NaOH pH 11	5
	0.1M glycine.HCl pH 2	4

Table 8

To establish what irreversible effects these conditions might have on the protein the free antibody was exposed to these solutions which were then removed before titration by ELISA against unexposed antibody (figure 47).

The free antibody was found to be irreversibly damaged and inactive after exposure to organic solvents which precludes their use as eluting buffers if the columns are to be reused. However, acid conditions at pH 3.0 were observed to be far less damaging to the antibody and if acetic acid was used the eluting solution could be removed *in vacuo* to give uncontaminated antigen.

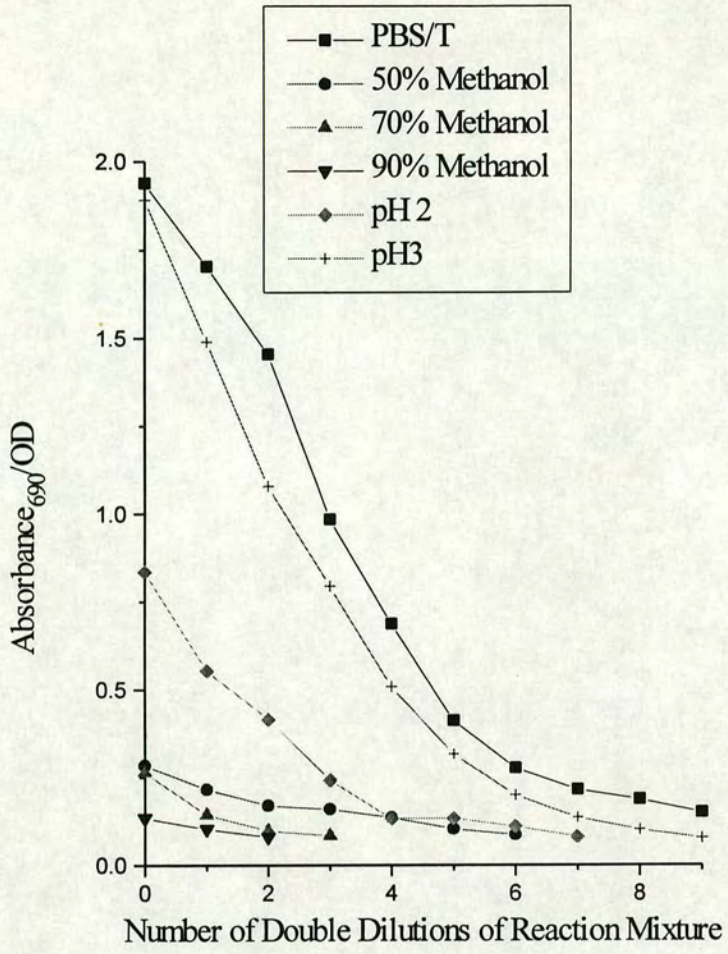

Figure 47: Comparison of Immunoreactivities After Exposure to Elution Conditions

ELISA was used to find the optimum pH that could release the antigen with the least damage to the antibody. It was found that pHs in the range 7.4 to 4.0 did not affect antibody binding of the antigen. Below pH 4.0 binding was reduced but at pH 3.0 binding dramatically increased before sharply falling below pH 2.5 (figure 48). It is known that the N^4 postion of εC can become protonated at low pH (figure 49) but no pK_a value has been reported[94-96]. A series of UV scans was recorded at a range of pHs and the absorbance was found to shift to higher wavelength at pH 3 (figure 50) indicating a structural change at this pH.

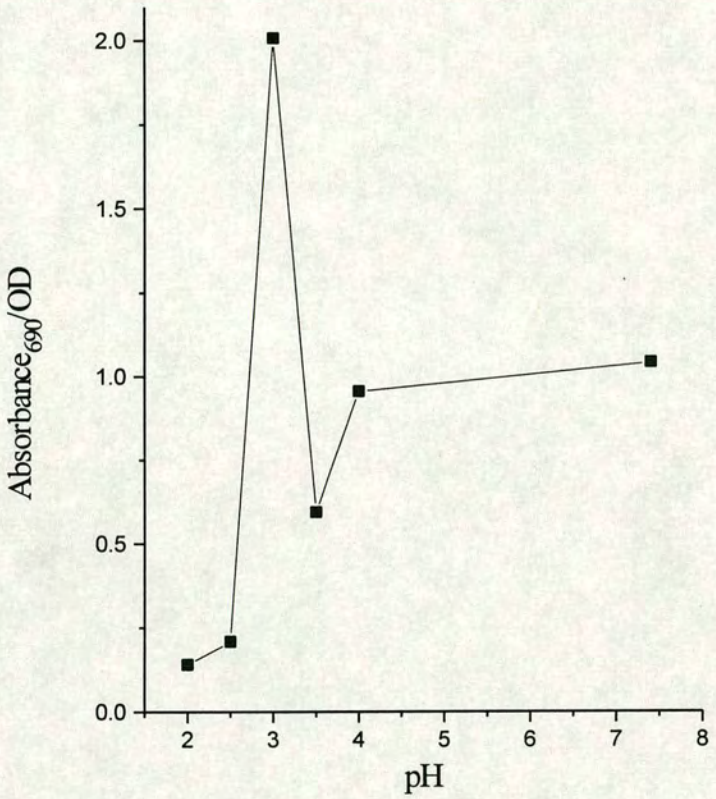

Figure 48: ELISA at a Range of pHs

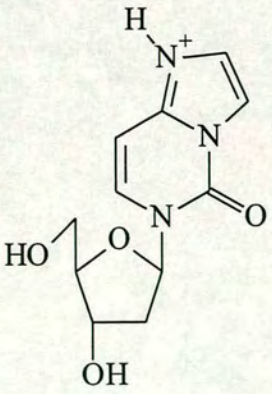

Figure 49: Protonated εC

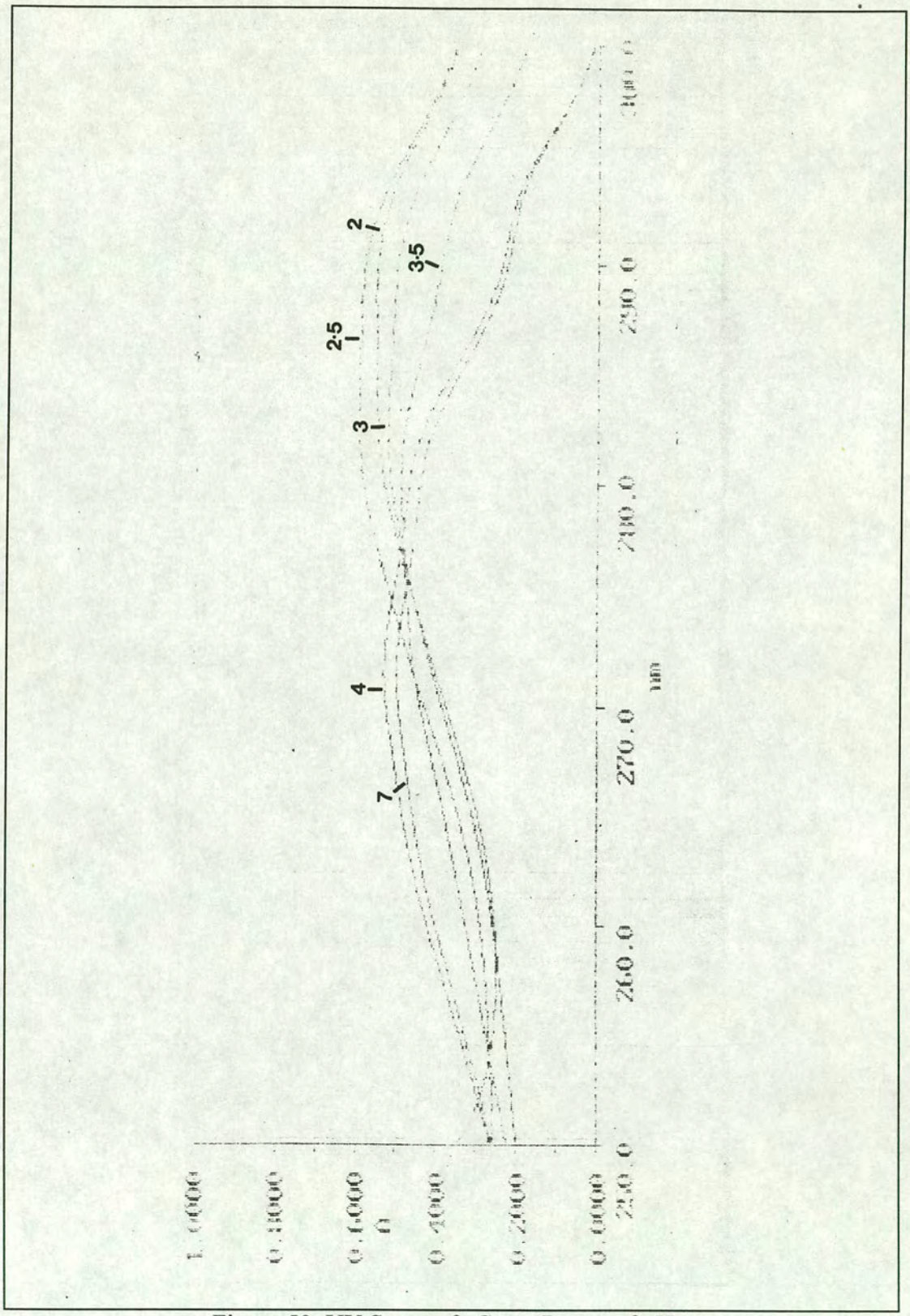

Figure 50: UV Scans of εC at a Range of pHs

The ELISA experiment suggests that the antibody is more reactive to the protonated form of εC. However at pHs below 3 these stronger interactions are disrupted possibly due to the denaturing of the protein structure and the antibody can no longer bind to the antigen. The optimal pH for antigen elution is therefore 2.5.

An Alternative to Immunoaffinity Column Chromatogaraphy

An alternative method of immunoaffinity chromatography using filters instead of columns was attempted (figure 51). This made use of commercially available centrifuge vials fitted with specific molecular weight cut-off filters (Amicon).

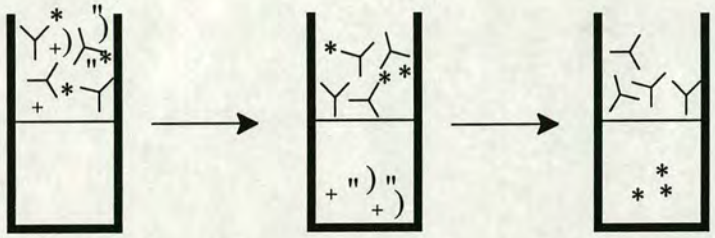

Figure 51: Immunoaffinity Purification Using Amicon Centrifuge Vials

In theory, the antibody and antigen would be incubated together in the vial above the filter and the vial then spun to remove unbound material. The antibody and bound antigen would remain above the filter by virtue of the antibody size. The bound material could then eluted by respinning the vial in the presence of an appropriate elution buffer.

Unfortunately, the experiment was unsuccessful. It is possible that the working centrifugal speeds required to successfully operate the vials generated forces that disrupted the binding between antibody and antigen. However this is speculative. This method of antigen purification was therefore discarded and immunoaffinity column chromatography with gravitational elution was the preferred method.

Antigen Detection

The method of antigen detection is dependent on the form of antigen. Initially, Oligos A and B were used in the immunoaffinity system as the sensitive dot-blot detection method could be employed. However, this proved problematic as

the highly charged oligonucleotides were prone to bind non-specifically to the column. To reduce such non-specific binding of charged molecules, high ionic strength buffers need to be used but these also disrupt the specific binding between antibody and antigen.

εC nucleoside was also used. Nucleosides cannot be bound to nylon membranes so the dot-blot method of detection was precluded and competitive ELISA was used. This method could detect picomole levels of εC but was prone to inaccuracies due to aberrant readings. In addition, using ELISA to detect the antigen means the antibody is used in both the purification and detection steps of this application. This could prove to have detrimental effects.

It has been demonstrated that the antibody cross-reacts with T and U and it may also cross-react with other molecules in a biological sample. Unknown quantities of these compounds could co-elute with εC and these contaminants could then be detected along with εC leading to inaccurate results. A preferred system is an orthogonal approach whereby the antibody is used to purify a sample but εC is detected by some physico-chemical means which would distinguish it from any contaminating compounds.

Capillary Zone Electrophoresis (CZE) was the technique used to identify and quantify the constituents of a purified sample. This method separates compounds on the basis of charge, hydrophobicity and structure. These substances are then detected by their absorbance at a defined wavelength. The absorbance can be integrated to provide quantitative data.

Only charged compounds can be run on CZE and therefore εC mono and bisphosphates were synthesised to test this system. It was thought that experimental levels of εC monophosphate running on CZE could be quantified by addition of εC bisphosphate. The bisphosphate spike being doubly charged would have a shorter retention time with respect to the monophosphate but, the UV absorbances would be very similar. CZE could be set at the UV maxima for these compounds (272nm) and the integrated quantity of monophosphate could be calculated from the known amount of bisphosphate. It was found that the charge difference between the mono

and bisphosphate made no difference to the quantities of these compounds picked up by the CZE.

Immunoaffinity Chromatography with CZE

Initially the column was used to capture samples of the synthesised εC monophosphate which were eluted from the column with 1ml fractions of acetic acid, than analysed and quantified by CZE on addition of the εC bisphosphate spike. The column proved to be extremely efficient and quantitative capture of small amounts of εC was obtained in a number of experiments (figure 52 and table 9).

εC monophosphate/nmol	% Retention
1.0	101
0.5	98
0.1	102

Table 9

To demonstrate column capture of εC in the presence of excesses of normal nucleotides, known quantities of herring sperm DNA were digested to mononucleotides with snake venom phosphodiesterase II. Complete digestion was verified by reverse phase HPLC. The immunoaffinity column was then used to purify 10 picomole samples of εC monophosphate (ecp) contaminated with different quantities of DNA hydrolysate and spiked before analysis with εC bisphosphate (pecp) (figure 53 and table 10). The immunoaffinity column could bind εC monophosphate even when mixed with 1000mg of DNA hydrolysate.

Digested DNA Added/mg	% Retention of εC Monophosphate
10	92
100	87
500	91
1000	/

Table 10

However, at the higher levels of sample contamination the eluted samples from the immunoaffinity column suffered from considerable run-through from normal nucleotides. At these higher levels the CZE apparatus could not resolve and integrate

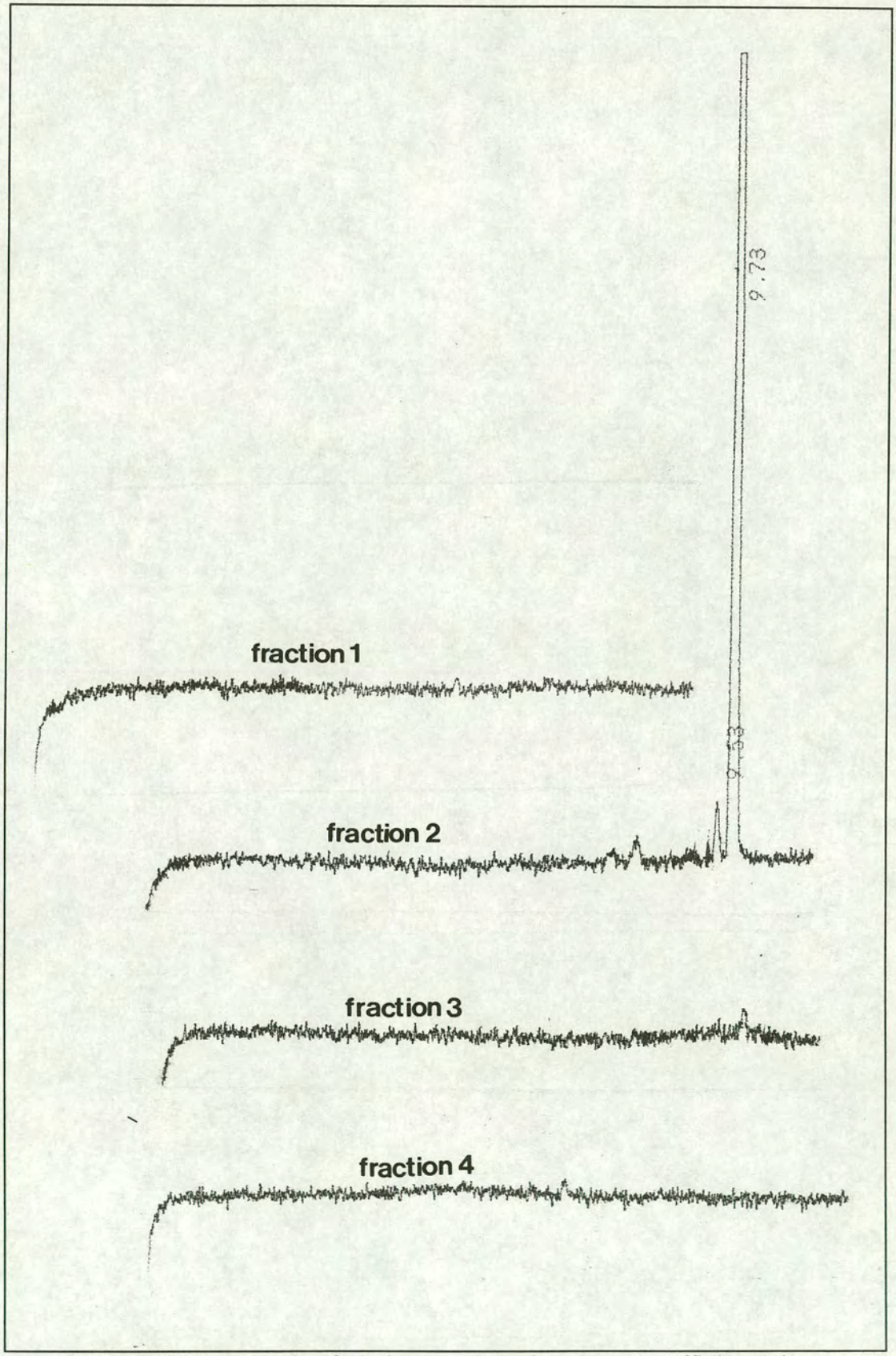

Figure 52: CZE Analysis of Elution Fractions from Immunoaffinity Column

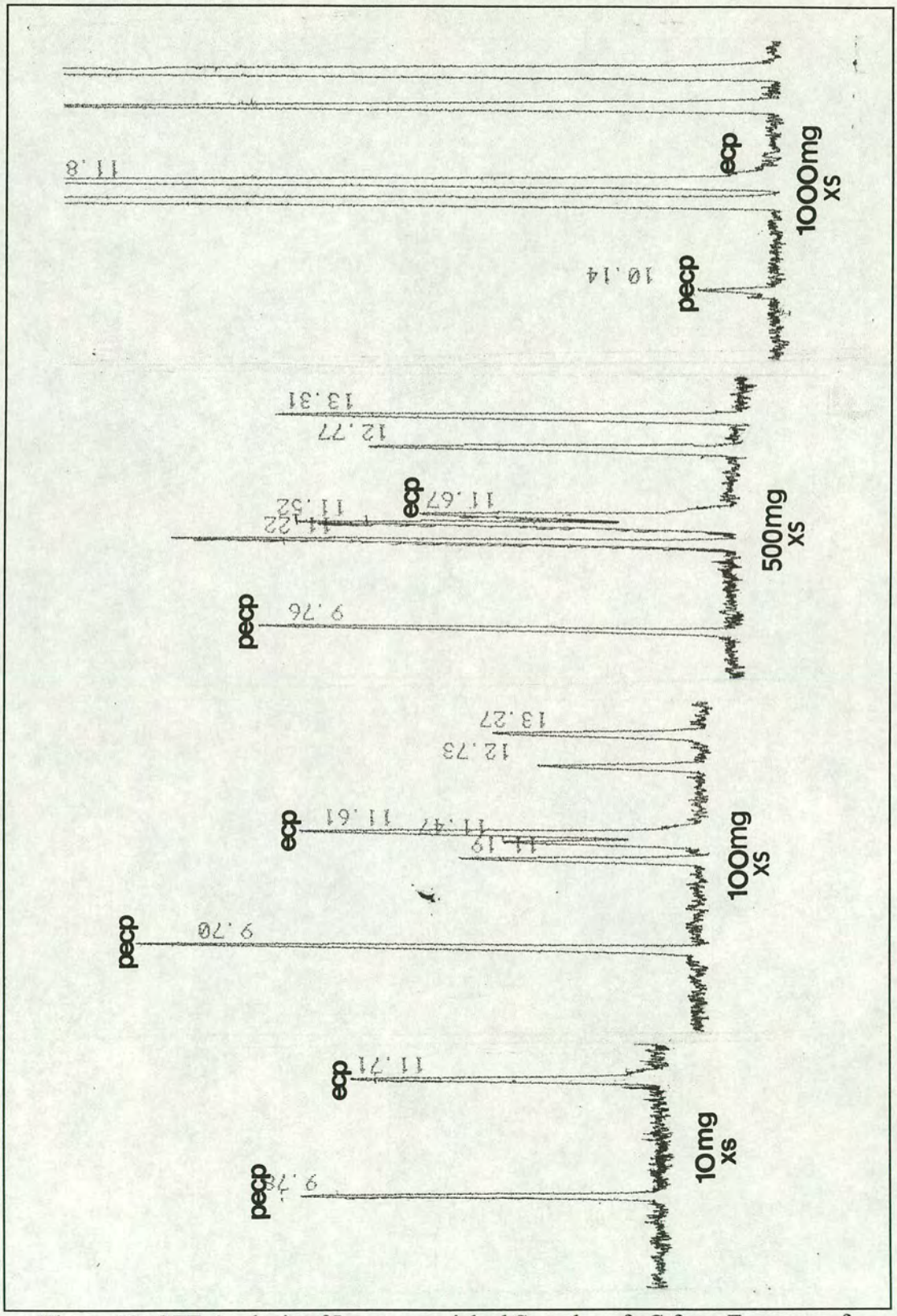

Figure 53: CZE Analysis of Immunoenriched Samples of εC from Excesses of Normal Nucleotides

εC monophosphate from the background nucleotides. As the quantities of the polluting nucleotides are approximately equal (given their differing UV absorbances at 272nm) this contamination is most likely due to non-specific binding to the solid phase matrix rather than cross-reaction of the normal nucleotides with the column antibodies.

These experiments demonstrated the capability of the column to successfully retain quantities of εC even in the presence of large excesses of normal nucleotides at levels greater than 1 εC in 3 x 10^8 nucleotides.

The column was also used to analyse εC formation in synthetic single and double stranded DNA (ssDNA and dsDNA) exposed to the vinyl chloride metabolite, CAA *in vitro*. Single and double stranded DNA was exposed at two concentrations of CAA and the formation of εC monitored with time using the immunoaffinity chromatography followed by CZE system (figure 54, figure 55, figure 56 and table 11).

Time/minutes	**0**	**1**	**5**	**10**	**15**	**30**	**60**
dsDNA at 60mM CAA	0	0	7.0	14.1	34.8	46.3	74.6
dsDNA at 60μM CAA	0	0	0	0	0	0.6	1.3
ssDNA at 60mM CAA	0	18.3	40.6	76.0	109.9	139.3	164.7
ssDNA at 60μM CAA	0	0	0.7	1.0	1.6	3.3	10.9

Table 11

As expected the production of adducts was greater and more rapid at the higher concentration of CAA. However, contrary to previous reports, adducts were found to form in both single and double stranded DNA[34]. The rate of adduct formation was significantly lower in double stranded DNA especially during the initial 10 minutes of CAA exposure. Thereafter the rates of adduct formation are similar. This is probably due to the disruption of the duplex structure by the destabilising effects of the etheno adducts (see later) making the interior structure of the DNA readily available to CAA.

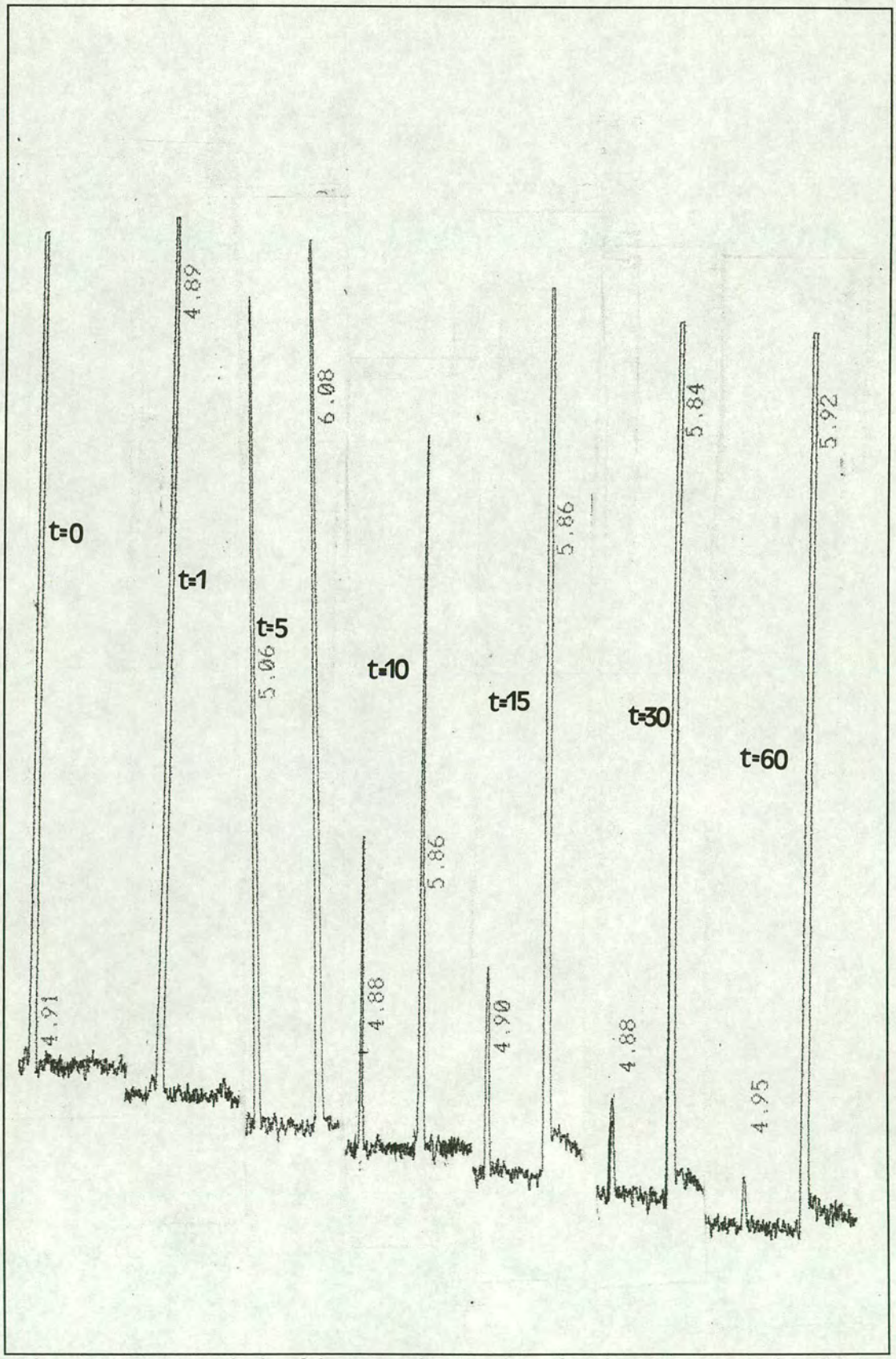

Figure 54: CZE Analysis of the Rate of Formation of εC in DNA Exposed to CAA

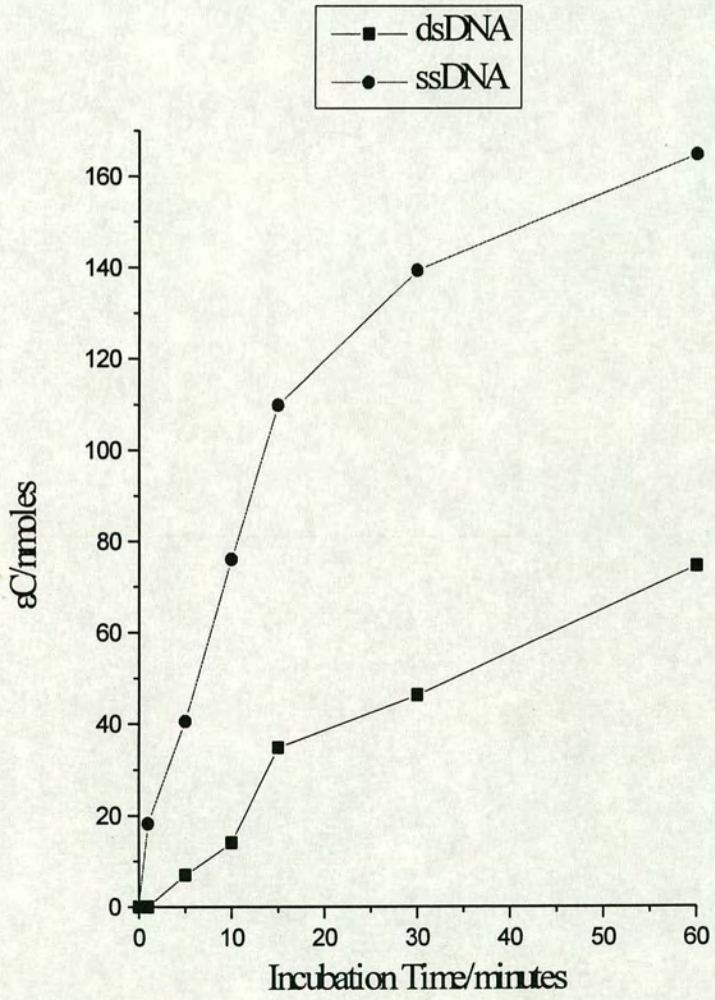

Figure 55: Rate of Formation of εC in Double Stranded and Single Stranded DNA at 60mM CAA

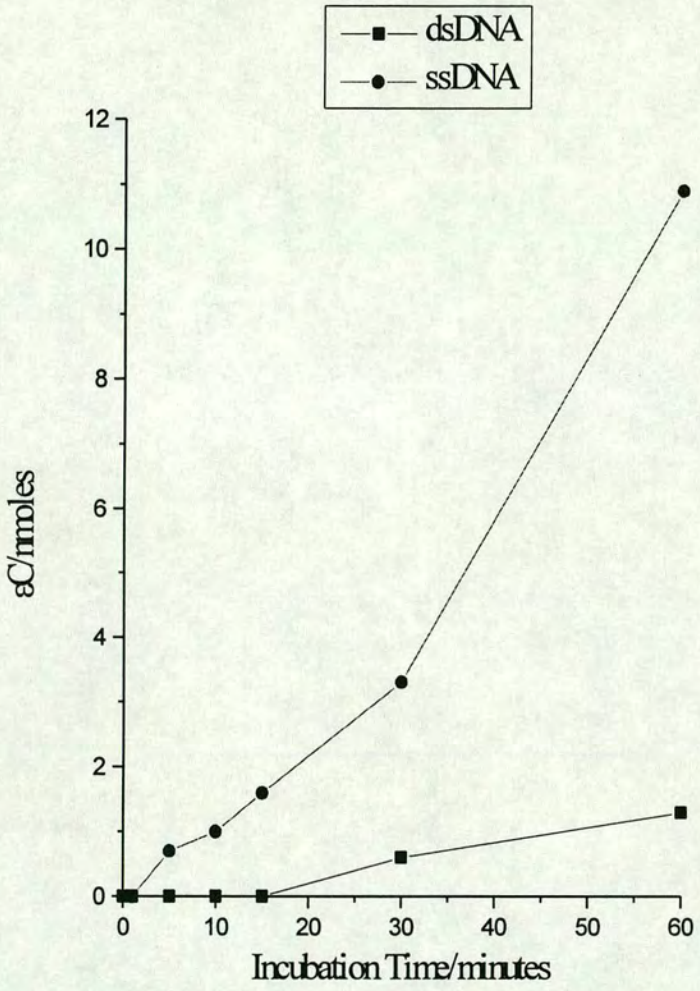

Figure 56: Rate of Formation of εC in Double and Single Stranded DNA at 60μM CAA

Structural Studies

In order to rationalise the base pairing properties of εC within DNA structural studies were undertaken. Milligram quantities of oligonucleotides incorporating εC were synthesised by automated DNA synthesis using the εC phosphoramidite made as before (table 12). The oligonucleotides were rigorously purified using an orthogonal purification strategy. The oligonucleotides were initially purified by reverse phase HPLC followed by anion exchange FPLC (Mono Q) and the purity was

measured by CZE. The oligonucleotides were mixed together to form a number of duplexes (table 13).

Sequence
CGC εCTT TTT GCG
CGC TTT TTεC GCG
CGC εCAA AAA GCG
CGC AAA AAεC GCG
CGC TTT TTT GCG
CGC AAA AAA GCG

Table 12

Code	Sequence
NS	d(CGC AAA AAA GCG / GCG TTT TTT CGC)
εC.T	d(CGC TTT TTT GCG / GCG εCAA AAA CGC)
εC.dA	d(GCG AAA AAA GCG / GCG εCTT TTT CGC)
T.εC	d(CGC TTT TTT GCG / GCG AAA AAεC CGC)
dA.εC	d(CGC AAA AAA GCG / GCG TTT TTεC CGC)

Table 13

Sample mixtures were analysed by CZE to allow the addition of oligonucleotides in the correct proportions. Duplexes are retained by CZE longer than single strands and therefore CZE can be used to measure duplex purity and the ratios of the two strands.

These DNA duplexes were used in:

1) UV thermal denaturing studies,

2) ^{31}P NMR studies,

3) Crystallisation studies.

1) UV thermal denaturing studies: The duplexes NS, εC.dA and εC.T were examined for their stability when exposed to heat. Heat induces double strands to separate and this dissociation can be detected. Base stacking interactions in the double helix reduce the levels of UV radiation absorbed by the heterocyclic bases and when the duplex dissociates this hyperchromicity can be measured. When monitored as a function of temperature a melting curve is produced. The point of

inflection is known as the melting temperature (Tm) and corresponds to equimolar concentrations of single and double strands. Measurement of the Tm at a range of duplex concentrations allows calculation of the thermodynamic properties of free energy, enthalpy and entropy given the equations:

$$1)\ 1/Tm = (R/\Delta H)\ \ln (C_T/4) + \Delta S/\Delta H$$

where: R is the gas constant (8.314 $JK^{-1}mol^{-1}$),

ΔH is enthalpy,

C_T is the concentration of single strands,

ΔS is entropy.

$$2)\ \Delta G = \Delta H - T\Delta S$$

where: ΔG is free energy,

T is temperature.

The thermodynamic parameters of hybridisation and the values for free energy (normalised to a temperature of 298K) for the three duplexes were calculated (figure 57, figure 58, figure 59 and table 13).

Duplex	**Tm/°C (1μM)**	**ΔH /kJmol^{-1}**	**ΔS /kJmol^{-1}K^{-1}**	**ΔG_{298} /kJmol^{-1}**	**$\Delta\Delta G_{298}$ /kJmol^{-1}**
NS	53.3	-307.92	-0.83	-60.58	/
εC.T	27.1	-217.69	-0.62	-32.32	28.26
εC.dA	25.2	-183.69	-0.50	-34.69	25.89

Table 13

Incorporation of εC within double stranded DNA leads to considerable drop in the stability of this structure lowering the Tm by 26.2°C and 28.1°C and dropping the free energy ($\Delta\Delta G_{298}$) by 25.89 and 28.26 for εC.dA and εC.T respectively. The small difference in stability between the εC.dA and the εC.T base pairs is consistent with the non-instructional nature of εC and also accounts for the slightly favoured εC.dA base pairing. The results mirror similar findings reported by Gibson *et al*[97] (see publication).

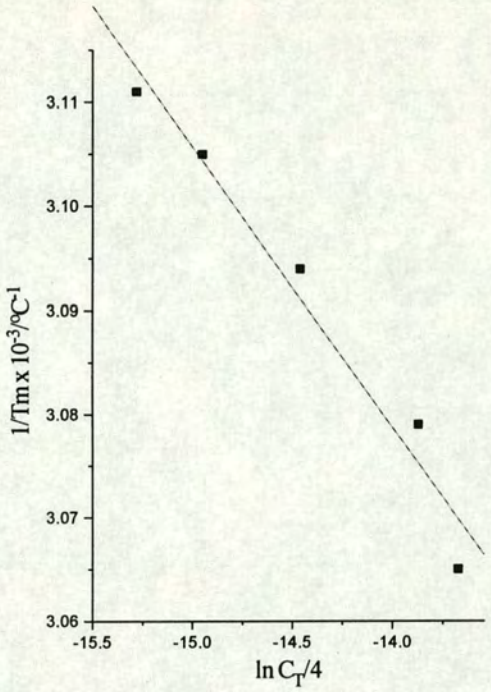

Figure 57: Plot of the Thermodynamic Parameters of NS Duplex Hybridisation

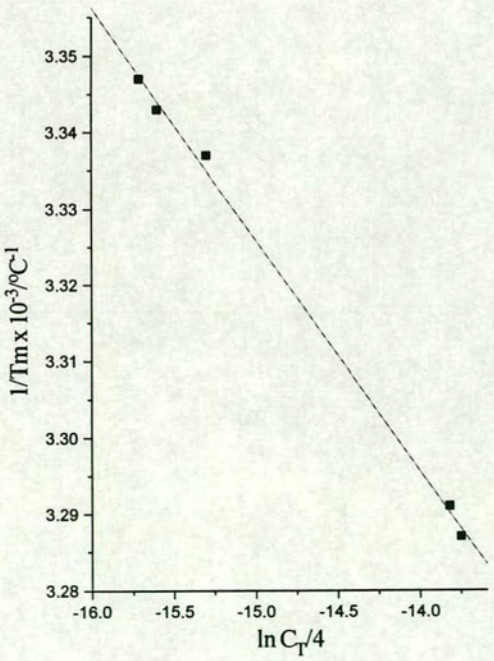

Figure 58: Plot of the Thermodynamic Parameters of εC.T Duplex Hybridisation

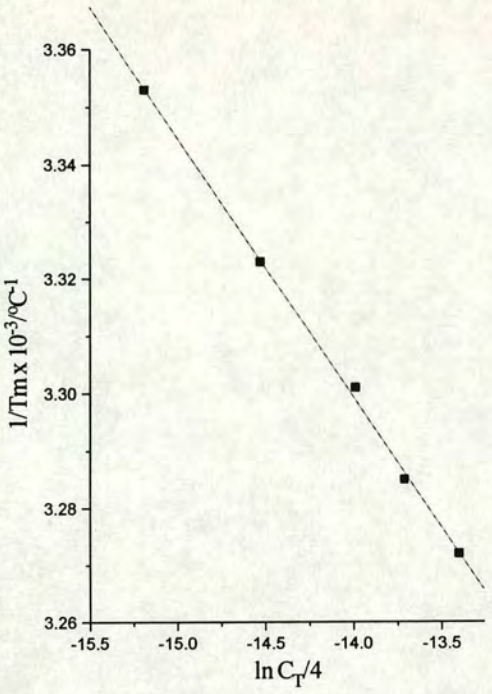

Figure 59: Plot of the Thermodynamic Parameters of εC.A Duplex Hybridisation

2) ^{31}P NMR studies: The duplexes NS, εC.dA and εC.T were also used in ^{31}P NMR studies comparing the phosphorus resonances of the DNA backbone in these three duplexes. Bulky lesions often perturb the overall double helical structure leading to conformational changes in the DNA backbone. This distinction can be seen in the signals of the neighbouring phosphorus atoms as they will lie outside the normal range of chemical shifts. The ^{31}P NMR spectra for all three duplexes show no significantly different resonances (figure 60) and so inclusion of εC opposite either a pyrimidine or a purine does not distort the overall duplex structure at NMR temperatures and DNA concentrations.

3) Crystallisation Studies: All the duplexes synthesised were designed to be suitable for crystallisations to obtain X-ray diffraction data on duplex structure. Often DNA crystals are grown from palindromic sequences as these immediately hybrise due to their self-complementarity thus producing pure duplexes with no more than one single stranded molecule as an impurity. As well as purity, a stable structure is also required for successful crystal growth but as has been seen, inclusion of εC

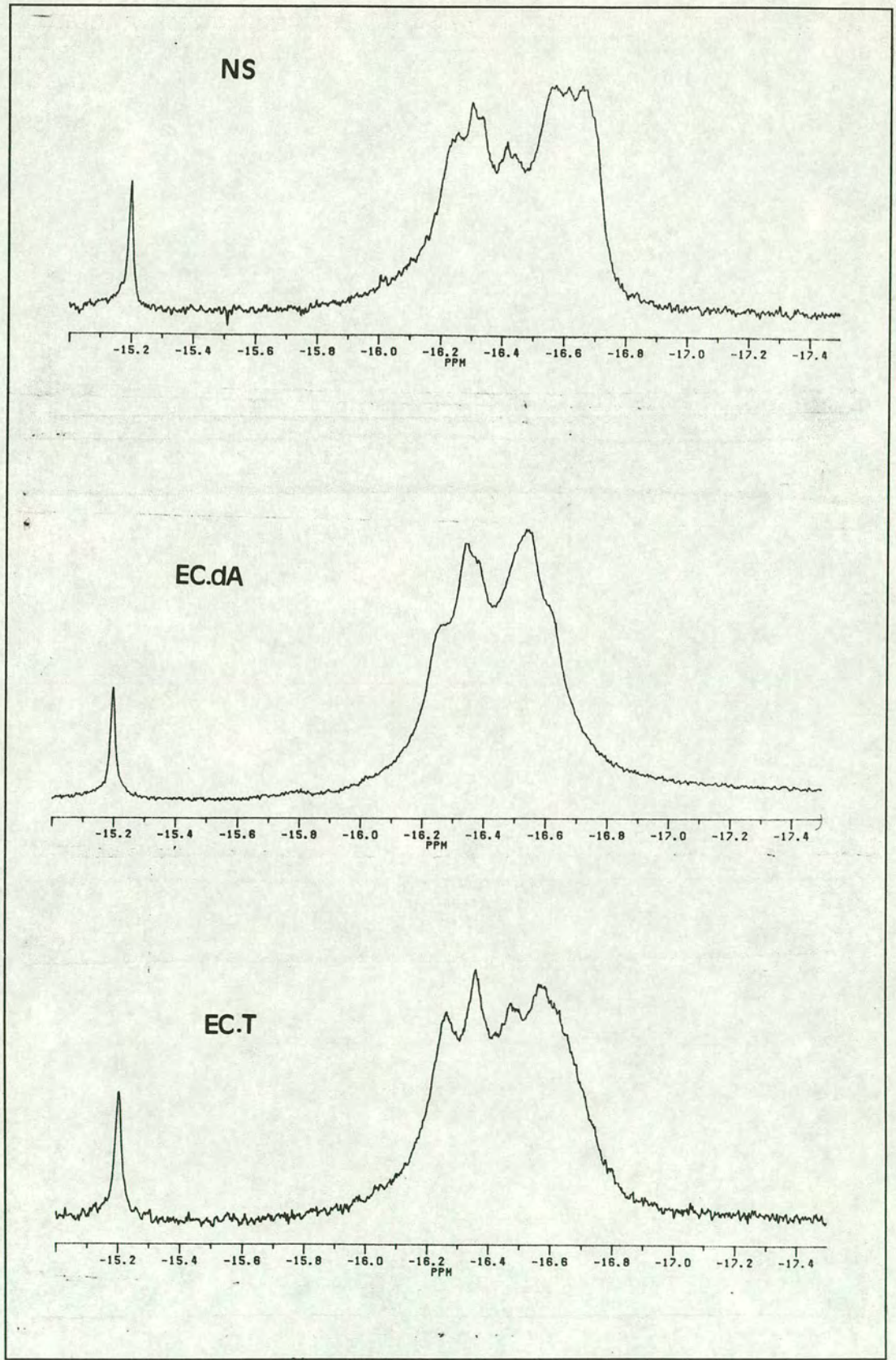

Figure 60: ^{31}P NMR Spectra of NS, εC.dA and εC.T

drastically destabilises duplexes. This precludes inclusion of εC in a palindromic sequence as it is unlikely that a stable duplex could form containing two such residues. Purity is paramount to crystal growth so all the duplexes were repurified by ion exchange FPLC under non-denaturing conditions. This separates any excess single strands from double stranded DNA. The native duplex sequence had previously been successfully crystallised and the X-ray crystal structure determined[98]. The conditions reported in that study were used in initial crystallisation trials and these were subsequently varied. Microcrystals were obtained from all the duplexes but no crystals of sufficient size and quality could be obtained for X-ray diffraction.

CONCLUSIONS AND FUTURE WORK

A highly selective and affinitive monoclonal antibody to εC was developed and successfully used in an immunoenrichment procedure. When used in tandem with a CZE detector this system could enrich picomole levels of εC from 1000mg excesses of DNA hydrolysate and quantify one εC from 10^8 normal nucleotides.

The detection sensitivity of this system could be improved by employing ^{32}P postlabelling followed by two-dimensional TLC post-immunoenrichment. This would allow femtomole or attomole levels of εC to be quantified.

Kinetic studies using the immunoaffinity/CZE system examined the relative rates of formation of εC in double and single stranded DNA when exposed to CAA. It was found that the rate of formation of εC in single stranded DNA exceeded that in double stranded DNA.

UV thermal denaturing and ^{31}P NMR studies on duplexes incorporating εC were carried to determine the base pairing properties of εC. It was found that εC has an extremely destabilising effect on the duplex although the overall structure is not greatly distorted relative to native DNA.

Attempts to crystallise duplexes incorporating εC failed to produce crystals of the necessary size and quality for X-ray diffraction and total structure determination. Additional crystallisations using altered crystallisation conditions and different DNA sequences may provide superior crystals.

EXPERIMENTAL

Materials

All chemicals, buffer tablets, proteins and enzyme substrates were obtained from Aldrich, Sigma or Fluka. Silica gel 60 was obtained from Fluka. All cell culture media were obtained from Gibco with the exception of myoclone from ICN Flow. Cell culture plasticware was obtained from Costar. Microtitre plates were obtained from Nunc. Secondary antibody horseradish peroxidase (HRP) conjugated to rabbit anti-mouse immunoglobulins was obtained from Dakopatts. Antibody isotyping kit was obtained from Sera-lab. Hibond nylon and nitrocellulose membranes were obtained from Amersham. Bovine alkaline phosphatase was obtained from Bohringer Mannheim. Protein-A coupled to agarose, Protein-A affinity columns and Immunopure Ag/Ab Immobilisation kits 1 and 4 were obtained from Pierce. NAP5 and NAP10 columns were obtained from Pharmacia.

Solvents

All solvents were of analytical or HPLC grade. Anhydrous pyridine was distilled over CaH_2. Anhydrous triethylamine (TEA) and diisopropylethylamine were stored over CaH_2. Anhydrous acetonitrile was purchased from Applied Biosystems as DNA synthesis grade. Anhydrous tetrahydrofuran (THF) and diethyl ether (ether) were distilled over sodium and benzophenone. Pyrogen-free, reverse osmosis purified water was used throughout.

Thin Layer Chromatography (TLC)

TLC was carried out on 0.22mm layer silica gel 60 F_{254} on aluminium backed sheets obtained from Merck using the following solvent systems:

A: ethyl acetate:methanol (5:1 v/v).

B: ethyl acetate:acetonitrile (1:1 v/v).

C: dichloromethane (DCM):methanol (9:1 v/v).

D: ethyl acetate:methanol (1:1 v/v).

Compounds were visualised by irradiation at 254nm. Sugar groups were visualised by anisaldehyde spray (*para*-methoxybenzaldehyde:acetic acid:conc.H_2SO_4:ethanol (5:1:1:100 v/v/v/v) with heating as dark blue to green colours. Dimethoxytrityl groups were visulalised by fuming HCl as bright orange colours.

Buffers, Cell Culyure Media and Substrates

Acetate buffer: 200mM sodium acetate and 200mM acetic acid at pH 4.5.

MES buffer: 100mM *N* -morpholinoethanesulphonic acid at pH 6.2.

HPLC buffers: details in appropriate experimental section.

Enzyme digest buffer: 2M sodium chloride and 100mM Tris at pH 8.8.

Phosphate buffered saline (PBS): tablets dissolved in water (200ml *per* tablet) gave 100mM phosphate and 50mM sodium chloride at pH 7.4.

PBS/T: PBS with 0.05% w/v Tween-20.

Blocking buffer: 10% w/v skimmed milk in PBS/T.

DAB substrate: 3,3'-diaminobenzidine.4HCl tablet and urea plus hydrogen peroxide tablet dissolved in water (15ml).

PBS/BSA: PBS with 1% w/v Bovine Serum Albumin (BSA).

pNPP substrate: *para* nitrophenyl-phosphate tablet dissolved in water (5ml).

RPMI: RPMI 1640 with glutamax.

RPMI/PS: RPMI with penicillin (200units.ml^{-1}) and streptomycin (200μg.ml^{-1}).

10% complete media: RPMI/PS with 10% v/v myoclone, 2mM sodium pyruvate and amphotericin B deoxycholate (2.5μg.ml^{-1}).

5% complete media: as for 10% complete media but with 5% v/v myoclone.

PBS/azide: PBS with 0.02% sodium azide.

Binding buffer: 100mM Tris at pH 8.5.

Eluting buffer: 100mM Glycine at pH 2.7.

Neutralising buffer: 1M Tris at pH 9.0.

SDS-PAGE solutions: details in appropriate experimental section.

Coating buffer: 15mM sodium carbonate and 35mM sodium hydrogen carbonate at pH 9.5.

TMB substrate: 3,3',4,4'-tetramethylbenzidine liquid substrate system containing chromagen, buffer and hydrogen peroxide.

Immunoaffinity column buffers: details in appropriate experimental section.

CZE buffers: details in appropriate experimental section.

UV melting buffer: 100mM sodium chloride, 10mM sodium hydrogen orthophosphate and 1mM sodium EDTA at pH 7.0.

Crystallisation solutions: details in appropriate experimental section.

FPLC buffers: details in appropriate experimental section.

Instrumentation

^{1}H NMR spectra were recorded on a Bruker WP-200 (200.13 MHz) Fourier transform spectrometer. ^{13}C NMR spectra were recorded on a Bruker WP-200 (50.32 MHz) Fourier transform spectrometer. ^{31}P NMR spectra were recorded on a Jeol FX90Q (90 MHz) Fourier transform spectrometer. UV spectra were recorded on a Perkin-Elmer Lambda 15 ultraviolet-visible specrophotometer. IR spectra were recorded on a Bio Rad FTS-7 Fourier transform spectrometer controlled by a Bio Rad SPC 3200 microcomputer. Positive ion fast atom bombardment (FAB) mass spectra were recorded on a Kratos MS 50 TC spectrometer using a 3-nitrobenzyl alcohol (3-NOBA) matrix. ELISA plates were read on a Molecular Devices Vmax kinetic microplate reader incorporating Softmax ELISA software package.

Bromoacetaldehyde [1][92]

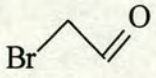

Bromoacetaldehyde diethyl acetal (86.4mmol, 20ml) and ethanol (10ml) were added to a solution of HCl (1M, 60ml) and the resulting biphasic mixture vigorously stirred at room temperature. After 7 d the title compound was obtained as a monophasic solution. This was used unpurified. Dinitrophenylhydrazine derivative gave *m/z* (FAB) 302.97029 ($M\text{-}1^{+}$; Calc. for $C_8H_7N_4O_4Br$, 302.97289).

5,6-Dihydro-5-oxo-6β-D-2'-deoxyribofuranosylimidazo-[1,2-*c*]-pyrimidine (εC) **[2]**[86]

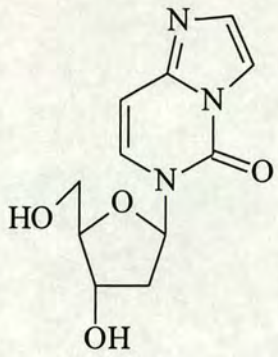

Compound [1] (43.2mmol, 6eq) was added in portions (9x5ml), to a stirred solution of 2'-deoxycytidine.HCl (1.9g, 7.2mmol, 1eq) in acetate buffer (40ml). The pH was periodically adjusted to 4.5 by the addition of sodium acetate solution (0.2M) and the solution warmed to 40°C. After 24 h the pH was adjusted to 8.5 with saturated $NaHCO_3$ solution and concentrated *in vacuo*. The resulting paste was washed with methanol (80ml) and filtered. The filtered solid was washed with methanol (50ml) and the combined filtrates concentrated *in vacuo*. The product was purified by wet flash silica gel chromatography eluting with 0 to 5% gradient of methanol in DCM. The appropriate fractions were collected and concentrated *in vacuo* to yield the title compound as a pale yellow foam (1.577g, 6.28mmol, 87%), R_f (in A), 0.16; $\delta_H([^2H_6]$-DMSO) 7.80 (1 H, s, 2-H), 7.75-7.73 (1 H, d, 7-H), 7.39 (1H, s, 3-H), 6.73-6.71 (1H, d,8-H), 6.44-6.40 (1H, t, 1'-H), 5.32-5.31 (1H, d, 3'OH), 5.10-5.07 (1H, t, 5'OH), 4.31-4.28 (1H, p, 3'-H), 3.87-3.84 (1H, q, 4'-H), 3.63-3.59 (2H, m, 5'-H) and 2.22-2.18 (2H, m, 2'-H); $\delta_C([^2H_6]$-DMSO) 146.51 (C), 133.12 (CH), 129.32 (2CH), 113.88 (C), 99.26 (CH), 88.27 (CH), 86.27 (CH), 71.24 (CH), 62.02 (CH_2) and 40.68 (CH_2); λ_{max} (H_2O)/nm 293(shoulder), 280(shoulder) and 272; υ_{max}(nujol mull)/cm^{-1} 3459 (OH), 1659 and 1622 (C=O and aromatic ring system); *m/z* (FAB) 252.09841 ($M+1^+$; Calc. for $C_{11}H_{14}N_3O_4$, 252.09842).

5,6-Dihydro-5-oxo-6β-D-5'-*O*-dimethoxytrityl-2'-deoxyribofuranosylimidazo-[1,2-*c*]-pyrimidine [3][86]

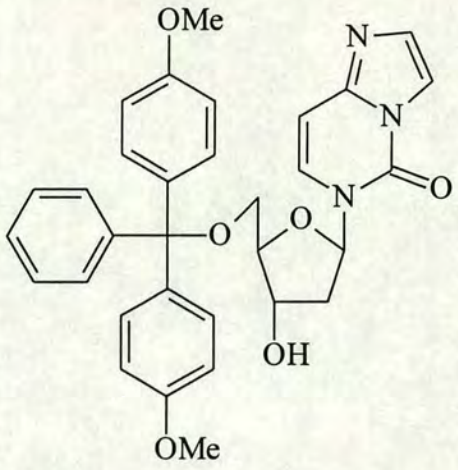

4-Dimethylaminopyridine (36mg, 280μmol, 0.1eq) and compound [2] (750mg, 2.98mmol, 1eq) were coevaporated with anhydrous pyridine (3 x 10ml) and dissolved in anhydrous pyridine (15ml) and anhydrous TEA (622μl, 451mg, 4.47mmol, 1.5eq). 4,4'-Dimethoxytrityl chloride (1.31g, 3.87mmol, 1.3eq, recrystallised from 1% acetyl chloride in hexane) was added in four portions with stirred, in the dark, under an argon atmosphere at room temperature. After 24 h the reaction was quenched with the addition of water (20ml), concentrated *in vacuo* and coevaporated with toluene (3 x 20ml). The resulting brown gum was dissolved in DCM (50ml) and washed with saturated KCl solution (50ml). The aqueous phase was washed with DCM (3 x 100ml) and the combined organic fractions dried over Na_2SO_4, filtered and concentrated *in vacuo*. The product was purified by wet flash silica gel chromatography eluting with a 0 to 4% gradient of methanol in 1% TEA in DCM. The appropriate fractions were concentated *in vacuo* to yield the title compound as a pale yellow foam (1.26g, 2.28mmol, 76%), R_f (in A) 0.79; $\delta_H([^2H_6]$-DMSO) 7.79 (1H, d, 2-H), 7.52-7.50 (1H, d, 7-H), 7.39-6.86 (14H, m, trityl-H and 3-H), 6.45-6.43 (1H, d, 8-H), 6.39 (1H, t, 1'-H), 5.46 (1H, d, 3'OH), 3.96-3.95 (1H, q, 4'-H), 3.72 (6H, s, Me), 3.54-3.38 (2H, m, 5'-H) and 2.52-2.48 (2H, m, 2'-H); $\delta_C([^2H_6]$-DMSO) 158.38 (C), 145.64 (C), 144.96 (C), 135.71 (C), 135.47 (C), 132.88 (CH), 130.06 (CH), 128.21 (CH), 127.98 (CH), 113.51 (CH), 113.17 (C), 98.54 (CH), 86.10 (CH), 85.94 (CH), 85.66 (CH), 70.16 (CH), 63.58 (CH_2) and 55.31

(CH_3); λ_{max}(50% ethanol)/nm 294(shoulder), 281, 273 and 234; υ_{max}(nujol mull)/cm^{-1} 1659 and 1621 (aromatic ring system); *m/z* (FAB) 554.22916 ($M+1^+$; Calc. for $C_{32}H_{32}N_3O_6$, 554.22916).

5,6-Dihydro-5-oxo-6β-D-5'-*O*-dimethoxytrityl-3'-*O*-succinyl-2'-deoxyribofuranosylimidazo-[1,2-*c*]-pyrimidine [4]

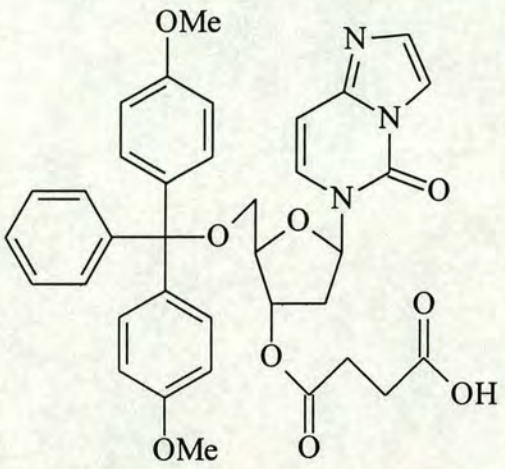

4-Dimethylaminopyridine (4.6mg, 46μmol, 0.1eq) and compound [3] (250mg, 460μmol, 1eq) were coevaporated with anhydrous pyridine (3 x 5ml) and dissolved in anhydrous pyridine (5ml). Succinic anhydride (60mg, 598μmol, 1.3eq) was added to the stirred solution under an argon atmosphere, in the dark at room temperature. After 72 h the solution was concentrated *in vacuo* and coevaporated with toluene (3 x 5ml). The resulting brown gum was dissolved in DCM (50ml) and washed with water (10ml). The organic phase was dried over Na_2SO_4, filtered and concentrated *in vacuo*. The product was purified by wet flash silica gel chromatography eluting with a 0 to 9% gradient of methanol in 1% TEA in DCM. The appropriate fractions were concentrated *in vacuo* to yield the title compound as a pale yellow foam (210mg, 322μmol, 70%), R_f (in A) 0.425; δ_H([$^2H_6$]-DMSO) 9.9-9.6 (1H, s, CO_2H), 7.65 (1H, s, 2-H), 7.58-7.56 (1H, d, 7-H), 7.37-6.78 (14H, m, trityl and 3-H), 6.59-6.55 (1H, t, 1'-H), 6.27-6.25 (1H, d, 8-H), 5.48-5.46 (1H, d, 3'-H), 4.20-4.19 (1H, d, 4'-H), 3.72 (6H, s, Me), 3.52-3.41 (2H, q, 5'-H), 3.02-2.98 (4H, m, 7'-H and 6'-H) and 2.46-2.42 (2H, m, 2'-H); δ_C([$^2H_6$]-DMSO) 176.16 (C), 172.50 (C), 158.38 (C), 145.48 (C), 144.61 (C), 143.99 (C), 135.01 (C), 134.84 (C), 132.14 (CH), 129.81 (CH), 127.85

(CH), 127.71 (CH), 127.10 (CH), 126.83 (CH), 112.99 (CH), 112.55 (CH), 98.93 (CH), 86.86 (C), 85.24 (CH), 84.05 (CH), 74.42 (CH), 54.94 (CH_3), 44.75 (CH_2), 38.30 (CH_2), 30.24 (CH_2) and 29.79 (CH_2); λ_{max}(50% ethanol)/nm 294(hump), 281(shoulder), 272, 265(shoulder), 257(shoulder) and 232; υ_{max}(nujol mull)/cm^{-1} 3200-2500 (CO_2H) and 1702 (C=O and aromatic ring system); *m/z* (FAB) 654.24518 ($M+1^+$; Calc. for $C_{36}H_{36}N_3O_9$, 654.24513).

5,6-Dihydro-5-oxo-6β-D-3'-*O*-succinyl-2'-deoxyribofuranosylimidazo-[1,2-*c*]-pyrimidine [5]

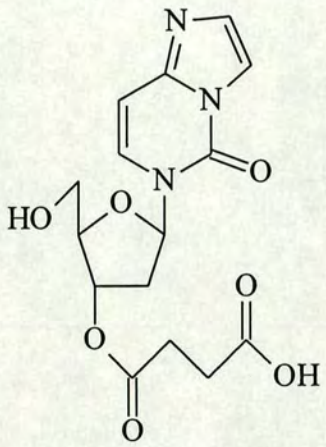

Compound [4] (50mg,77μmol) was dissolved in acetonitrile (500μl) and HCl solution (500μl, 1M) added. After stirred at room temperature for 24 h the product was purified by reverse phase HPLC as described below eluting with: buffer A-water and buffer B-20% acetonitrile and using the following gradient:

Time/min	Flow Rate/ml.min^{-1}	% Buffer B
0	3	0
3	3	0
4	3	15
25	3	70
26	3	100
28	3	100
29	3	0
32	0	0

The appropriate peak was collected, concentated *in vacuo* and freeze dried to yield the title compound as a white solid (14mg, 40μmol, 52%), R_f (in A) 0.06; λ_{max}(50% ethanol)/nm 293(shoulder), 281(shoulder), 272, 264(shoulder) and 257(shoulder); *m/z* (FAB) 352.11488 ($M+1^+$; Calc. for $C_{15}H_{17}N_3O_7$, 352.11489).

Preparation of Ethenodeoxycytidine (εC) Immunogen

BSA (Sigma) (6mg) and 1-ethyl-3-(3-dimethylaminopropyl)carbodiimide.HCl (13mg, 84μmol, 3eq) were added to MES buffer (2ml) and warmed to 32°C. A solution of [5] (10mg, 28μmol, 1eq) in DMSO (2ml) also warmed to 32°C was added dropwise and a slight precipitate formed. The suspension was incubated at 32°C and after 24 h the product was purified by gel filtration NAP-10 column chromatography to the manufacturer's specifications eluting with 50% ethanol. The conjugate was stored in 50% ethanol at -20°C until used.

Preparation of εC Screen

As for the εC immunogen replacing BSA with CγG.

Characterisation of εC Immunogen

εC immunogen (1ml of 500μgml^{-1} in 50% ethanol) was warmed to 40°C. 4% $NaHCO_3$ (1ml) and 0.1% 2,4,6-trinitrobenzenesulphonic acid (1ml) were added and the mixture incubated at 40°C. After 2 h 10% sodium dodecyl sulphate (1ml) and HCl (500μl, 1M) were added. BSA (1ml of 500μgml^{-1} in 50% ethanol) was treated identically and the absorbance of both solutions read at 335nm against a blank of 50% ethanol treated as above.

2-Cyanoethyl-*N*,*N*-(diisopropyl)chlorophosphoramidite [6][99]

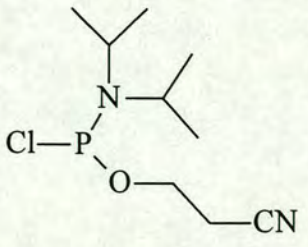

3-Hydropropionitrile (3.4ml, 3.55g, 50mmol, 0.14eq) dissolved in anhydrous acetonitrile (20ml) was added dropwise, *via* a double ended needle under argon pressure, to a stirred solution of phosphorus trichloride (30.6ml, 350mmol, 1eq) in anhydrous acetonitrile (20ml), at room temperature. After 15min the solution was concentrated *in vacuo* and the resulting cloudy oil purified by Kugelrohr distillation (60°C, 0.4mmHg) to yield 2-cyanoethylphosphodichloride. *N,N*-diisopropylamine (10.5ml, 74.9mmol, 0.21eq) dissolved in anhydrous ether (40ml) was added dropwise, *via* a double ended needle under argon pressure, to a stirred solution of the 2-cyanoethylphosphdichloride in anhydrous ether (40ml) at room temperature. After 5min a white precipitate formed and the reaction mixture was filtered twice and concentrated *in vacuo*. The resulting yellow oil was purified by Kugelrohr distillation (140°C, 0.3mm Hg) to yield the title compound as a clear, colourless oil (5.2g, 16%), $\delta_P([^2H_1]\text{-}CDCl_3)$ 180.25 (1P, s, P^{III}).

5,6-Dihydro-5-oxo-6β-D-5'-*O*-dimethoxytrityl-2'-deoxyribofuransylimidazo-[1,2-*c*]-pyrimidine-3'-*O*-cyanoethyl-*N,N*-(diisopropyl)phosphoramidite [7][86]

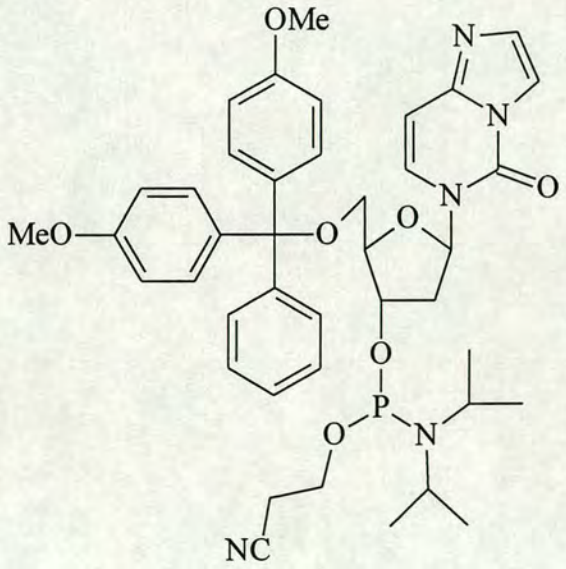

Compound [3] (392mg, 709mmol, 1eq) was coevaporated with anhydrous pyridine (3 x 5ml) then with anhydrous THF (5ml) and dissolved in anhydrous THF (5ml) and anhydrous diisopropylethylamine (400µl, 2,3mmol, 3.2eq). Compound [6] (210µl, 222mg, 940µmol, 1.3eq) was added dropwise with stirred, in the dark, under an

argon atmosphere at room temperature. After 10min solid diisopropylethylammonium chloride precipitated and the suspension stirred for a further 2 h. The reaction was quenched with the addition of anhydrous ethyl acetate (50ml) and the organic phase washed quickly with saturated KCl solution (10ml). The organic phase was dried over Na_2SO_4, filtered and concentrated *in vacuo*. The resulting yellow oil was purified by wet flash silica gel chromatography (pre-washing the silica gel with 1% triethylamine in anhydrous ethyl acetate) eluting with anhydrous ethyl acetate. The appropriate fractions were collected and concentrated *in vacuo* to yield the title compound as a white foam (335mg, 445μmol, 63%), R_f (in B), 0.70; $\delta_P([^2H_1]\text{-}CDCl_3)$ 149.42 and 149.02 (1P, d, P^{III}); *m/z* (FAB) 754.33698 ($M+1^+$, Calc. for $C_{41}H_{49}N_5O_7P$, 754.33694).

Oligonucleotide Synthesis

Oligonucleotide synthesis was performed using solid phase cyanoethyl-*N*,*N*-diisopropylphosphoramidite chemistry on an Applied Biosystems 394 automated DNA sythesiser equipped with on-line long wave detector (498nm). All DNA synthesis reagents and phosphoramidite monomers were supplied by Applied Biosystems. Compound [7] was dried *in vacuo* with P_2O_5 for 24 h and used as a 0.12M solution in anhydrous acetonitrile. In general all coupling efficiencies were >98.5%. "Trityl-off" sythesis was carried out and oligonucleotides were cleaved from the resin with concentrated ammonia and deprotected by incubation at 55°C in concentrated ammonia for 6 h.

HPLC Analysis and Purification of Oligonucleotides

Oligonucleotide analysis and purification was carried out by HPLC on a Gilson Model 306 equipped with a Brownlee Aquapore Octyl reverse phase column (10mm x 250mm).The eluting buffers used were: buffer A-100mM NH_4OAc and buffer B-100mM NH_4OAc plus 25% acetonitrile eluting with the following gradient:

Time/min	Flow Rate/ml.min^{-1}	% Buffer B
0	3	0
3	3	0
5	3	20
24	3	70
26	3	100
28	3	100
29	3	0
32	0	0

Analytical scale runs were performed at 260nm and 0.5aufs. Preparative scale runs were performed at 298nm and 1aufs.

Enzymatic Digestion of Oligonucleotides

Oligonucleotides (3 to 6 OD_{260} units) dissolved in enzyme digest buffer (500µl) were incubated at 37°C with snake venom phosphodiesterase I (0.05 units) and calf thymus alkaline phosphatase (0.75 units). After 48 h the solutions were analysed by HPLC as above using the following buffers: buffer A-0.1M NH_4OAc and buffer B-0.1M NH_4OAc plus 20% acetonitrile.

Oligonucleotide Storage

Oligonucleotides were desalted by gel filtration NAP-10 column chromatography to the manufacturer's specifications eluting with distilled water and stored at -20°C in frozen solutions or freeze dried solids.

Dot Blot Protocol

1) Oligonucleotide solution (500nl) was spotted onto nylon membrane and allowed to dry.

2) The membrane was irradiated at 254nm for 5min

3) Blocking buffer (20ml) was applied and incubated at room temperature for 30min

4) The membrane was washed with PBS/T (5x).

5) Anti-εC antibody (20ml diluted to 1/1000 with PBS/T from approximately 1mgml^{-1} stock solution) was applied and incubated at room temperature for 3 h.

6) Repeated 4).

7) Rabbit anti-mouse antibody/HRP (20ml diluted 1/1000 with PBS/T) was applied and incubated at room temperature for 1 h.

8) Repeated 4).

9) DAB substrate (10ml) was applied and incubated at room temperature for 30min

This dot blot protocol was modified for protein fixation by using nitrocellulose membrane. This only required drying, irradiation being unnecessary.

3β-D-2'-deoxyribofuranosyl imidazo-[2,1-*i*]-purine (εA) **[8]**[86]

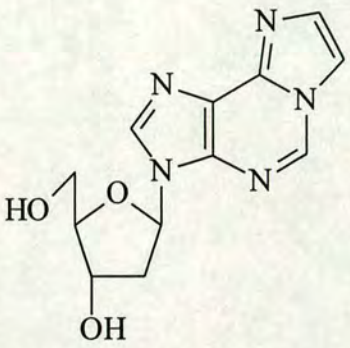

Compound [1] (8.7mmol, 6eq) was added in portions (9 x 1ml) to a stirred solution of 2'-deoxyadenosine.H_2O (400mg, 1.45mmol, 1eq) in acetate buffer (20ml). The pH was periodically adjusted to 4.5 by the addition of sodium acetate solution (0.2M) and the solution warmed to 40°C. After 24 h the solution was concentrated *in vacuo* and triturated with 50% ether in ethyl acetate (100ml). The resulting solid was filtered and washed with 50% ether in ethyl acetate and dried *in vacuo* to yield the title compound as a white solid (361mg, 1.33mmol, 91%), R_f (in A) 0.35; δ_H([$^2H_6$]-DMSO) 9.28 (1H, s, 5-H), 8.54 (1H, s, 2-H), 8.07-8.06 (1H, d, 7-H), 7.56-7.55 (1H, d, 8-H), 6.50-6.45 (1H, t, 1'-H), 5.43-5.41 (1H, d, 3'OH), 5.05-5.00 (1H, t, 5'OH), 4.47-4.44 (1H, p, 3'-H), 3.93-3.88 (1H, q, 4'-H), 3.68-3.50 (2H, m, 5'-H), 2.80-2.69 (1H, m, 2'-H) and 2.43-2.34 (1H, m, 2'-H); δ_C([$^2H_6$]-DMSO) 140.62 (C), 139.77 (CH), 138.21 (C), 137.09 (CH), 132.83 (CH), 123.15 (C), 112.30 (CH), 88.99 (CH), 83.99 (CH), 70.74 (CH), 61.70 (CH_2) and under DMSO (CH_2); λ_{max}(H_2O)/nm 296, 275, 266, 259; υ_{max}(nujol mull)/cm^{-1} 3284 (OH) and 1642 (aromatic ring system); *m/z* (FAB) 276.10966 ($M+1^+$; Calc. for $C_{12}H_{13}N_5O_3$, 276.10961).

2-Amino-6-oxo-3β-D-5',3'-*O*-(1,1,3,3-tetraisopropyldisiloxy)ribofuranosylpurine [9][100]

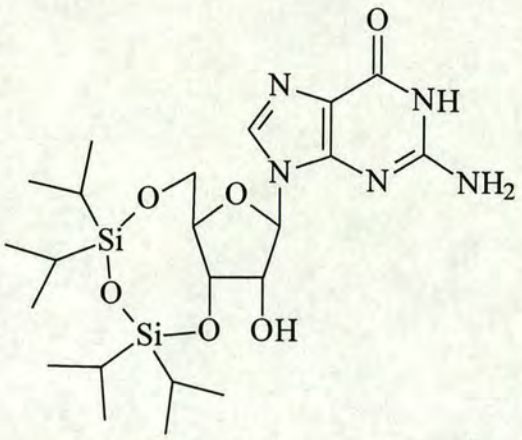

Guanosine (1.108g, 3.92mmol, 1eq) and 4-dimethylaminopyridine (49mg, 0.4mmol, 0.1eq) were coevaporated with anhydrous pyridine (3 x 25ml) and dissolved in anhydrous pyridine (75ml). 1,3-dichloro-1,1,3,3-tetraisopropyldisiloxane (1.526ml, 1.36g, 4.312mmol, 1.1eq) was added, dropwise, with stirred at room temperature. After 72 h the suspension was concentrated *in vacuo* and coevaporated with toluene (3 x 30ml). The resulting oil was dissolved in DCM (50ml), washed with saturated KCl solution (30ml) and the aqueous phase extracted with DCM (3 x 50ml). The combined organic fractions were dried over Na_2SO_4, filtered, concentrated *in vacuo* and purified by wet flash silica gel chromatography eluting with 0 to 5% gradient of methanol in DCM. The appropriate fractions were collected and concentrated *in vacuo* to yield the title compound as a white solid (1.605, 3.06mmol, 78%), R_f (in C) 0.26; $\delta_H([^2H_6]\text{-DMSO})$ 7.76 (1H, s, 8-H), 7.34 (2H, s, NH_2), 6.53 (1H, s, OH), 5.69-5.68 (1H, d, 1'-H), 4.37-4.11 (1H, m, 2'-H), 4.05-3.88 (2H, m, 4'-H and 3'-H), 3.48 (6H, s, 5'-H and propyl-H) and 1.03-0.97 (24H, ds, Me); $\delta_C([^2H_6]\text{-DMSO})$ 157.05 (C), 154.06 (C), 150.78 (C), 128.50 (CH), 116.94 (C), 88.11 (CH), 81.18 (CH), 74.18 (CH), 69.75 (CH), 60.83 (CH), 17.51 (CH_3), 17.35 (CH_3), 17.11 (CH_3), 17.04 (CH_3), 13.00 (CH), 12.66 (CH), 12.55 (CH) and 12.22 (CH); $\lambda_{max}(H_2O)$/nm 282, 259, 232(hump) and 213; υ_{max}(nujol mull)/cm^{-1} 3336, 3188 (OH, NH), 1699, 1625, 1578 and 1539 (C=O and aromatic ring system); *m/z* (FAB) 526.25026 ($M+1^+$; Calc. for $C_{22}H_{39}N_5O_6Si_2$).

1-*N*-(2,2-diethoxyethyl)-2-amino-6-oxo-3β-D-5',3'-(1,1,3,3-tetraisopropyldisiloxy)ribofuranosylpurine [10][91]

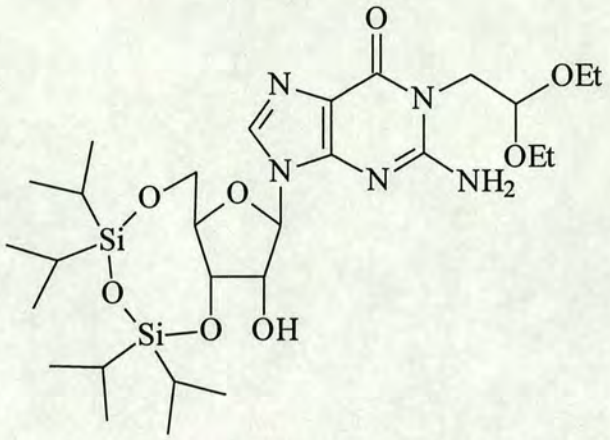

To a solution of compound [9] (800mg, 1.52mmol, 1eq) in DMF (50ml), bromoacetaldehyde diethylacetal (356μl, 450mg, 2.28mmol, 1.5eq) and powdered potassium carbonate (314mg, 2.28mmol, 1.5eq) were added. The suspension was stirred at 90°C and after 24 h the solution was concentrated *in vacuo*. The resulting oil was dissolved in DCM (50ml) and washed with saturated KCl solution (30ml). The aqueous phase was extracted with DCM (3 x 50ml) and the combined organic fractions were dried over Na_2SO_4, filtered and concentrated *in vacuo*. The product was purified by wet flash silica gel chromatography eluting with 0 to 2% gradient of methanol in DCM and the appropriate fractions were concentrated *in vacuo* to yield the title compound as a pale yellow foam (809mg, 1.26mmol, 55%), R_f (in C) 0.77; $\delta_H([^2H_6]$-DMSO) 7.78 (1H, s, 8-H), 7.33 (2H, s, NH_2), 6.88 (1H, s, OH), 5.70-5.68 (1H, d, 1'-H), 4.73-4.68 (1H, t, 11-H), 4.38-4.27 (1H, m, 2'-H), 4.11-3.88 (2H, m, 4'-H and 3'-H), 3.70-3.53 (2H, m, 5'-H), 3.48 (4H, s, propyl-H) and 0.90-1.33 (36H, m, 10-H, ethoxy-H and Me); $\delta_C([^2H_6]$-DMSO) 156.84 (C), 154.90 (C), 148.89 (C), 128.47 (CH), 116.24 (C), 100.51 (CH), 87.84 (CH), 81.25 (CH), 74.13 (CH), 69.84 (CH), 63.21 (CH_2), 63.13 (CH_2), 60.90 (CH_2), 44.79 (CH_2), 17.48 (CH_3), 17.34 (CH_3), 17.08 (CH_3), 17.01 (CH_3), 15.36 (CH_3), 13.00 (CH), 12.67 (CH), 12.55 (CH) and 12.22 (CH); $\lambda_{max}(H_2O)$/nm 275(hump) and 258; υ_{max}(nujol mull)/cm^{-1} 3398, 3195 (OH and NH), 1681, 1648, 1609,1570 and 1539 (C=O and aromatic ring system); *m/z* (FAB) 642.33501 ($M+1^+$; Calc. for $C_{28}H_{51}N_5O_8Si_2$, 642.33545).

8,9-Dihydro-9-oxo-3-β-D-furanosylimidazo-[2,1-*a*]-purine (εG_2) **[11]**[91]

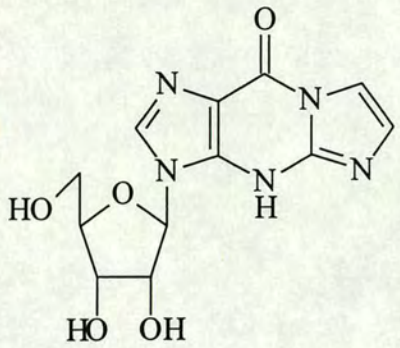

Compound [10] (500mg, 780μmol) was dissolved in methanol (10ml) and HCl solution (50ml, 1M) added. The solution was stirred at room temperature and after 24 h the pH was adjusted to 7 with NaOH solution (2M). The solution was concentrated *in vacuo* and the resulting yellow oil purified by wet flash silica gel chromatography eluting with 0 to 9% gradient of methanol in 1% triethylamine in DCM. The appropriate fractions were concentrated *in vacuo* to yield the title compound as a pale yellow solid (158mg, 515μmol, 66%), R_f (in C) 0.17; $\delta_H([^2H_6]$-DMSO) 8.17 (1H, s, 2-H), 7.62-7.61 (1H, d, 7-H), 7.45-7.44 (1H, d, 8-H), 5.83-5.81 (1H, d, 1'-H), 4.49-4.45 (1H, t, 2'-H), 4.15-4.11 (1H, t, 3'-H), 3.94-3.89 (1H, q, 4'-H) and 3.68-3.51 (2H, m, 5'-H); $\delta_C([^2H_6]$-DMSO) 151.48 (C), 150.50 (C), 145.93 (C), 137.41 (CH), 116.77 (CH), 115.50 (C), 107.04 (CH), 86.94 (CH), 85.35 (CH), 73.87 (CH), 70.44 (CH) and 65.09 (CH_2); $\lambda_{max}(H_2O)$/nm 285 and 226; υ_{max}(nujol mull) 3390 (OH), 1709, 1594, 1578 and 1531 (C=O and aromatic ring system); *m/z* (FAB) 308.10084 ($M+1^+$; Calc. for $C_{12}H_{14}N_5O_5$, 308.09949).

2-Amino-6-oxo-N^7-(2-hydroxyethyl)-3-β-D-ribofuranosyl purine [12][93]

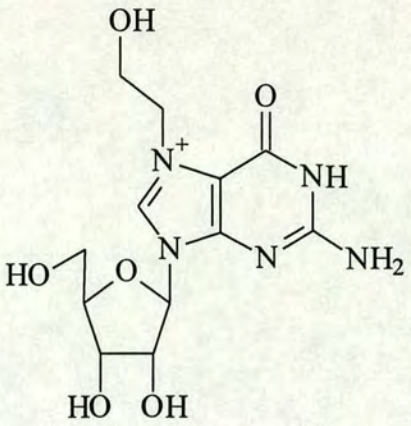

Ethylene oxide was bubbled into a stirred suspension of guanosine (2.83g, 10mmol) in glacial acetic acid (100ml) at room temperature until the turbid mixture cleared. After stirred for a further 20 min the reaction mixture was added to acetone (200ml) and ether (800ml) was added to precipiate the product. The solid was filtered, washed with ether (200ml) and dried *in vacuo* to yield the title compound as a white solid (3.195g, 8.26mmol, 83%), R_f (in A) 0.00; $\delta_H([^2H_6]$-DMSO) 9.32 (1H, s, 8-H), 7.80-7.50 (2H, s, NH_2), 6.50-6.10 (4H, s, OH), 5.85-5.84 (1H, d, 1'-H), 4.42-4.38 (3H, t, 11-H and 2'-H), 4.18-4.14 (1H, t, 3'-H), 4.00-3.98 (1H, d, 4'-H), 3.78-3.57 (4H, m, 10-H and 5'-H) and 1.79 (3H, s, acetate-H); $\delta_C([^2H_6]$-DMSO) 153.88 (C), 153.02 (C), 147.62 (C), 105.54 (C), 88.01 (CH), 83.24 (CH), 72.21 (CH), 67.06 (CH), 58.15 (CH_2), 56.96 (CH_2), 49.68 (CH_2) and 20.84 (CH_3); $\lambda_{max}(H_2O)$/nm 280, 256, 210; υ_{max}(nujol mull)/cm^{-1} 3333, 3479 (OH and NH), 1711, 1672, 1625, 1562 and 1523 (C=O and aromatic ring system); *m/z* (FAB) 328.12563 ($M+1^+$; Calc. for $C_{12}H_{18}N_5O_6$, 328.12571).

Imidazole ring opening of 2-amino-6-oxo-N^7-(2-hydroxyethyl)-3-β-D-ribofuranosylpurine [13][94]

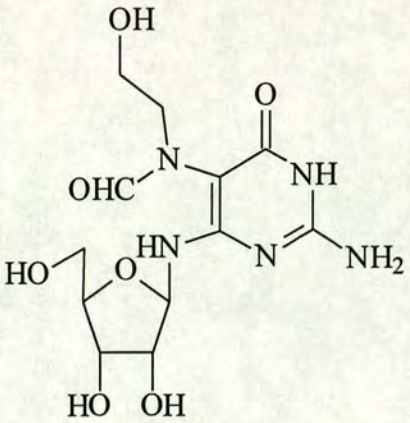

Compound [12] (1g, 258mmol) was dissolved in H_2O (10ml) and conc. NH_4OH (40ml) added. The solution was stirred at room temperature and after 24 h was concentrated *in vacuo* and then freeze dried to yield the title compound as a white solid (854mg, 2.48mmol, 96%), R_f (in D) 0.32; $\lambda_{max}(H_2O)$/nm 274; υ_{max}(nujol mull)/cm^{-1} 3328, 3156 (OH and NH), 1660 and 1578 (C=O and aromatic ring system); *m/z* (FAB) 346.13605 ($M+1^+$; Calc. for $C_{12}H_{19}N_5O_7$, 346.13627).

Preparation of Alkaline Phosphatase Labelled εC (εC/AP)

A solution of compound [5] (1mg, 2.85μmol, 1eq) in MES buffer (500μl) was warmed to 25°C and 1-ethyl-3-(3-dimethylaminopropyl)-carbodiimide.HCl (1mg, 2.85μmol, 1eq) was added. After 10min calf intestine alkaline phosphatase (50μl, 500μg in 3M NaCl, 1mM $MgCl_2$, 100μM $ZnCl_2$ and 30mM triethanolamine) was added with MES buffer (450μl) and incubated at 25°C for 5 h.The conjugate was purified by NAP-10 gel filtration chromatography to the manufacturer's specifications, eluting with PBS/BSA. A portion (100μl) was freeze dried and weighed against freeze dried PBS/BSA (100μl) to determine the quantity of conjugate. The conjugate was stored in PBS/BSA at 4°C until used.

Thawing Frozen Cell Lines

Cryotubes containing the anti-εC monoclonal antibody cell line were removed from liquid nitrogen storeage and rapidly thawed with warm water. The contents were transfered, within a laminar flowhood to a sterile container and diluted with RPMI/PS (10ml). The suspension was spun (500G, 5min) and the supernatant discarded. The pellet was resuspended in warm RPMI/PS (10ml) and kept at 37°C for 30min The suspension was spun (500G, 5min) and the supernatant discarded. The pellet was resuspended in 10% complete media (2ml), divided into two, 2ml wells and stored in a CO_2 incubator at 37°C.

Maintaining and Expanding Cell Culture

All cell manipulations were performed within a laminar flowhood. 5% complete medium was exchanged 3 times weekly. The culture was examined for cell growth and for growth exceeding 70% confluency the cells were suspended and transfered to a larger, sterile flask. This process was concluded when the culture was maintained in six, 1000ml flasks. The old medium was removed and spun (500G, 5min) and the supernatant retained and stored at 4°C or frozen at -4°C. Fresh 5% complete medium, warmed to 37°C, was added in equal volume and the cell culture returned to the CO_2 incubator at 37°C. Every month the cultures were transfered to fresh, sterile flasks to prevent microbial growth.

Methods of Antibody Purification

A) Ammonium Sulphate Precipitation

Antibody was concentrated from hybridoma culture media by $(NH4)_2SO_4$ precipitation. Saturated $(NH4)_2SO_4$, cooled to 4°C, was slowly added to an equal volume of hybridoma culture medium whilst stirred on ice, to give a 50% saturated $(NH4)_2SO_4$ solution. After 1 h the suspension was spun (8000G, 30min) and the supernatant discarded. The pellet was dissolved in the minimum quantity of H_2O and dialysed against PBS/azide (3 x 3000ml).

B) Ion Exchange HPLC

Antibody purification was carried out by HPLC on a Gilson Model 306 equipped with 3 pumps and a fraction collector.

Method 1: The HPLC apparatus was equipped with an Anachem Hydropore-AX Dynamax II ion exchange column (4.6mm x 100mm). The eluting buffers used were: buffer A-10mM K_2HPO_4 at pH 7.4, buffer B-10mM K_2HPO_4 at pH 7.4 plus 500mM NaCl. The sample buffer was: buffer C-Post $(NH4)_2SO_4$ concentrated antibody pre-filtered through 0.45um and 0.2um filters. The following elution gradient was used:

Time/mins	Flow Rate/mlmin^{-1}	% Buffer B	% Buffer C
0	1.5	0	0
1	1.5	0	0
3	1.5	0	100
13	1.5	0	100
14	2.0	0	0
18	2.0	0	0
19	2.0	0	0
21	2.0	0	0
22	2.0	0.5	0
23	2.0	25	0
25	2.0	60	0
28	2.0	60	0
30	2.0	0	0
34	2.0	0	0
35	0.0	0	0

Chromatography was performed at 280nm and 1aufs. The fraction collector started after 10 min and collected 2ml fractions, the antibody eluting in fractions 13 to 19.

Method 2: The HPLC apparatus was equipped with an Anachem Hydropore-SCX Dynamax II ion exchange column (4.6mm x 100mm). The eluting buffers used were: buffer A-20mM MES at pH 6.3 and buffer B-20mM MES plus 500mM NaCl at pH 6.3. The sample buffer was: buffer C-Post $(NH4)_2SO_4$ concentrated antibody pre-filtered through 0.45μm and 0.2μm filters. The following elution gradient was used:

Time/min	Flow Rate/ml.min^{-1}	%Buffer B	%Buffer C
0	2	0	0
1	2	0	0
2	2	0	100
11	2	0	100
12	2	0	0
17	2	0	0
18	2	70	0
23	2	70	0
24	2	70	0
25	2	70	0
26	2	0	0
30	0	0	0

Chromatography was performed at 280nm and 1aufs. The fraction collector started at 12 min and collected 2ml fractions, the antibody eluting in fractions 7 to 11.

C) Protein-A Affinity Chromatography Protocol

1) The affinity column was equilibrated with binding buffer (30ml).

2) Post $(NH_4)SO_4$ concentrated antibody (15ml) pre-filtered through 0.45μm and 0.2μm filters was double diluted with binding buffer and applied to the column.

3) The column was washed with binding buffer (50ml).

4) Eluting buffer was applied (10ml) and fractions (2ml) were collected with the addition of neutralising buffer (200μl).

5) The fractions were collected and analysed monitored spectrophotometrically at 280nm.

6) The peak fractions were pooled and dialysed against PBS/azide (3 x 1000ml).

7) The column was washed with binding buffer (30ml) then 20% ethanol (10ml) and stored in 20% ethanol at 4°C.

SDS-Polyacrylamide Gel Electrophoresis (SDS-PAGE)

SDS-PAGE analysis of purified of purified antibody was performed on a Hoefer Vertical Electrophoresis Sturdier SE-410 apparatus using the following solutions:

12% Resolving Gel	Volume/ml
Water	16.5
30% Acrylamide Mix	20.0
1.5M Tris pH 8.8	12.5
10% SDS	0.5
10%Ammonium Persulphate	0.5
TEMED	0.02

5% Stacking Gel	Volume/ml
Water	6.8
30% Acrylamide Mix	1.7
1.0M Tris pH 6.8	1.25
10% SDS	0.1
10% Ammonium Sulphate	0.1
TEMED	0.01

Antibody was desalted with Amicon-30 concentrators according to the manufacturer's specifications and 1 to 10μg fractions applied *per* well under denaturing conditions. The following low molecular weight markers were also applied to the outside wells:

Marker	Molecular Weight/kDaltons
Phosphorylase B	94
Albumin	67
Ovalbumin	43
Carbonic Anhydrase	30
Trypsin Inhibitor	20
α Lactalbumin	14

The gels were run at a constant current of 20mA (voltage going from 90 to 200V) for 3 h and developed with coomassie blue stain.

Antibody Storage

Purified antibody samples were stored for short periods of time (days or weeks) in PBS/azide at 4°C. For long periods of time (months) purified antibody samples were stored in PBS/azide at -20°C.

General ELISA Protocol

1) 96 well microtitre plates were coated with εC screen (100µl *per* well with 10µgml^{-1} in coating buffer) at room temperature overnight.

2) The plates were washed with PBS/T (5x), shaken and aspirated dry.

3) The plates were covered and stored at 4°C until used.

4) Anti-εC antibody (100µl *per* well diluted in PBS/T) was applied to the εC coated plates and incubated overnight.

5) Repeated 2).

6) Rabbit anti-mouse antibody/HRP (100µl *per* well at 1/1000 dilution in PBS/T) was applied and incubated at room temperature for 2 h.

7) Repeated 2).

8) TMB substrate (100µl *per* well) was applied and after 30 min incubation at room temerature the resultant blue colour was quantified spectrophotometrically at 690nm on an ELISA plate reader.

This ELISA protocol was modified for the following applications:

Antibody Titre

As above except 4) Anti-εC antibody (100µl double diluted in PBS/T) was applied in triplicate at each dilution to εC coated plates and incubated at room temperature overnight.

Inhibition

As above except 4) Anti-εC antibody dilution that gave approximately 2OD at 690nm was applied (50µl *per* well) in triplicate with a range of concentrations of inhibitor (50µl *per* well in PBS) to εC coated plates and incubated at room temperature overnight.

Isotyping

As above except 6) Secondary antibody/HRP specific to the different mouse antibody isotypes (IgM, IgG_1, IgG_{2a}, IgG_{2b}, IgG_3, κ and λ) were applied (100µl *per* well at 1/100 dilution with PBS/T) and incubated at room temperature for 1 h.

εC/AP Titre

As above except 1) 96 well microtitre plates were coated with anti-εC antibody (100µl *per* well with 10µgml^{-1} in 100mM $NaHCO_3$ at pH=9.5) at room temperature for 1 h.

3) Plates were used immediately.

4) εC/AP (100µl *per* well diluted to 1/100 then double diluted with PBS/T) was applied in triplicate at each dilution to antibody coated plate and incubated at room temperature for 2 h.

6) Step omitted.

7) Step omitted.

8) pNPP substrate (100µl *per* well) was applied and after 30min incubation at room temperature the resultant yellow colour was quantified spectrophotometrically at 405nm with a reference at 450nm on an ELISA plate reader.

Antibody Affinity

As above except 1) 96 well microtitre plates were coated with anti-εC antibody (100µl *per* well with 10µg.ml^{-1} in 100mM $NaHCO_3$ at pH=9.5) at room temperature for 1 h.

3) Plates were used immediately.

4) εC/AP (100µl *per* well double diluted from 1/160 to 1/81920 with PBS/T) was applied in triplicate to rows B to D on εC coated plate. PBS/T (100µl *per* well) was applied in triplicate to rows E to G on the same plate and the plate incubated for 2 h.

6) Step omitted.

7) Step omitted.

8) εC/AP (50µl *per* well double diluted from 1/80 to 1/40960 with PBS/T) was applied in triplicate to rows E to G. pNPP substrate (100µl *per* well) was applied in triplicate to rows B to D and (50µl *per* well at double strength) to rows E to G. After 30min incubation at room temperature and the resultant yellow colour quantified spectrophotometrically at 410nm on an ELISA plate reader.

Isoelectric Focusing Gel

Isoelectric focusing gel was run using Pharmacia Phastgel apparatus with a pre-set isoelectric focusing gel and an isoelectric focusing pH 3 to pH 10 calibration kit:

Protein	pI
Trypsinogen	9.30
Basic Lentil Lectin	8.65
Middle Lentil Lectin	8.45
Acidic Lentil Lectin	8.15
Basic Horse Myoglobulin	7.35
Acidic Horse Myoglobulin	6.85
Human Carbonic Anhydrase	6.55
Bovine Carbonic Anhydrase	5.85
b-Lactoglobulin A	5.20
Soybean Trypsin Inhibitor	4.55
Amyloglucosidase	3.50

Anti-εC antibody (2μg) was loaded and the gel run according to the manufacturer's specifications.

Immunoaffinity Column Construction

Method 1: Coupling to Cyanogen Bromide (CNBr) Activated Sepharose

Used CNBr activated sepharose 4B purchased from Pharmacia. The following buffers were prepared:

a) Swelling Buffer: 1mM HCl.

b) Coupling Buffer: 200mM $NaHCO_3$ and 500mM NaCl at pH 8.5-9.0.

c) Blocking Buffer: 50mM Tris at pH 8.0.

d) Acetate Buffer: 100mM NaOAc and 500mM NaCl at pH 4.0.

Protocol:

1) Anti-εC antibody (11.4mg in 2ml PBS) was dialysed against coupling buffer (3 x 500ml) and made upto 6ml with coupling buffer.

2) CNBr activated Sepharose 4B (860mg) was poured onto a glass sinter funnel (porosity 4) and washed with swelling buffer (200ml) for 15minThe gel swelled to approximately 3ml.

3) The gel was quickly washed with coupling buffer (6ml) and aspirated dry.

4) The gel was transfered to the antibody solution from 1) to give a 2:1 (v/v) antibody:gel suspension.

5) The suspension was slowly tumbled on an end-to-end mixer for 20 h at 4°C.

6) The suspension was filtered and washed with blocking buffer (6ml) and the combined filtrate and washing solution was analysed spectrophotometrically at 280nm for unbound antibody.

7) The gel was resuspended in blocking buffer (6ml) and slowly tumbled on an end-to-end mixer at room temperature for 2 h.

8) The gel was poured into a column (12mm x 107mm with porous polyethylene discs at top and bottom of gel bed). The column was washed with acetate buffer (10ml) and then blocking buffer (10ml). The washing was repeated.

9) The column was washed with PBS/azide (10ml) and stored in PBS/azide at 4°C.

Method 2: Coupling to Aldehyde Functionalised Agarose

Used Pierce Immunopure Ag/Ab Immobilization Kit 1. The kit contained:

Coupling Buffer: 100mM sodium phosphate and 0.05% sodium azide at pH 7.0.

Quenching Buffer: 1M Tris.HCl at pH 7.4.

Washing Buffer: 1M NaCl.

Reductant: $NaCNBH_3$.

Pre-swollen aldehyde functionalised agarose pre-packed in a column (12mm x 107mm with porous polyethylene discs at top and bottom of gel bed).

Protocol:

1) The column was equilibrated with coupling buffer (6ml).

2) Anti-εC antibody (28.3mg in 2.5ml of PBS) was added to the column. The column was capped at each end and slowly tumbled on an end-to-end mixer at room temperature for 2 h.

3) Reductant (200µl, 1M in coupling buffer) was added. The column was slowly tumbled on an end-to-end mixer for 2 h and then left standing at room temperature for 4 h.

4) The column was drained and equilibrated with quenching buffer (4ml) and the combined eluents analysed spectrophotometrically at 280nm for unbound antibody.

5) Quenching buffer (2ml) and reductant (200µl, 1M in quenching buffer) were added. The column was slowly tumbled on an end-to-end mixer for 30min

6) The column was washed with washing buffer (4 x 5ml) and PBS/azide (4 x 5ml). The column was stored in PBS/azide at 4°C.

Method 3: Coupling to Prepacked Pharmacia HiTrap Protein-A Column

Used pre-packed HiTrap Protein-A column from Pharmacia. The following buffers were prepared:

Binding Buffer: 100mM Tris at pH 7.4.

Coupling Buffer: 200mM Triethanolamine at pH 8.0.

Crosslinking Buffer: 20mM Dimethylpimelimidate in coupling buffer (made fresh).

Quenching Buffer: 20mM Ethanolamine in coupling buffer.

Protocol (all manipulations were carried out by 5 and 20 ml syringes):

1) The column was equilibrated with binding buffer (20ml).

2) Anti-εC antibody (19.2mg in 20ml of binding buffer) was slowly passed (3x) through the column.

3) The column was equilibrated with coupling buffer (20ml).

4) Over 45min crosslinking buffer (20ml) was passed through the column.

5) Over 5min quenching buffer (5ml) was passed through the column.

6) The column was washed with PBS/azide (40ml) and stored in PBS/azide at 4°C.

Method 4: Coupling to Protein-A Derivatised Agarose

Used Protein-A coupled to agarose purchased from Pierce. The following buffers were prepared:

Binding Buffer: 3M NaCl and 1.5M Glycine at pH 8.9.

Coupling Buffer: 200mM Triethanolamine at pH 8.0

Crosslinking Buffer: 20mM Dimethylpimelimidate in coupling buffer (made fresh).

Quenching Buffer: 20mM Ethanolamine in coupling buffer.

Protocol:

1) The gel (2ml) was suspended in binding buffer (30ml), spun (30G, 5min) and the supernatant discarded. This was repeated twice.

2) Anti-εC antibody (13.2mg in 4ml PBS/azide) with binding buffer (10ml) was added to the gel and slowly tumbled on an end-over-end mixer at room temperature for 1 h.

3) The suspension was spun (30G, 5min) and the pellet resuspended in coupling buffer (30ml). The washing was repeated twice and the washings combined and analysed spectrophotometrically at 280nm for unbound antibody.

4) Crosslinking buffer (30ml) was added and the suspension slowly tumbled on an end-to-end mixer at room temperature for 1 h.

5) The suspension was spun (30G, 5min) and the supernatant discarded.

6) Quenching buffer (30ml) was added and the suspension slowly tumbled on an end-to-end mixer for 5min

7) The gel was poured into a column (12mm x 107mm with porous polyethylene discs at top and bottom of gel bed) and washed with PBS/azide (50ml). The column was stored in PBS/azide at 4°C.

The above method was also used with the following modifications:

Modified Protocol 1: As above except:

1) Step omitted.

2) The suspension was spun (30G, 5min) and the supernatant discarded and the pellet resuspended in coupling buffer (30ml). The washing was repeated twice.

3) Crosslinking buffer (30ml) was added and the suspension slowly tumbled on an end-to-end mixer at room temperature for 1 h.

4) Anti-εC antibody (9.8mg in 4ml PBS/azide) with binding buffer (10ml) was added to the gel and slowly tumbled on an end-over-end mixer at room temperature for 1 h.

5) The suspension was spun (30G, 5min) and the supernatant analysed spectrophotometrically at 280nm for unbound antibody.

Modified Protcol 2: As above except:

2) Anti-εC antibody (7.1mg in 4ml PBS/azide) with binding buffer (10ml) was equilibrated with εC (1μmol) for 1 h then added to the gel and slowly tumbled on an end-over-end mixer at room temperature for 1 h.

Method 5: Coupling to Hydrazide Functionalised Agarose

Used Pierce Immunopure Ag/Ab Immobilization Kit 4. The kit contained:

Coupling Buffer: 100mM sodium phosphate and 0.05% sodium azide at pH 7.0.

Oxidation Vial: sodium *m*-periodate (5mg).

Desalting Column.

Pre-swollen hydrazide functionalised agarose pre-packed in a column (12mm x 107mm with porous polyethylene discs at top and bottom of gel bed).

Protocol:

1) Anti-εC antibody (31.1mg in 3ml PBS/azide) was concentrated to 1ml by Amicon-30 to the manufacturer's specifications.

2) The desalting column was equilibrated with coupling buffer (8ml) and the antibody solution (1ml) was desalted through the column. The antibody containing fractions were analysed specrophotometrically at 280nm.

3) The antibody solution (3ml) was added to the oxidation vial and gently swirled for 5min The vial was incubated at room temperature for a further 30min

4) The desalting column was equilibrated with coupling buffer (15ml) and the antibody solution (3ml) desalted through the column. The antibody containing fractions were analysed spectrophotometrically at 280nm.

5) The antibody solution (5ml) was added to the gel and slowly tumbled on an end-to-end mixer at room temperature for 16 h.

6) The column was drained and washed with coupling buffer (6ml) and the eluents analysed spectrophotometrically at 280nm for unbound antibody.

7) The column was washed with PBS/azide (20ml) and stored in PBS/azide at 4°C.

General Protocol for the Use of Immunoaffinity Columns to Trap εC Antigens

1) Storage buffer drained from column.

2) Column conditioned with 500mM NaCl (2 x column volume).

3) Column equilibrated with cold PBS (3 x column volume).

4) εC antigen in cold PBS (25% of the column volume) was added to column and allowed to enter gel bed.

5) Cold PBS (5% of the column volume) was added to the column and allowed to enter the gel bed.

6) The column was capped at the bottom and cold PBS (1ml) added. The column was capped at the top.

7) Incubate for 1 h at room temperature.

8) Caps were removed. Wash column with cold PBS (8 x column volume).

9) Washed column with cold water (4 x column volume).

10) Add elution buffer (2 x column volume) and collect fractions.

11) Washed column with PBS/azide (5 x column volume).

12) Capped column at bottom and add PBS/azide (2ml). Capped column at top and stored at 4°C.

On the first initial trial of the immunoaffinity column all fractions eluting from the column were collected.

Alkylation of the Antibody with Dimethylpimelimidate

Anti-εC antibody (200μg) was incubated with dimethyl pimelimidate.HCl (2ml of 10 to 20mM in 200mM triethanolamine buffer at pH 8.0) in Amicon microcon-30 at room temperature. After 45 min the vials were spun (3,500G, 5min) and PBS (1ml) added. The vial was inverted and spun (3,500G, 5min). The antibody solutions were analysed by ELISA titration with an antibody solution treated identically with dimethyl pimelimidate absent.

Alkylation of the Antibody with Acetic Acid

Anti-εC antibody (200μg) was incubated with a solution of acetic acid (100mM) and 1-ethyl-3-(3-dimethylaminopropyl)carbodiimide.HCl (5mg) in MES buffer (2ml) adjusted to pH 6.0. The mixture was incubated overnight at 40°C. The antibody solution was analysed by ELISA titration with an antibody solution treated identically with 1-ethyl-3-(3-dimethylaminopropyl)carbodiimide absent.

The Use of Amicon Concentators to Trap εC Antigens

Protocol:

1) εC oligonucleotides (1nM to 10μM in 100μl PBS) and anti-εC antibody (7μM in 100μl PBS) were added to Amicon microcon-100 and incubated for 16 h at 4°C.

2) The Amicon microcon-100 were spun (4,000G, 15min) and the eluent collected.

3) PBS (200μl) was added to the Amicon microcon-100 and spun (4,000G, 15min) and the eluent was collected.

4) 8M Urea (200μl) was added to the Amicon microcon-100 and incubated at room temperature for 2 h.

5) The Amicon microcon-100 was spun (10,000G, 15mins) and the eluent collected.

6) PBS (200μl) was added to the Amicon microcon-100 with the filter reversed and spun (4,000G, 15mins). The eluent was collected.

7) The collected eluent fractions were analysed using the dot blot protocol described above.

Preparation of 5,6-dihydro-5-oxo-6β-D-2'deoxyribofuranosylimidazo-[1,2-*c*]-pyrimidine 3'-Mono and 5',3'-Bis-phosphates (εC monophosphate and εC bisphosphate)

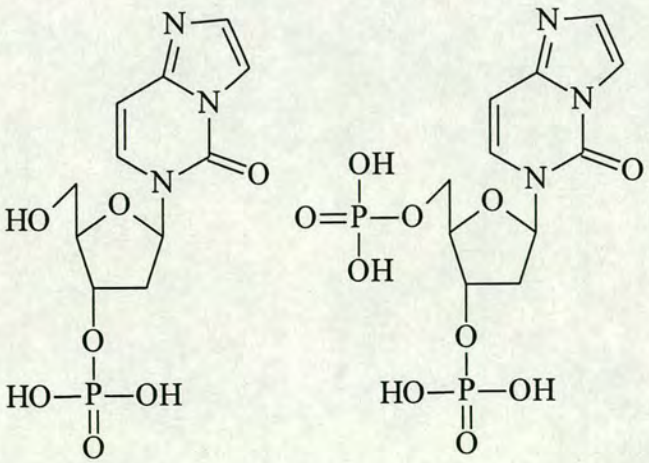

εC monophosphates and bisphosphates were prepared using the oligonucleotide synthesis methodology described above but incorporating a phosphate addition monomer supplied by Cruachem. Purification was achieved by reverse phase HPLC as above and desalting by gel filtration (G25 Sephadex) chromatography. The

appropriate fractions were collected and freeze dried to obtain the title compounds as white solids, εC monophosphate (2.0μmol), $\delta_P([^2H_2]\text{-}D_2O)$ 0.269 (1P, s, P^V); $\lambda_{max}(H_2O)$/nm 292(shoulder), 281(shoulder) and 272; *m/z* 330.05169 ($M\text{-}1^+$; Calc. for $C_{11}H_{13}N_3O_7P$, 330.04911), εC bisphosphate (2.86umol), $d_P([^2H_2]\text{-}D_2O)$ 2.423 (2P, d, P^V); $\lambda_{max}(H_2O)$/nm 292(shoulder), 281(shoulder) and 272; *m/z* 412.03115 ($M+1^+$; Calc. for $C_{11}H_{15}N_3O_{10}P$, 412.03110).

Analysis and Quantification of εC in Immunoaffinity Column Eluents

Method 1: When the antigen is an εC oligonucleotide

Collected fractions were aspirated dry, votexed with PBS (20μl) and analysed using the dot blot protocol described above with standard dilutions of εC oligonucleotide.

Method 2: When the antigen is an εC nucleoside

Collected fractions were aspirated dry, vortexed with PBS (50μl) and analysed using the collected fractions as competitors in the inhibition ELISA protocol described above with standard dilutions of εC nucleoside.

Method 3: When the antigen is an εC monophosphate

Collected fractions were freeze dried and vortexed with water (20μl). εC bisphosphate (10nmol to 10pmol) was added. The samples were analysed by CZE on an Applied Biosystems Model 270A Capillary Electrophoresis system with Microgel capillaries using 75mM Tris-phosphate with 10% methanol at pH 7.6 elution buffer. The on-line detector was set at 272nm with the loading voltage at -5kV, temperature at 30°C the running voltage at -15kV and the sample uptake time at 5 to 30s. Sample runs were recorded on a chart recorder set at: chart speed 1cm.min^{-1}, attenuation 16, offset 5 and peak threshold 1000.

Incubation of Double Stranded DNA with Chloroacetaldehyde

DNA duplex $d(GCGCTTAAGCGC)_2$ (1mg freeze dried) was dissolved in PBS (500μl) and an aliquot (50μl) removed. Chloroacetaldehyde (50μl diluted 1/10 with PBS from a 50% stock solution in water) was added and the solution incubated at 37°C. Aliquots (50μl) were removed at the following time intervals: t=1, 5, 10, 15,

30, 60 min The aliquots were immediately desalted by NAP5 gel filtration chromatography to the manufacturer's specifications eluting with enzyme digest buffer. The samples (1ml) were incubated at 80°C for 90 min and cooled to 37°C. Snake venom phosphodiesterase I (0.05 units) was added to each sample and incubated for 24 h at 37°C. The samples were purified by immunoaffinity chromatography as described above and the εC present quantified by method 3, adding εC bisphosphate (5nmol).

This experiment was repeated using a 100 fold dilution of chloroacetaldehyde

Incubation of Single Stranded DNA with Chloroacetaldehyde

As for the double stranded DNA incubation with chloroacetaldehyde but using single stranded DNA d(ACTCATGCCGGG) (1mg freeze dried) and using εC biphosphate (10nmol, 5nmol when chloroacetaldehyde diluted 100 fold) in analysis method 3.

Large Scale DNA Digestion to Nucleotides

Herring sperm DNA (2.21g freeze dried) was dissolved in enzyme digest buffer (10ml) and snake venom phosphodiesterase I (1 unit) added. The thick, brown suspension was incubated for 96 h at 37°C afterwhich the suspension became slightly turbid. Trypsin (100μg) was added and incubated for 24 h at 37°C. Soybean trypsin inhibitor (100μg) was added to the resulting clear solution and incubated for 2 h at 37°C. The solution was freeze dried to yield a brown powder.

CZE Analysis of Oligonucleotide Purity

Samples of puified oligonucleotides were analysed by CZE as described above.

^{31}P NMR of Oligonucleotides

DNA duplexes (approximately 450nmol freeze dried) were dissolved in 5mM KH_2PO_4 and 100mM KCl at pH 7.0. The samples were freezed dried in Eppendorf vials. The samples were dissolved in D_2O and ^{31}P NMR spectra recorded at 9.4T on a Bruker AM400 spectrometer using a 5mm phosphorus probe, and at 298K. The aquisition time was 1.708secs. with an additional delay of 1.2s. (recycle time of

2.9s.). The 90° pulse width was 1199.04Hz. WALTZ was used for proton decoupling, centred at 4.1ppm. Free induction decays were zero-filled once and apodised with 0.5Hz line-broadening exponential Fourier transformation

UV Thermal Denaturing Studies of Oligonucleotides

UV thermal denaturing was performed on a Perkin Elmer Lambda 15 UV/visible spectrophotometer equipped with a Perkin-Elmer Peltier block and controlled by an IBM PS2 microcomputer running a Perkin-Elmer PECSS2 software package to present absorbance versus time melting curves. Single stranded oligonucleotides were dissolved in UV melting buffer. Solutions were mixed to give double stranded oligonucleotides to give 5μM to 500nM solutions when made upto 2.5ml with UV melting buffer in a cuvette. UV thermal denaturing runs were performed in triplicate at 5 different concentrations at a linear gradient of $1^{\circ}C.min^{-1}$ from 10°C to 80°C at 260nm. The absorbance at 80°C was recorded and the concentrations of single strands determined using excinction coefficients. TCONV31 software package was used to convert to absorbance versus temperature and Perkin-Elmer PECSS2 software package to calculate the first derivative and the point of inflection.

Crystallisations of Oligonucleotides

The following solutions were made up and filtered through 0.2μm filters:

100mM $MgCl_2$.

10mM Spermine.4HCl.

50% Methylpentanediol (MPD).

50mM Sodium cacodylate at pH 6.5.

Pure, desalted and freeze dried DNA was dissolved in sodium cacodylate solution to give 50μl of a 2mM DNA solution and crystallisation plates made up as follows:

μl	1	2	3	4	5	6	7	8	9
Water	9	9	9	9	9	9	9	9	9
DNA	5	5	5	5	5	5	5	5	5
$MgCl_2$	X	X	X	X	X	X	X	X	X
MPD	5	5	5	5	5	5	5	5	5
Spermine	X	X	X	X	X	X	X	X	X

Where X was a variable quantity. The plates were covered with glass slides and sealed with vacuum grease. The plates were incubated at room temperature, 8°C or 4°C and periodically examined for crystal growth by microscope.

The Ratio of Double to Single Stranded DNA Analysed by CZE

Two duplex forming single strands of DNA (5mg/strand) were dissolved in water (25ml) and mixed together in the following solutions to make a total volume of 40μl:

Solution	**1**	**2**	**3**	**4**	**5**	**6**	**7**	**8**	**9**	**10**	**11**
Strand1/μl	25	24	23	22	21	20	19	18	17	16	15
Strand2/μl	15	16	17	18	19	20	21	22	23	24	25

The solutions were analysed by CZE as described above but at a running temperature of 25.5°C and using an eluting buffer of 75mM Tris-phosphate at pH 7.6.

FPLC Analysis and Purification of Oligonucleotides

Oligonucleotide analysis and purification by FPLC was carried out using a Pharmacia GP-250 Plus system with two LKB P-500 pumps equipped with a Pharmacia Resourse Q ion exchange column. The eluting buffers used for denaturing conditions were: buffer A-10mM NaOH at pH 12 and buffer B-10mM NaOH plus 1.5M NaCl at pH 12 and for non-denaturing conditions were: buffer A-50mM Tris at pH 7.4 and buffer B-50mM Tris plus 1.0M NaCl at pH 7.4. The following elution gradient was used:

Time/min	Flow Rate/mlmin^{-1}	% Buffer B
0	3	10
2	3	10
20	3	100
22	3	100
23	3	10
25	3	10

Analytical scale runs were performed at 260nm and 0.5aufs. Preparative scale runs were performed at 298nm and 1aufs.

REFERENCES TO CHAPTER ONE

1. Cairns J. (1978) Cancer: Science and Society, W.H. Freeman and Company, 15-33.

2. Cairns J. (1978) Cancer: Science and Society, W.H. Freeman and Company, 89-118.

3. DeVita V.T., Hellman S. and Rosenberg S.A. (1995) Biologic Therapy of Cancer, second edition, J.B. Lippincott Company, 95-102.

4. Blackburn G.M. and Kellard B. (1986) Chemistry and Industry, 606-613.

5. Watson J.D. and Crick F.H. (1953) Nature, 171, 737-738.

6. Watson J.D. and Crick F.H. (1953) Nature, 171, 964-967.

7. Zamenhof S., Brawerman G. and Chargaff E. (1952) Biochemistry and Biophysics Acta, 9, 402.

8. Saenger W. (1984) Principals of Nucleic Acid Structure, Springer-Verlag New York Inc., 116-158.

9. Crick F.H. (1970) Nature, 227, 561-563.

10. Lehninger A.L., Nelson D.L. and Cox M.M. (1993) Principals of Biochemistry, second edition, Worth Publishers New York, 324-358.

11. Lehninger A.L., Nelson D.L. and Cox M.M. (1993) Principals of Biochemistry, second edition, Worth Publishers New York, 814-858.

12. Franks L.M. and Teich N.M. (1991) An Introduction to the Cellular and Molecular Biology of Cancer, second edition, Oxford Medical Publications, 125-175.

13. Viola P.L., Bigotti A. and Caputo A. (1971) Cancer Research, 31, 516-522.

14. Drew R.T., Boorman G.A., Haseman J.K., McConnell E.E., Busey W.M. and Moore J.A. (1983) Toxicology and Applied Pharmacology, 68, 120-130.

15. Hong C.B., Winston J.M., Thornburg L.P. and Lee C.C. (1981) Journal of Toxicology and Environmental Health, 7, 909-924.

16. Berlin A., Draper M., Krug E., Roi R. and van der Venne M.T. (1990) The Toxicology of Chemicals: Carcinogenicity Volume 2, Commission of the European Communities, 127-136.

17. Heldaas S., Langard S.L. and Andersen A. (1984) British Journal of Industrial Medicine, 41, 25-30.

18. Laplanche A., Clavel F., Contassot J.C. and Lanouziere C. (1987) British Journal of Industrial Medicine, 44, 711-715.

19. Funes-Cravioto F., Lambert B., Linsten J., Ehrenberg L., Natarajan A.T. and Osterman-Golkar S. (1975) The Lancet 1, 459.

20. Purchase I.F.H., Richardson C.R. and Andersen D. (1975) The Lancet 2, 410-411.

21. Griem H., Bonse G., Radwan Z., Reichert D. and Henschler D. (1975) Biochemical Pharmacology, 24, 2013-2017.

22. Loprieno N., Barale R., Baroncelli S., Bronzetti G., Cammellini A., Corsi G., Leponini C., Niere R. and Rossi A.M. (1976) Screening Tests in Chemical Carcinogenesis, IARC Scientific Publications, 505-516.

23. Bolt H.M. (1986) The Role Of Cyclic Nucleic Acid Adducts in Carcinogenesis and Mutagenesis, IARC Scientific Publications, 261-268.

24. Barbin A., Bresil H., Croisey A., Jacquignon P., Malaveille C., Montesano K. and Bartsch H. (1975) Biochemical and Biophysical Research Communications, 67, 596-603.

25. Laib R.J., Klein K.P. and Bolt H.M. (1985) Carcinogenesis, 6, 65-68.

26. Guengerich F.P., Mason P.S., Stott W.T., Fox T.R. and Watanabe P.G. (1981) Cancer Research, 41, 4391-4398.

27. Laib R.J., Pellio T., Wunschel U.M., Zimmermann N. and Bolt H.M. (1985) Carcinogenesis, 6, 69-72.

28. Gwinner L.M., Laib R.J., Filser J.G. and Bolt H.M. (1983) Carcinogenesis, 4, 1483-1486.

29. Wade D.E., Alry S.C. and Sinsheimer J.E. (1978) Mutation Research, 58, 217-223.

30. Zajdela F., Croisey A., Barbin A., Malaveille C., Tomatis L. and Bartsch H. (1980) Cancer Research, 40, 352-356.

31. McCann J., Simmon V., Streitwieser D. and Ames B.N. (1975) Proceedings of the National Academy of Sciences USA, 72, 3190-3193.

32. Crebelli R., Conti G., Conti L. and Carere A. (1990) Mutagenesis, 5, 165-168.

33. Daniel F.B., DeAngelo A.B., Stober J.A., Olson G.R. and Page N.P. (1992) Fundamental and Applied Toxicology, 19, 159-168.

34. Krzyzosiak W.J., Wiewiorowski M. and Jaskolski M. (1986) The Role Of Cyclic Nucleic Acid Adducts in Carcinogenesis and Mutagenesis, IARC Scientific Publications, 75-81.

35. Singer B., Holbrook S.R., Fraenkel-Conrat H., Kusmierek J.T. (1986) The Role Of Cyclic Nucleic Acid Adducts in Carcinogenesis and Mutagenesis, IARC Scientific Publications, 45-56.

36. O'Neill I., Barbin A., Friesen M. and Bartsch H. (1986) The Role Of Cyclic Nucleic Acid Adducts in Carcinogenesis and Mutagenesis, IARC Scientific Publications, 57-73.

37. Park K.K., Liem P., Stewart B.C. and Miller J.A. (1993) Carcinogenesis, 14, 441-450.

38. Marnett L.J. and Burcham P.C. (1995) Chemical Research in Toxicology, 6, 771-785.

39. Vaca C.E., Wilhelm J. and Harms-Ringodahl M. (1988) Mutation Research, 195, 137-149.

40. Sodum R.S. and Chung F.L. (1988) Cancer Research, 48, 320-323.

41. Kandela J.C., Mrema J.E.K., DeAngelo A., Daniel F.B. and Guintaka R.V. (1990) Biochemical and Biophysical Research Communications, 167, 457-463.

42. Spengler S. and Singer B. (1981) Nucleic Acids Research, 9, 365-373.

43. Barbin A., Bartsch H., Leconte P. and Radman M. (1981) Nucleic Acids Research, 9, 374-387.

44. Hall J.A., Saffhill R., Green T. and Hathaway D.E. (1981) Carcinogenesis, 2, 141-146.

45. Jacobsen J.S., Perkins C.P., Callahan J.T., Sambamurti K. and Humayun M.Z. (1989) Genetics, 121, 213-222.

46. Kouchakdjian M., Eisenberg M., Yarema K., Basu A., Essigmann J. and Patel D.J. (1991) Biochemistry, 30, 1820-1828.

47. de los Santos C., Kouchakdjian M., Yarema K., Basu A., Essigmann J. and Patel D.J. (1991) Biochemistry, 30, 1828-1835.

48. Leonard G.A., McAuley-Hecht K.E., Gibson N.J., Brown T., Watson W.P. and Hunter W.N. (1994) Biochemistry, 33, 4755-4761.

49. Kusmierek J.T. and Singer B. (1982) Biochemistry, 21, 5723-5728.

50. Simha D., Yadau D., Rzepka K.W., Palejawala V.A. and Humayun M.Z. (1994) Mutation Research, 304, 265-269.

51. Jacobsen J.S. and Humayun M.Z. (1990) Biochemistry, 29, 496-504.

52. Palejawala V.A., Simha D. and Humayun M.Z. (1991) Biochemistry, 30, 8736-8743.

53. Singer B. and Spengler S.J. (1986) The Role Of Cyclic Nucleic Acid Adducts in Carcinogenesis and Mutagenesis, IARC Scientific Publications, 359-371.

54. Barbin A., Laib R.J., and Bartsch H. (1985) Cancer Research, 45, 2440-2444.

55. Singer B., Spengler S.J., Chavez F. and Kusmierek J.T. (1987) Carcinogenesis, 8, 745-747.

56. Cheng K.C., Preston B.D., Cahill D.S., Dosanjh M.K., Singer B. and Loeb L.A. (1991) Proceedings of the National Academy of Sciences USA, 88, 9974-9978.

57. Lindahl T. (1982) Annual Reviews in Biochemistry, 51, 61-87.

58. Swenberg J.A., Fedtke N., Groussel F., Barbin A. and Bartsch H. (1992) Carcinogenesis, 13, 727-729.

59. Oesch F., Adler S., Rettelbach R. and Doejer G. (1986) The Role Of Cyclic Nucleic Acid Adducts in Carcinogenesis and Mutagenesis, IARC Scientific Publications, 373-379.

60. Matijasevic Z., Sekiguichi M. and Ludlum D.B. (1992) Proceedings of the National Academy of Sciences USA, 89, 9331-9334.

61. Dosanjh M.K., Roy R., Mitra S. and Singer B. (1994) Biochemistry, 33, 1624-1628.

62. Dosanjh M.K., Chenna A., Kim E., Fraenkel-Conrat H., Samson L. and Singer B. (1994) Proceedings of the National Academy of Sciences USA, 91, 1024-1028.

63. Goding J.W. (1986) Monoclonal Antibodies: Principals and Practice, second edition, Academic Press, 5-58.

64. Yarmush M.L., Weiss A.M., Antonsen K.P., Odde D.J. and Yarmush D.M. (1992) Biotechnology Advances, 10, 413-446.

65. Cuatrecasas P. and Anfinsen C.B. (1974) Methods in Enzymology, 34, 345-378.

66. Hermanson G.T., Mallia A.K. and Smith P.K. (1992) Immobilised Affinity Techniques, Academic Press Inc., 52-60.

67. Wilchek M., Miron T. and Kohn J. (1984) Methods in Enzymology, 104, 3-23.

68. Affinity Chromatography: Principals and Methods (1979) Pharmacia Fine Chemicals Handbook, 92-94.

69.Erlanger B.F. and Beiser S.M. (1964) Proceedings of the National Academy of Sciences USA, 52, 68-74.

70. Strickland P.T. and Boyle J.M. (1984) Progress in Nucleic Acid Research and Molecular Biology, 31, 1-58.

71. Adamkiewicz J., Ahrens O., Eberle G., Nehls P. and Rajewsky M.F. (1986) The Role Of Cyclic Nucleic Acid Adducts in Carcinogenesis and Mutagenesis, IARC Scientific Publications, 403-411.

72. Poirier M.C. (1984) Environmental Mutagenesis, 6, 879-887.

73. Laib R.J., Bolt H.M., Cartier R. and Bartsch H. (1989) Toxicology Letters, 45, 231-239.

74. Bedell M.A., Dyroff M.C. and Doejer G. (1986) The Role Of Cyclic Nucleic Acid Adducts in Carcinogenesis and Mutagenesis, IARC Scientific Publications, 425-436.

75. Misra R.R., Chiang S.Y., Swenberg J.A. (1994) Carcinogenesis, 15, 1647-1652.

76. Young T.L. and Santella R.M. (1988) Carcinogenesis, 9, 589-592.

77. Eberle G., Barbin A., Laib F.C., Thomale J., Bartsch H. and Rajewsky M.F. (1989) Carcinogenesis, 10, 209-212.

78. Ciroussel F., Barbin A., Eberle G. and Bartsch H. (1990) Biochemical Pharmacology, 39, 1109-1113.

79. Swenberg J.A., Fedtke N., Ciroussel F., Barbin A. and Bartsch H. (1992) Carcinogenesis, 13, 727-729.

80. Guichard Y., Nair J., and Barbin A. and Bartsch H. (1993) Postlabelling Methods for Detection of DNA Adducts, IARC Scientific Publications, 263-269.

81. Barbin A., El Ghissassi F., Nair J. and Bartsch H. (1993) Proceedings of the National American Association for Cancer Research, 34, 136.

82. Butler V.P., Beiser S.M., Erlanger B.F., Tanenbaum S.W., Cohen S. and Bendich A. (1962) Proceedings of the National Academy of Sciences, 48, 1597-1602.

83. Jacob E.L. (1982) Journal of Immunology, 128, 895-901.

84. Ji T.H. (1983) Methods in Enzymology, 91, 580-609.

85. Erlanger B.F. (1980) Methods in Enzymology, 70, 85-104.

86. Srivastava S.C., Raza S.K. and Misra R. (1994) Nucleic Acids Research, 22, 1296-1304.

87. Habeeb A.F.S.A. (1966) Analytical Biochemistry, 14, 328-336.

88. Langone J.J., Boyle M.D.P. and Borsos T. (1978) Journal of Immunology, 121, 327-332.

89. Weir D.M. (1984) Immunochemistry Volume One, forth edition, Blackwell Scientific Publications, 38.1-38.17.

90. Boryski J. (1990) Nucleosides and Nucleotides, 9, 803-813.

91. Khazanchi R., Yu P.L. and Johnson F. (1993) Journal of Organic Chemistry, 58, 2552-2556.

92. Roe R., Paul J.S. and Montgomery P.O.B. (1973) Journal of Heterocyclic Chemistry, 10, 849-857.

93. van Delft J.H.M., van Weert E.J.M., Schellekens M.M., Claassen E. and Baan R.A. (1991) Carcinogenesis, 12, 1041-1049.

94. Jaskolski M., Krzyzosiak W., Sierzputowska-Gracz H. and Wiewiorwski M. (1981) Nucleic Acids Research, 9, 5423-5442.

95. Krzyzosiak W., Jaskolski M., Sierzputowska-Gracz H. and Wierwiorwski M. (1982) Nucleic Acids Research, 10, 2741-2753.

96. Kozerski L., Sierzputowska-Gracz H., Krzyzosiak W., Brateck-Wiewiorowska M., Jaskolski M. and Wiewiorowski M. (1984) Nucleic Acids Research, 12, 2205-2223.

97. Gibson N.J., Parkinson J.A., Barlow T., Watson W.P. and Brown T. (1994) Journal of the Chemical Society, Chemical Communications, 2241-2242.

98. Nelson H.C.M., Finch J.T., Luisi B.F. and Klug A. (1987) Nature, 330, 221-226.

99. Sihna N.D., Biernat J. and Koster H. (1983) Tetrahedron Letters, 24, 5843-5846.

100. Markiewicz W.T. (1979) Journal of Chemical Research, Synopsis, 24.

CHAPTER TWO

Immunochemical Detection of Oligonucleotide Probes Labelled with Dansyl Reporter Groups

Tae a Moose

"Wee sleeket, cowrin' tim'rous beastie,
O, what a panic's in thy breastie!
Thou need na start awa' sae hasty,
Wi' bickerin' brattle!'
I wad be laith to rin an' chase thee,
Wi' murderin' pattle!

I'm truly sorry man's dominion,
Has broken nature's social union,
An' justifies that ill opinion,
Which makes thee startle,
At me, thy poor, earth-born companion,
An' fellow mortal!"

Robert Burns (November 1785)

INTRODUCTION

It is well established that the macromolecule, DNA, with the exception of RNA viruses is the genetic information store for all cellular life. In recent years it has been shown that illnesses can be the result of abnormalities in the genetic code, due to viral infection or inherited genetic disease. It is now possible to diagnose such illnesses by probing genomic DNA for such abnormalities. The ability to synthesise and modify oligonucleotides that are complementary to intra-gene sequences has allowed the recognition of specific genomic DNA. A variety of methods have been employed to modify oligonucleotide probes to enable their detection.

Labelling synthetic oligonucleotides with radionuclides was the established technique. However, this methodology suffers from some serious drawbacks:

a) The three commonly used radionuclides, ^{32}P, ^{35}S and ^{125}I have short half-lives, 14.2, 87.4 and 59.6 days respectively, thus diagnostic experiments must be rapidly performed after labelling and long term storage is precluded.

b) Due to constant radioisotopic decay the intensity of emitted radiation is variable resulting in uncertain detection sensitivity.

c) The cost of these potentially hazardous materials and their safe handling is becoming increasingly prohibitive.

These factors can outweigh the advantages of the inherent sensitivity of this technique thus necessitating the development of cheap, safe and sensitive non-radioactive labelling methods.

Non-radioactive Labelling

Non-radioactive labelling of oligonucleotides is well established and has been reviewed in great detail[1-4], hence only a brief outline of non-radioactive labelling methods will be given here.

Oligonucleotide probes can be covalently tagged with labels that are themselves directly detectable or that promote the indirect binding of a detectable molecule. Directly detectable labels include fluorescent dyes which emit a quantifiable signal when irradiated or enzymatic labels which produce colourimetric

or chemiluminescent signals upon addition of a substrate. Indirectly detectable labels bind a protein-enzyme conjugate which is then detected in a second step. Commonly, this is an antibody-enzyme conjugate when the label is a hapten or a streptavadin-enzyme conjugate when the label is biotin (figure 1).

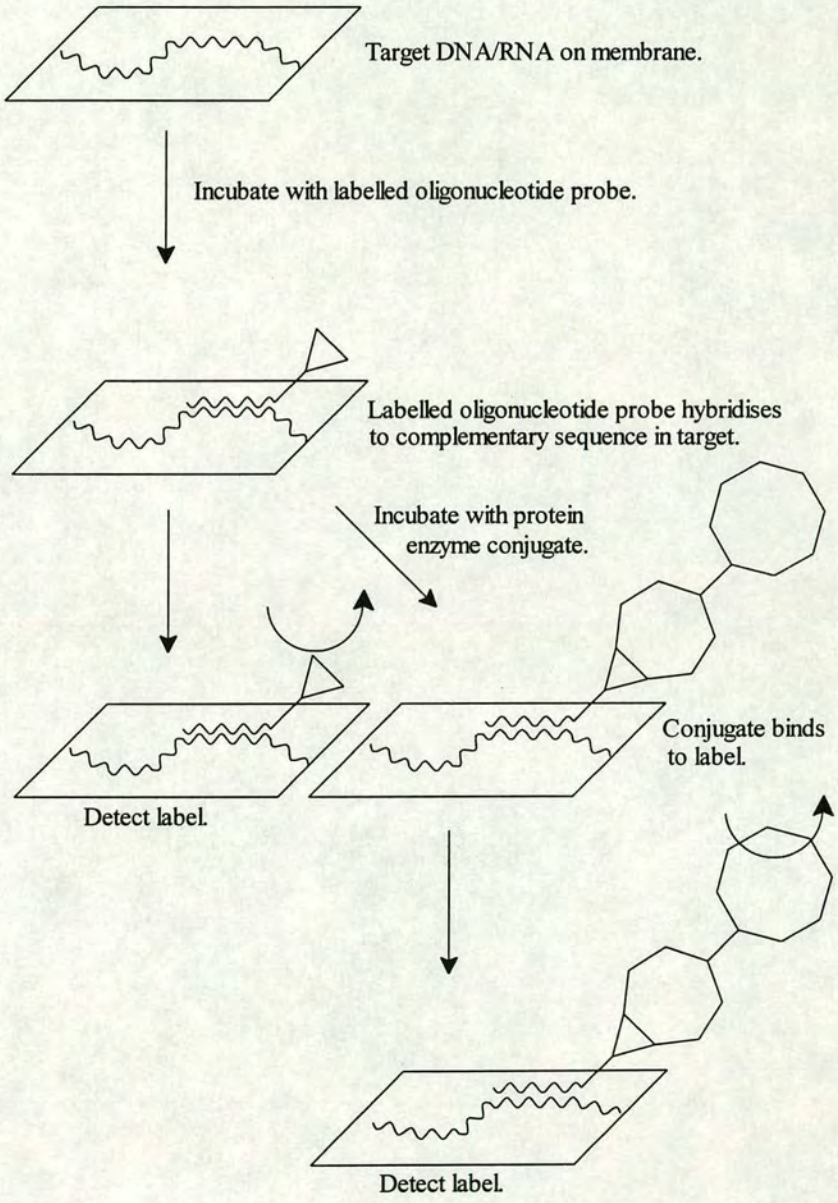

Figure 1: The Experimental Steps in Direct and Indirect Labelling Systems

Labels have been incorporated into oligonucleotides in a number of ways. They have been introduced enzymatically by the action of transferase and polymerase enzymes on modified nucleotide triphosphates and chemically by employing modified phosphoramidite monomers during automated oligonucleotide

synthesis. The modifications either include the labels themselves or reactive functionalities capable of incorporating labels post-synthetically (figure 2).

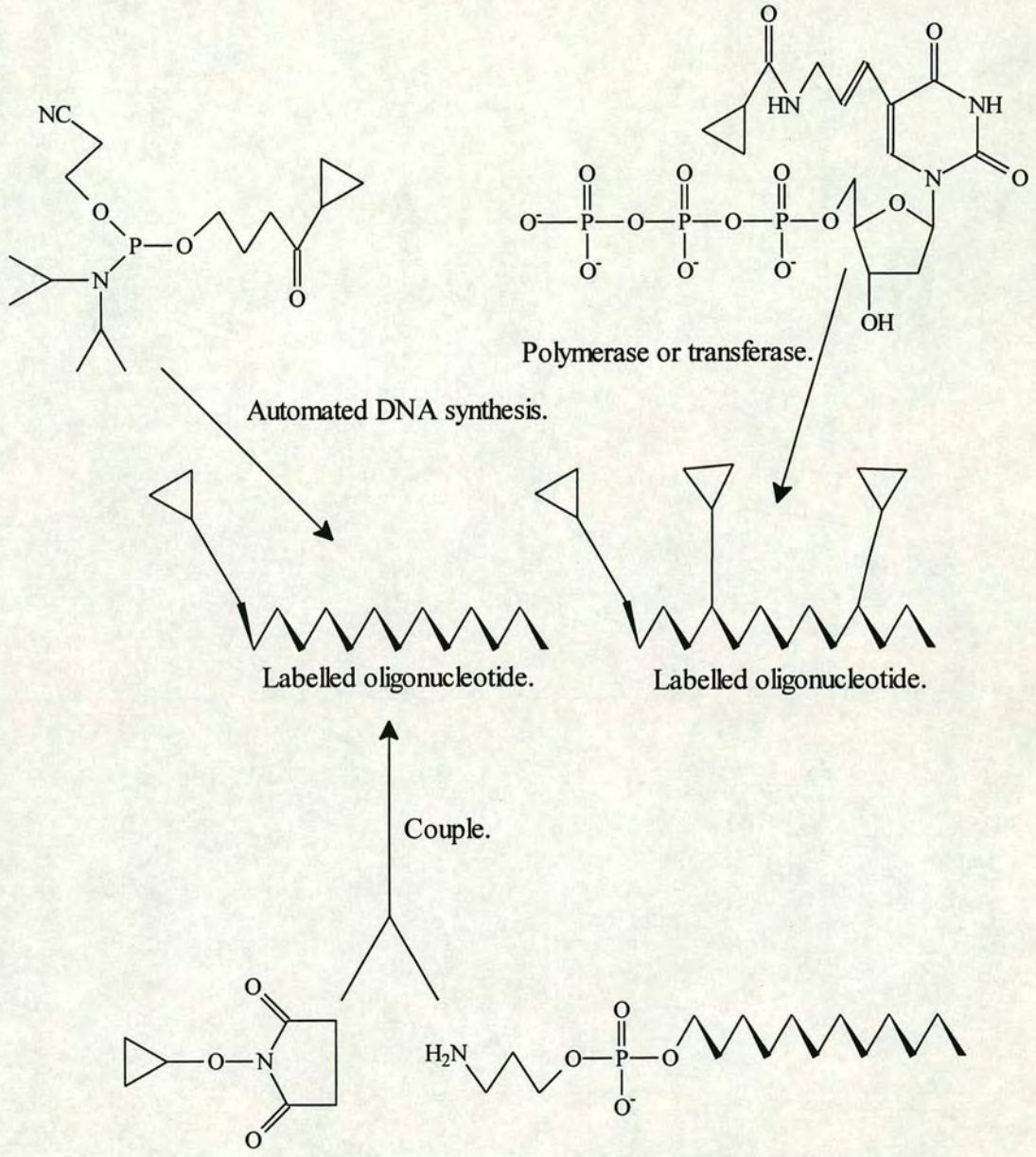

Figure 2: Label Incorporation into Oligonucleotides

Fluorescent dyes such as fluorescein, 7-nitrobenzo-2-oxa-1,3-diazole (NBD), tetramethylrhodamine and Texas Red (figure 3) have been introduced during automated oligonucleotide synthesis via their phosphoramidites[5,6] or by post-synthetically coupling electrophilic dervatives such as *N*-hydroxysuccinimides[7], isothiocyanates[8] and halides [8] to amino[9,10] or thiol[11] derivatised DNA.

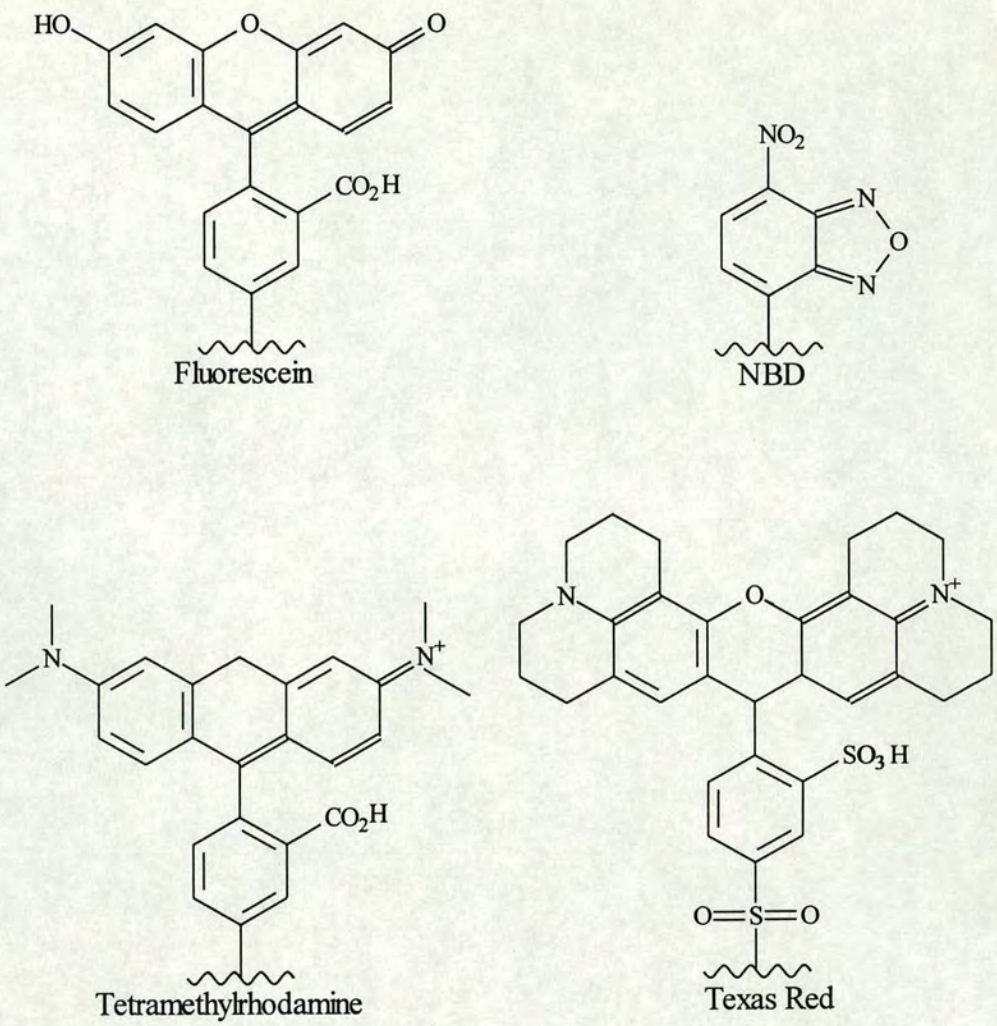

Figure 3: Fluorescent Labels

The enzymes horseradish peroxidase (HRP) and alkaline phosphatase (AP) have been covalently crosslinked to oligonucleotides by a variety of coupling methods[12-15]. The signal produced by such enzymes is entirely dependent on the choice of substrate. Colourimetric detection is based on enzymatic action converting a pale coloured or colourless, soluble substrate into a highly coloured soluble or insoluble product. Substrates which produce soluble products are 3,3',5,5'-tetramethylbenzidine (TMB) with HRP[16] and *para*-nitrophenyl phosphate (pNPP) with AP[17]. Substrates which produce insoluble products include 3,3'-diaminobenzidine (DAB) with HRP[18] and 5-bromo-4-chloro-3-indoyl phosphate/nitro blue tetrazolium (BCIP/NBT) with AP[19].

Although the fluorescent dyes and HRP and AP *via* a substrate are directly detectable they have disadvantages:

a) Experimental conditions such as solvent polarity heat and pH can distort fluorescent properties and can denature enzymes.

b) The size of these molecules, particularly enzymes may sterically inhibit the hybridisation of the probe to the target sequence.

c) Fluorescent dyes and detectors are costly and oligonucleotide-enzyme conjugates are time consuming and expensive to synthesise and purify.

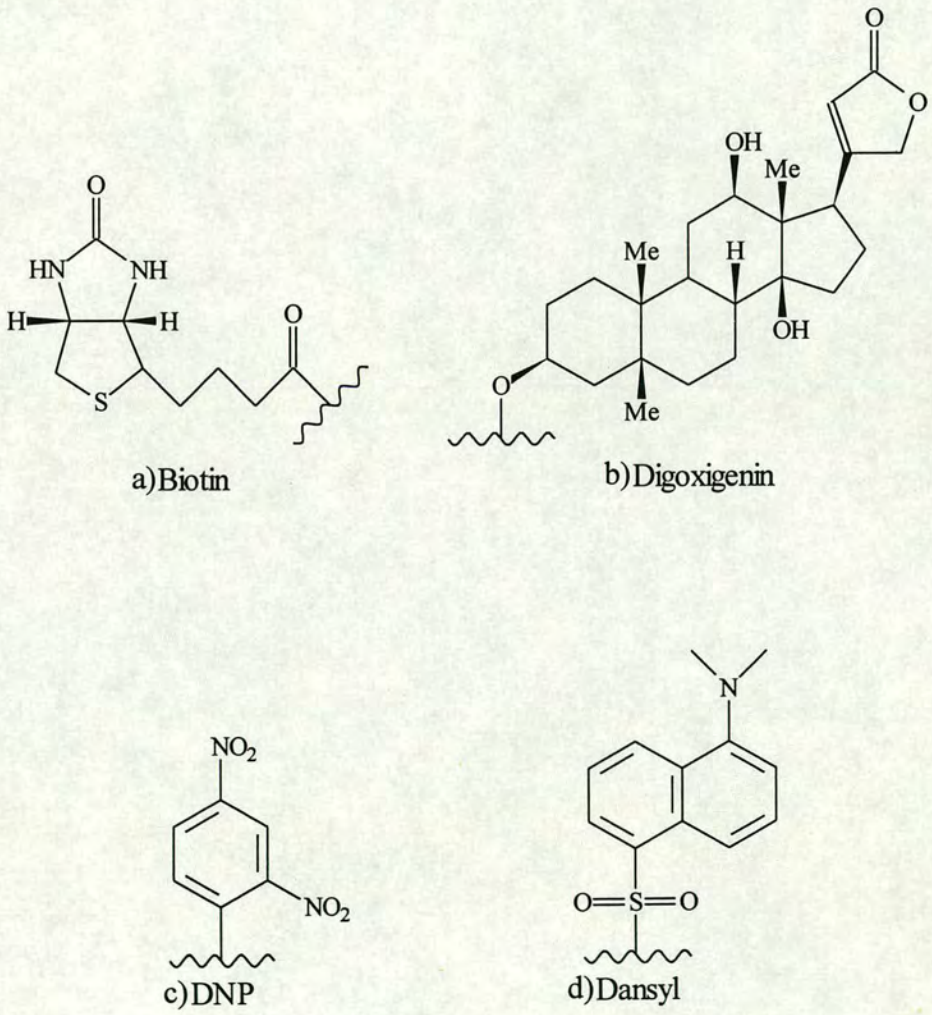

Figure 4: Indirect labels

The strong affinity between biotin (Vitamin H) (figure 4a) and the bacterial analogue of avidin, streptavidin, is commonly used in indirectly detectable labelling systems. Oligonucleotides have been labelled enzymatically *via* biotin labelled

deoxyuridine[20], deoxyadenosine[21] and deoxycytidine[21] triphosphates, during oligonucleotide synthesis *via* a variety of biotin phosphoramidites[22-25] and post-synthetically *via* *N*-hydroxysuccinimide[26,27], hydrazide[28] and azide[29] derivatives. Detection is accomplished by the secondary binding of a streptavidin-enzyme conjugate. The enzyme is commonly either HRP or AP using the colourimetric signal production outlined above. As with directly detectable labels, biotin and streptavidin-enzyme conjugates are expensive and biotin, which is of biological origin can also suffer problems with background contamination from the target sample.

Digoxigenin (figure 4b) is a large terpenoid which when used as a label circumvents the background contamination problems of biotin[30]. It has been incorporated into oligonucleotides enzymatically[31], during automated synthesis and post-synthetically[32]. This label is detected immunochemically by anti-digoxigenin antibodies conjugated to AP. The drawbacks with the use of digoxigenin as a label are its expense, instability to normal automated oligonucleotide synthesis conditions and multiple functionality, making it difficult to derivatise.

The potential of the 2,4-dinitrophenyl (DNP) group (figure 4c) as an oligonucleotide label has only recently been realised[33-37]. DNP's properties as a cheap, highly coloured, chemically simple, extremely immunogenic small molecule make it very attractive as a non-radioactive label. As the molecule is not found *in vivo* the background signal is low and high affinity anti-DNP antibodies are readily available. Detection is either by anti-DNP antibody-enzyme conjugates or by a two step anti-DNP antibody then anti-antibody-antibody enzyme conjugate system (figure 5).

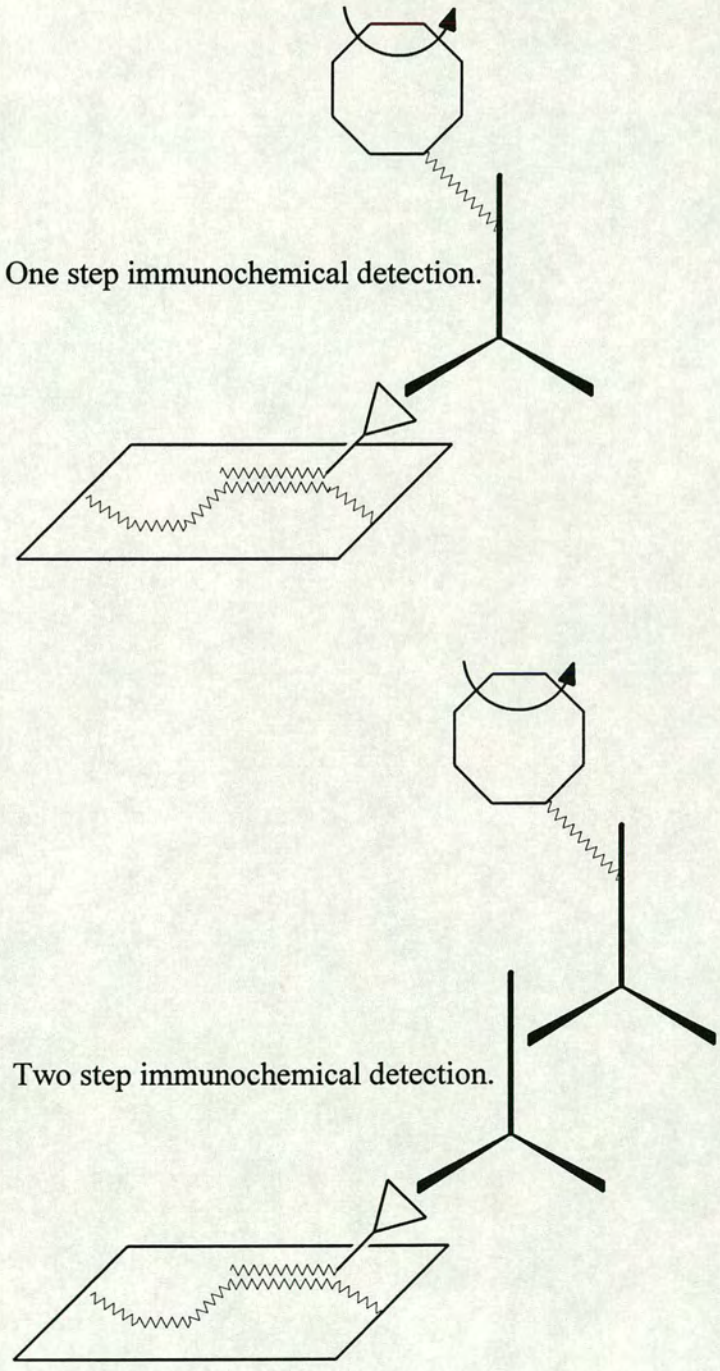

Figure 5: Immunochemical Detection

Antibodies

The Immune System

The immune system has developed to protect the host from attack by invading micro-organisms, parasites and cancer cells[38]. The mechanisms of innate and acquired immunity respond in tandem to foreign bodies whilst tolerating substances found in the host tissue[39]. Innate immunity is mediated by macrophages, natural killer cells and the activation of compliment. It is non-specific and non-adaptive, therefore unable to enhance the immune response upon repeated exposure[40]. Acquired immunity is dependent on cellular mechanisms capable of memorising exposure and eliciting specific responses[41].

Acquired Immunity

The mechanisms of acquired immunity are dependent on the recognition of foreign bodies by T and B lymphocytes *via* receptors on their surface[42]. The immune system is capable of synthesising vast repertoires of receptors and binding sites ($>10^8$) due to rearrangement of its genes and gene reading frames and also through point mutations. In this way highly specific binding sites are created[43].

Upon entering the host, foreign bodies, or antigens are recognised, engulfed and degraded into fragments by Antigen Presenting Cells (APC). The fragments are displayed on the cellular surfaces as complexes with glycoproteins. These Major Histocompatibility Complexes (MHC) bind specific T cell receptors activating InterLeukin (IL) growth factors which signal T cell proliferation (figure 6). As the binding of T cells is specific to the antigen-glycoprotein complex only a small fraction of the total T cell population is activated ie. only those capable of recognising the antigen. T cells then stimulate mechanisms to destroy the invading organism and participate in B cell proliferation[44].

B cells also bear antigen specific receptors which on binding the antigen are withdrawn and degraded. The antigen is presented as a MHC by the B cell, binding antigen specific T cells. T cell binding activates interleukin production, stimulating B cell differentiation and proliferation[45]. The majority of daughter B cells produce large antigen specific glycoproteins known as antibodies. However, some become memory

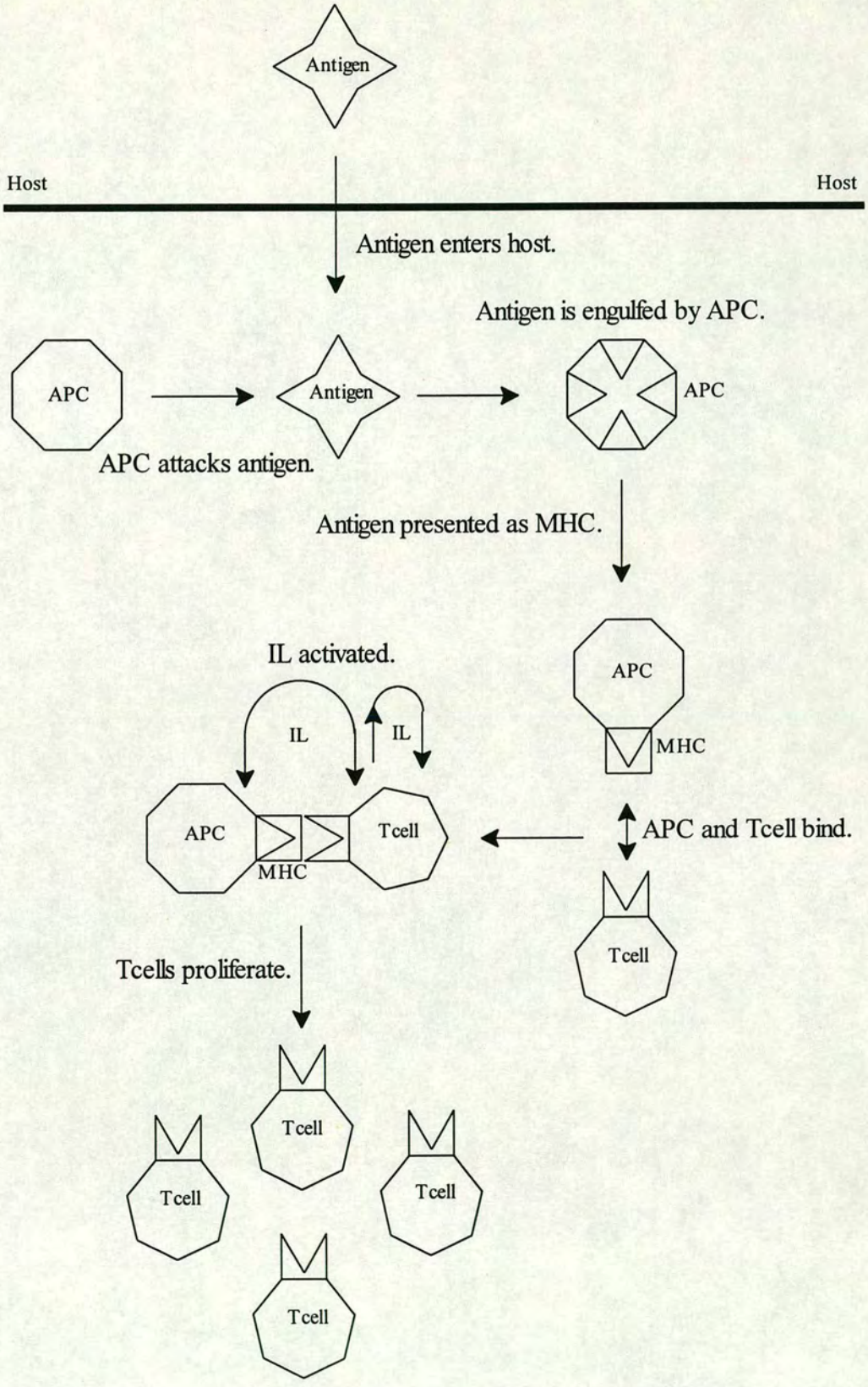

Figure 6: T Cell Mediated Immunity

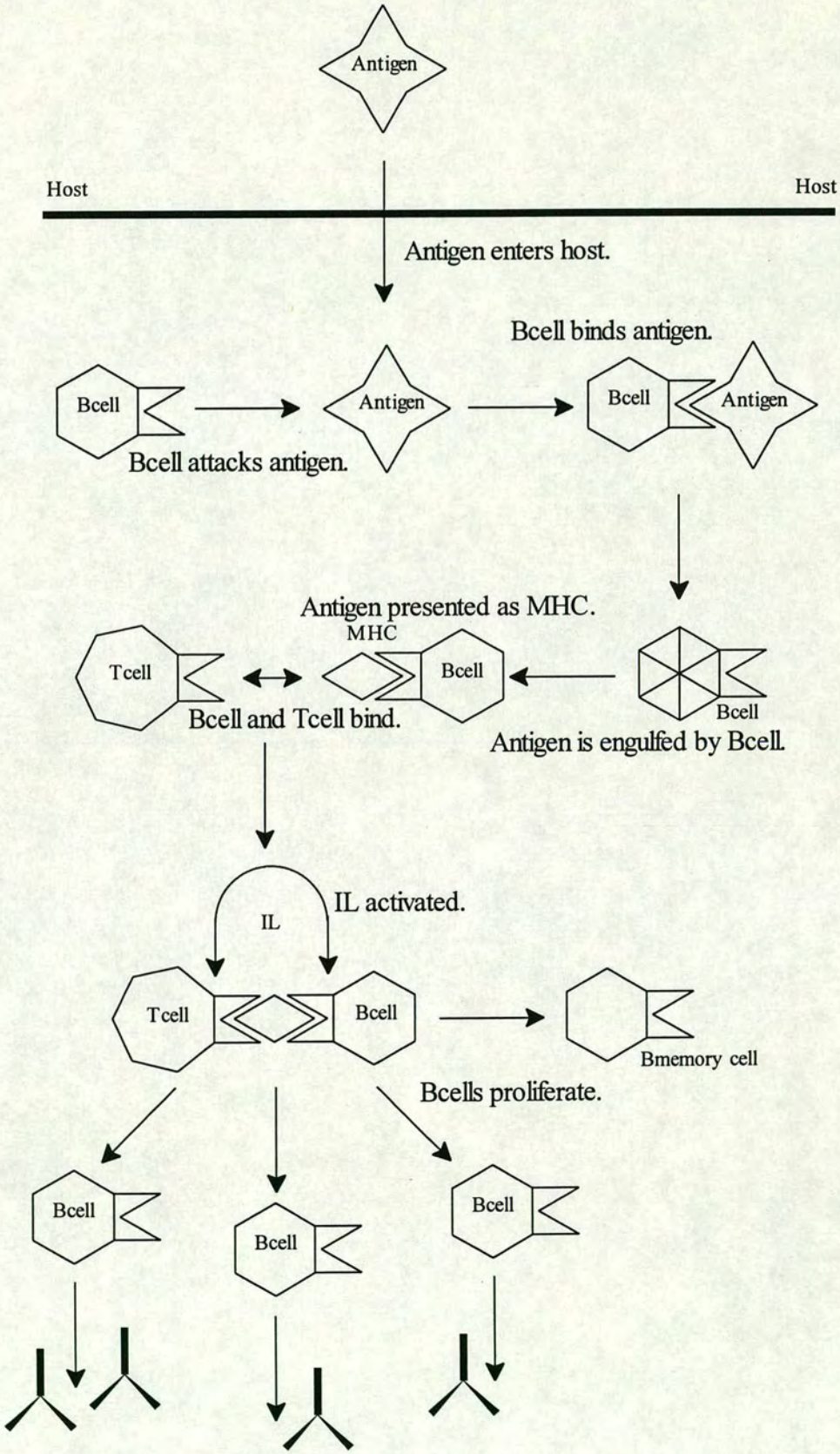

Figure 7: B Cell Mediated Immunity

cells capable of speedy reactivation of the immune system in reponse to further exposure to the antigen[46] (figure 7).

During differentiation, the B cells which bind most strongly to the antigen proliferate preferentially thus increasingly higher affinity antibodies are selected. There are five major classes of antibody IgA, IgD, IgE, IgG and IgM although only two, IgG and IgM, are present in large amounts within the plasma. Initially the immune system produces antibodies of the IgM class. However, these are often quickly superseeded by higher affinity antibodies of the IgG class when class switching takes place[47]. Initially the immune system responds to antigen presentation by synthesising antibodies of the IgM isotype. These are superseeded by mature IgG antibodies which have undergone successive cycles of gene recombination and mutation, selecting antibody binding sites of increasing affinity and specificity[48]. The biological functions of these antibodies are primarily antigen binding, coating it in an inactivating layer and promoting phagocytosis and compliment activation[49].

Production of Antibodies

In recent years the acquired immune system has been artificially harnessed to produce specific biochemical tools, antibodies with tailor-made binding sites.

Initially antibodies were produced by immunising mammals with the immunogen of interest. After boost immunisations the animals could be bled and the antibodies purified from the sera. This produced polyclonal antibodies. Most antigens have multiple antigenic determinants or epitopes, the regions where the antibody binds. These can be recognised by receptors on different B cells. Thus antibodies of different epitope specificities are generated, in a polyclonal response. Polyclonal antibodies are of variable affinity and specificity especially when impure immunogens are used[51].

Hybridoma technology was developed to allow the production of antibodies from a single B cell and these were termed monoclonal antibodies. These antibodies are advantageous in that they are of single determinant specificity and can be selected in terms of their affinity. This makes them desirable as diagnostic tools as they can be selected for their reproducible properties. The principle of the technique centres

on isolating mortal B cells from an immunised animal and fusing them with immortal myeloma cells creating hybrids of the two. In practice, the fusion process is random and a mixture of B cells, myeloma cells and multiple hybrids are formed, only some of which produce useful antibodies. These can be isolated by feeding the cells with a selective medium containing Hypoxanthine, Aminopterin and Thymidine (HAT). Aminopterin inhibits nucleotide biosynthesis and thus poisons cells. However, B cells express an enzyme, Hypoxanthine Guanine PhosphoRibosyl Transferase (HGPRT) which provides an alternative salvage pathway to nucleotide biosynthesis. Cells that express this enzyme survive aminopterin poisoning. Myeloma cells are deficient in the HGPRT gene and die in the presence of aminopterin. B cells, due to their mortality also decline in number over time thus leaving only cells capable of expressing the surviving HGPRT gene product ie. fused B cell-myeloma cells known as hybridomas (figure 8). The cells remaining are assayed for production of the required antibody and isolated from all the other cells in culture by cloning. This selection of hybridomas negates the need for immunogens of high purity[51]. Cloning is a process whereby the cells of interest can be isolated from all the other cells in culture. It is essential soon after the positive identification of antibody producing cells to reduce the risk of overgrowth by non-secreting cell lines. Cloning is also required to ensure monoclonality of the secreting cell lines.

Cells have been cloned by limiting dilution or in soft agar. Cloning by limiting dilution involves successive dilution of the selected hybridoma cell population into wells within culture plates resulting in a number of wells containing single cells. Cloning in soft agar separates cells by a solid phase barrier. This method often requires an additional reculturing step in liquid medium before antibody production can be screened. In practice several rounds of cloning are required before a monoclonal cell line has been achieved.

Hybridomas rarely survive culturing in isolation. However, it is possible to increase the efficiency of cell survival and growth by a factor of 10^4 by the addition of "feeder cells"[52]. The reasons for this are not understood but it is possible that feeder cells provide essential growth factors and signals for hybridoma

proliferation[53]. Cells that have been used as feeders are thymocytes, spleenocytes and peritoneal cells[51].

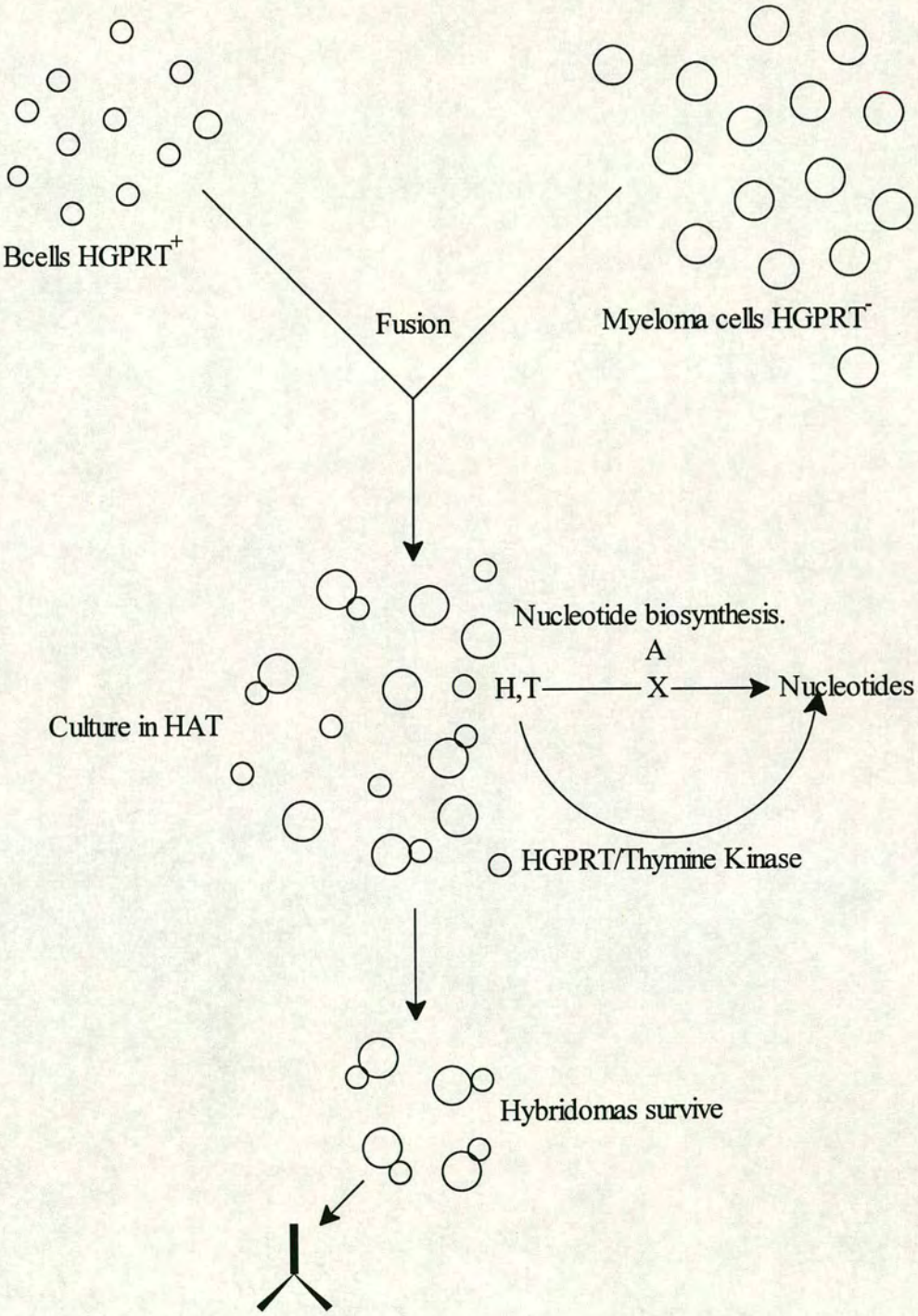

Figure 8: Cell Fusion

AIMS OF THE PROJECT

In order to provide an alternative to the biotin and digoxigenin oligonucleotide labelling systems and to complement the existing DNP system, a further potential labelling group was studied. The dansyl group (figure 4d) has been used in the past to label amino acids, proteins and oligonucleotides[53,54]. This approach has only made use of the fluorescent properties of this group. However, dansyl is highly immunogenic and immunochemical detection of dansyl labelled probes could provide an extremely sensitive reporter system. Dansyl labelled oligonucleotides have been synthesised, as has the DNP system, for immunochemical detection[55]. The aim of this project was to raise a cell line secreting monoclonal anti-dansyl antibodies and to evaluate and compare this system to the DNP system.

RESULTS AND DISCUSSION

Preparation of Dansyl Immunogen

In order to elicit an immune response, the dansyl group was conjugated to a larger carrier molecule as, in general, substances of molecular weight below 1000 are not immunogenic[57]. Bovine serum albumin (BSA) was selected as the carrier molecule as the numerous lysine residues on the protein's surface can be easily functionalised with dansyl chloride (figure 9). BSA is a protein of molecular weight of 67,000 Daltons and therefore provokes a large immune response in mice due to the large number of potential determinants foreign to the self-configurations that induce tolerance within the animal.

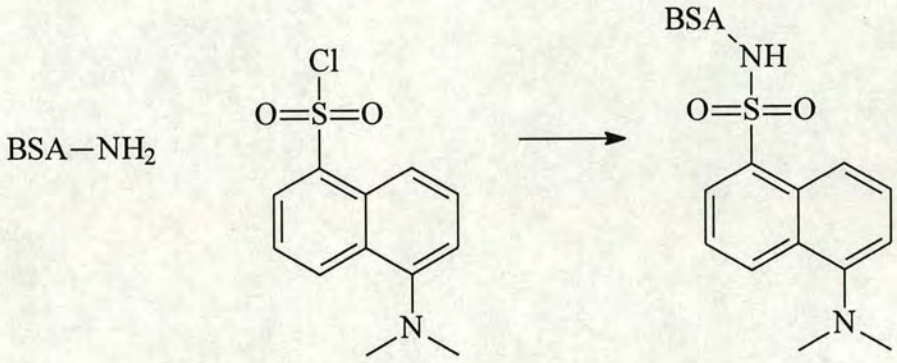

Figure 9: Functionalisation of BSA with Dansyl

The inherent hydrophobicity of dansyl chloride prevented reaction with BSA in the aqueous buffer required for the protein, therefore DMSO was added and the conjugation mixture warmed to solubilise the reagent. 50% ethanol was used as the elution buffer in the subsequent chromatographic step to stop excess dansyl chloride precipitating and blocking the desalting column.

Evidence of dansyl-BSA conjugation was obtained by an obvious change in colour of the eluted protein (from colourless to yellow), strong fluorescence when irradiated at 320nm and comparison of the UV absorbance scans of dansyl chloride, BSA and the eluted protein in the region 240 to 300nm (figure 10). The eluted protein exhibits considerable dansyl-like character in the UV scan.

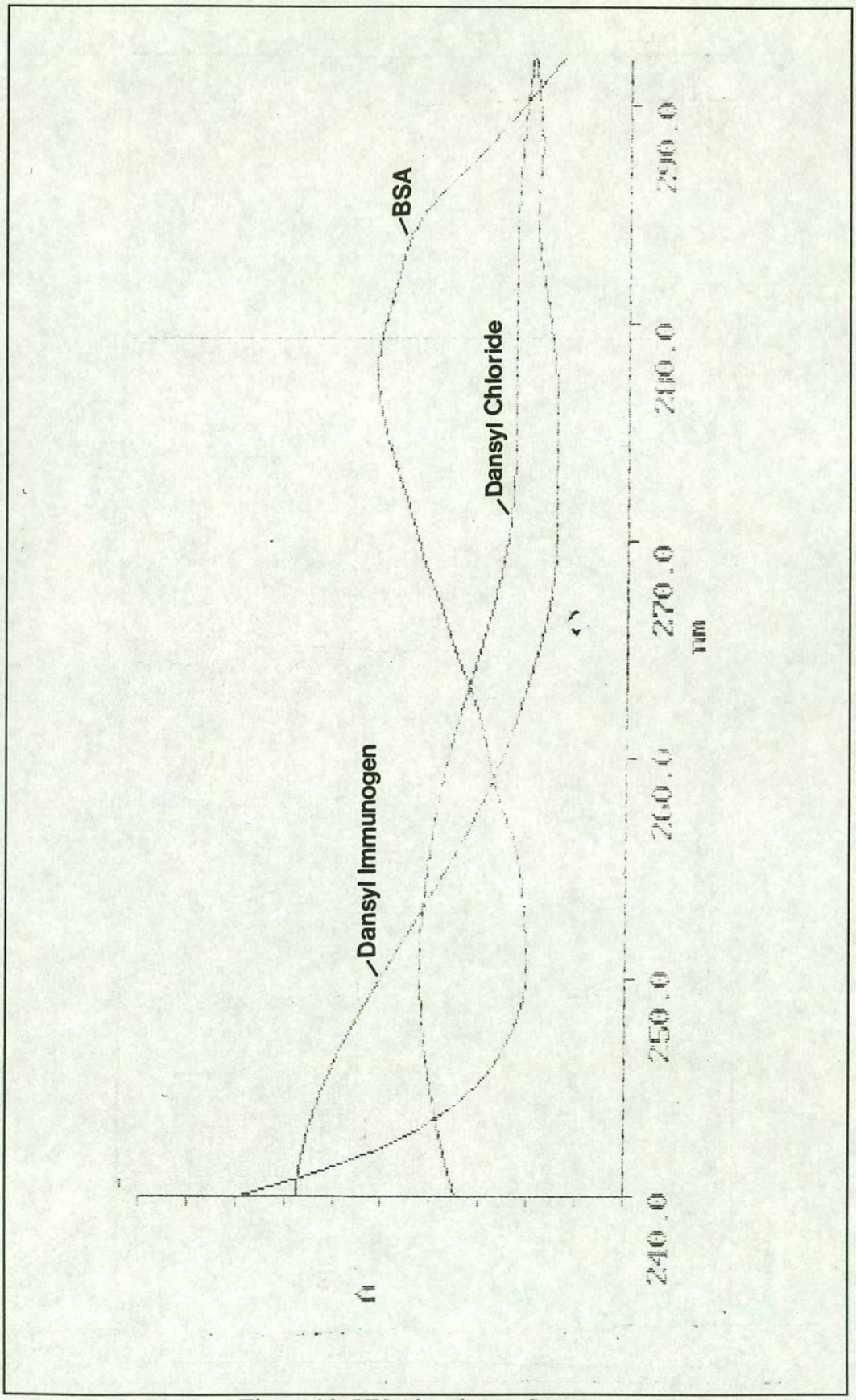

Figure 10: UV Absorbance Scans

Immunisation

The dansyl-BSA conjugate was emulsified with Freund's Complete Adjuvant for primary immunsation. This contains a suspension of killed mycobacteria in mineral oil which potentiates the immune response[58]. Freund's Incomplete Adjuvant, containing no mycobacteria, was used for the secondary immunisation.

The conjugate was used as the 50% ethanol storage solution. In hindsight, removal of ethanol would have been advantageous as it is an immune system surpressant[59]. It was also observed to be harmful to immunised animals as a number of older mice died after immunisation with this solution in separate experiments. Two mice (A and B) were immunised and boosted pre-fusion with dansyl immunogen.

Fusion

The fusion protocol used was developed at Shell Research Ltd. by Dr. Paul Aston and was based on the methods of Kohler and Milstein[60] and Galfre *et al*[61]. This involved blending splenocytes isolated from the spleens of the immunised mice with myelomas in ratios of between 10:1 to 1:1 splenocytes:myelomas. Next, the controlled addition of the fusion agent, PolyEthylene Glycol (PEG) causes the cellular membranes to fuse and multinuclear cells to form. During post-fusion cellular division, the nuclei of these so called heterokaryons fuse and the resulting daughter hybridoma cells possess a share of the genetic material[62]. These cells were cultured in media containing HAT for 14 days to isolate the viable hybridomas. Two fusion experiments were undertaken using a spleen from each mouse. Each fusion was divided into 360 wells in 6 culture plates.

Bleed Assay

During the period of HAT culture, blood removed from the mice was analysed to assess the titre of anti-dansyl antibodies circulating in the animals prior to fusion. This provides a measure of the immune reponse *in vivo* towards the dansyl immunogen.

Sera were isolated from red blood cells by centrifugation and double diluted across microtitre plates coated with dansyl screen.

Dansyl screen was prepared in the same manner as dansyl immunogen, replacing BSA with Chicken Gamma Globulin (CγG). As the immune system produces antibodies to the immunogen as a whole, many serum antibodies have epitope specificity to determinants on BSA, not to the dansyl group. Using dansyl screen removes many BSA-like determinants thereby helping to provide a clearer representation of anti-dansyl titre.

An Enzyme Linked ImmunoSorbent Assay (ELISA) revealed quantifiable titres of reactivity in the sera towards the dansyl screen (figure 11 and table 1).

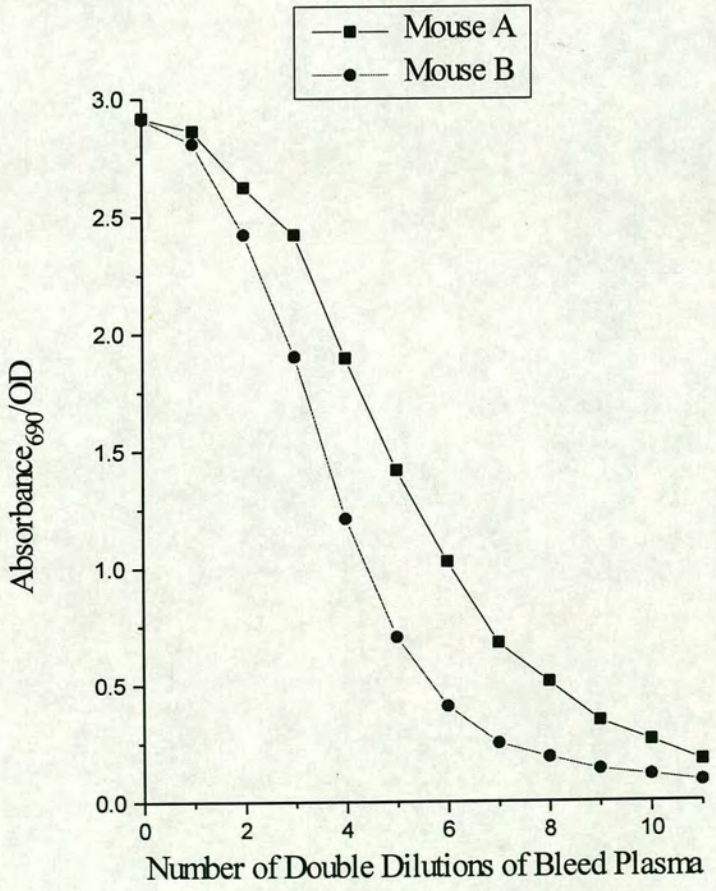

Figure 11: Antibody Titre in Mouse Bleeds

To further establish specificity within the sera towards the dansyl group a competitive ELISA using ammonium dansylate as an inhibitor was performed.

Mouse Bleeds	Titre	IC_{50} with Ammonium Dansylate/μM
A	1/700	7.5
B	1/250	2.5

Table 1: Reactivity of Mouse Bleeds to Dansyl

Dansyl chloride could not be used here as it is insoluble in the aqueous buffer required by ELISA. Therefore, it was converted to the ammonium salt of the sulphonic acid by reaction with ammonium hydroxide (figure 12). The ELISA revealed that the sera reactivity to dansyl immobilised on the microtitre plate could be reversed by dansyl in solution (figure 13, table 1).

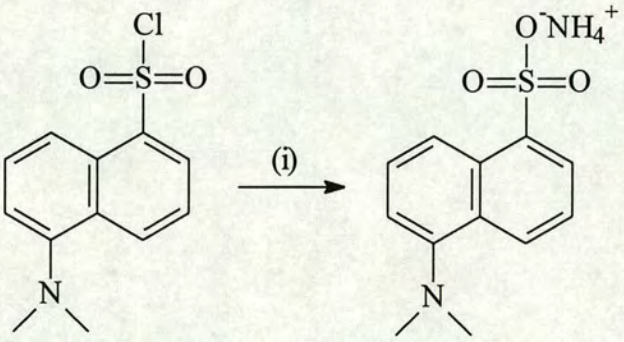

(i) ammonium hydroxide

Figure 12: Synthesis of ammonium dansylate

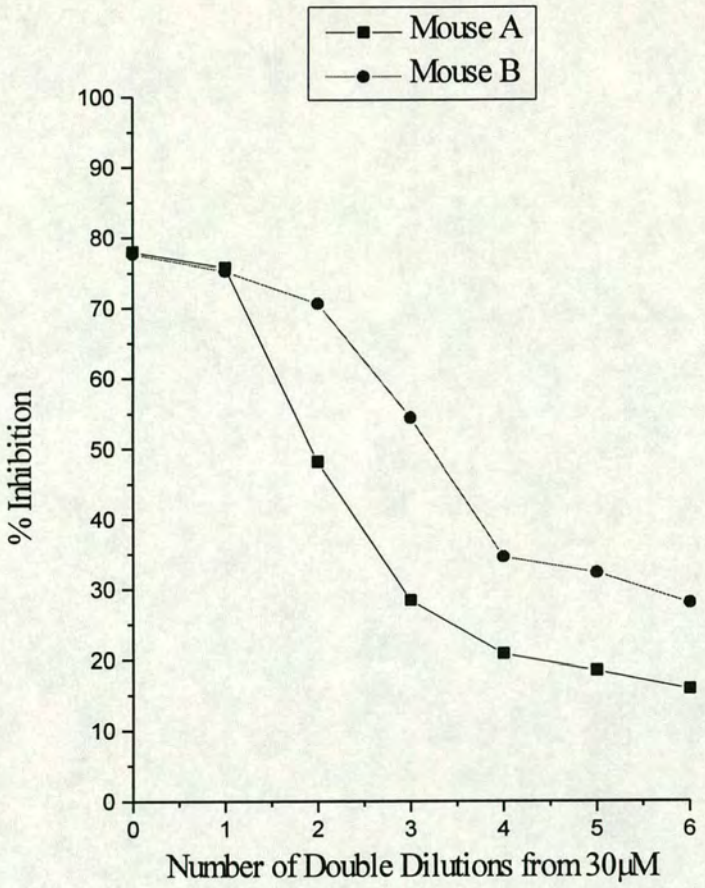

Figure 13: Antibody Specificity to Ammonium Dansylate in Mouse Bleeds

Screening of Fusion Plates

14 days post-fusion the 6 culture plates from each fusion were assayed for anti-dansyl antibody production. Medium was transfered from the culture plates to microtitre plates coated with dansyl screen. ELISA revealed many positive wells from both fusions. A total of thirty-five and thirty-two wells were chosen from fusions A and B, respectively. The selection criterion was a positive reading six times greater than that of the background. Further examination by competitive ELISA using ammonium dansylate identified seven wells with specificity to the dansyl group for cloning, three wells from Mouse A and four wells from Mouse B (tables 2 and 3). On the basis of these results it appeared that the cell fusion using the

splenocytes from mouse B produced viable hybridomas with reactivity towards dansyl.

Fusion Plate Number	Positive Wells in Initial Screening	% Inhibition by 300μM Ammonium Dansylate	Selection for Cloning
3	D7	7	No
3	F2	25	Yes
3	F4	7	No
3	G5	22	Yes
3	G11	42	Yes

Table 2: Screening of Fusion Wells from Mouse A

Fusion Plate Number	Positive Wells in Initial Screening	% Inhibition by 300μM Ammonium Dansylate	Selection for Cloning
1	C7	45	No
1	E8	18	No
2	B2	32	No
2	F6	31	No
3	D10	70	Yes
3	F10	78	Yes
5	B9	82	Yes
5	E2	36	No
5	F6	43	No
5	F8	43	No
5	F9	51	Yes
6	B7	27	No

Table 3: Screening of Fusion Wells from Mouse B

Cloning

Cloning was achieved by the limiting dilution method. Thymuscytes isolated from murine thymus lobes were the feeder cells of choice and supplemented the hybridoma cell population at limiting dilution. The hybridoma lines were screened and cloned twice sucessively before monoclonality was confirmed (tables 4 and 5). Cell lines were assigned a code which denoted the line's lineage from mouse, fusion well and cloning wells. The positive wells containing the lowest number of

individual clones which showed the greatest antibody titre were selected for recloning. These criterion favour cell lines which produce high affinity antibodies in high titre.

Cell Line	Number of Positive Wells Found on Screening	Selection for Recloning
A3F2	0	0
A3G5	0	0
A3G11	9	E4
B3D10	3	C7
B3F10	13	A7
B5B9	38	E4
B5F9	0	0

Table 4: Screening of First Cloning

Cell Line	Monoclonality
A3G11E4	Yes
B3D10C7	Yes
B3F10A7	No Clones
B5B9E4	Yes

Table 5: Screening of Second Cloning

From the seven cell lines chosen from the fusion experiments for cloning, four cell lines remained positive after screening. Positive wells were selected for recloning on the basis of assumed high affinity and titre. Three of the four cell lines were cloned successfully. All the isolated clones of these cell lines gave positive results on screening indicating monoclonality.

Monoclonal Cell Lines

The cell lines A3G11E4, B3D10C7 and B5B9E4 were characterised in detail to ascertain the cell line most suitable for the non-radiactive labelling application. This was determined using the following criterion:

1) titre,

2) affinity,

3) isotype,

4) ease of purification.

Monoclonal Cell Line	Titre	IC_{50} with Ammonium Dansylate/nM	Isotype	Protein A Binding?	Protein G Binding?
A3G11E4	/	950	IgM	No	No
B3D10C7	1/16	200	IgM	No	Yes
B5B9E4	1/600	60	IgM	Yes	Yes

Table 6: Monoclonal Antibody Characteristics

Titration of cell culture dilutions by ELISA on dansyl screen coated microtitre plates gave the titre at half maximal absorbance (approximately $1OD_{650}$) (figure 14 and table 6). These dilutions were used in competitive ELISA with increasing concentrations of ammonium dansylate to obtain IC_{50} values for the antibodies (figure 15 and table 6). To select the highest affinity antibody the method of Rath *et al*[63] was employed. The IC_{50} values clearly indicate that cell lineB5B9E4 has the greatest relative affinity. Important additional criteria are antibody isotype and ease of purification from serum proteins.

Antibody isotype determines the physico-chemical properties of the antibody. Antibodies of the IgG isotype are the immunochemical reagents of choice due to their high solubility, ease of functionalisation and digestion into smaller, active fragments. They also tend to be of higher affinity relative to the larger IgM isotype (IgG molecules are of approximately 170,000 Daltons and IgM molecules are of approximately 900,000 Daltons). IgM antibodies are prone to flocculation, insolubility and insusceptiblity to fragmentation with retention of activity[64-68]. An isotyping kit containing anti-class and anti-subclass specific antibody conjugates was used to isotype the antibodies. All 3 were found to be of the IgM isotype (table 6). This was a disappointing and statistically surprising result as IgM antibodies only constitute approximately 5% of the total serum immunoglobuliulins[69]. This warranted further investigation and the dansyl immunogen was re-examined as it may have influenced the immune system response. It is known that epitope density influences immunological properties as high hapten:carrier protein ratios can potentiate an IgM reponse[70]. The method of Habeeb[71] was employed to determine the

mean hapten:carrier protein ratio. This involved counting the free amino groups on the dansyl immunogen and native BSA by labelling the free lysine residues with trinitrobenzene sulphonic acid (TNBS) and reading spectrophotometrically at 335nm (the absorbance at this wavelength of the dansyl immunogen not exposed to TNBS had to be subtracted from that of the dansyl immunogen-TNBS complex as the dansyl group also absorbs at 335nm). As may have been anticipated from the immunochemical results the hapten:carrier protein ratio was extremely high with 57 of the possible 61 lysine residues labelled with the dansyl group.

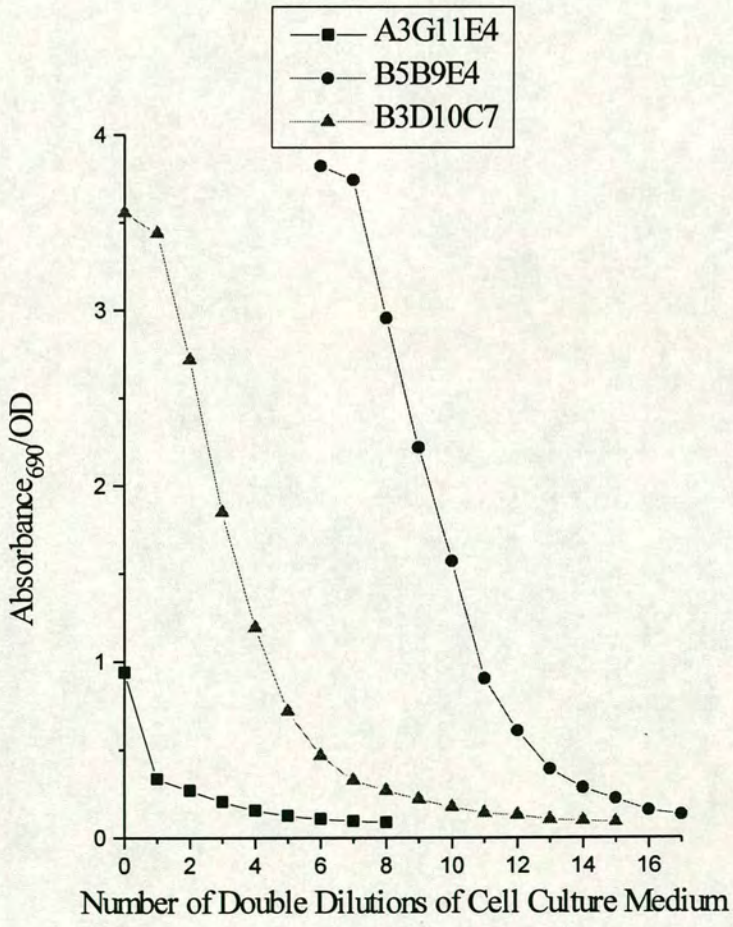

Figure14: Monoclonal Antibody Titrations

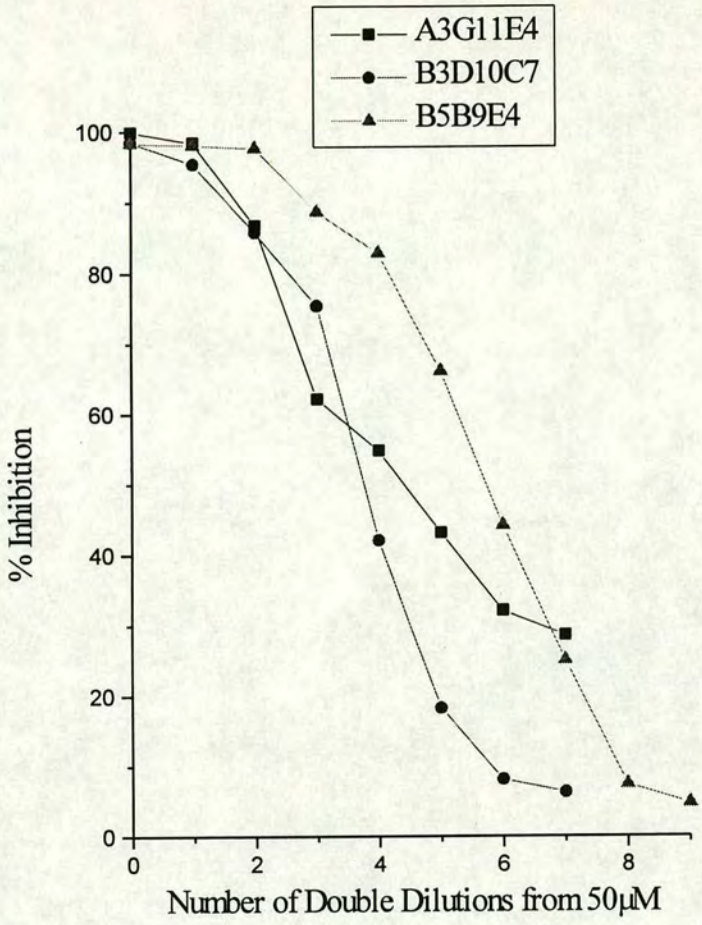

Figure 15: Monoclonal Antibody Specificity to Ammonium Dansylate

The antibody binding proteins, Protein-A and Protein-G, can be immobilised on solid supports and provide convenient affinity chromatographic methods to separate immunoglobulins from other serum proteins. It has become established that only murine antibodies of the IgG isotype bind to Protein-A and Protein-G[72]. In practice, however, many IgM antibodies will also bind[73]. Indeed, when cell culture media from the two higher affinity antibodies were applied to Protein-A and Protein-G affinity columns strong binding was observed (table 6). The antibodies could also be obtained by elution from the column with acid in pure form. As the levels of antibody in the media were too low to detect spectrophotometrically by UV absorbance at 280nm, a dot blot assay was performed to detect antibody elution. One millilitre fractions were eluted from the column and spotted onto a nitrocellulose

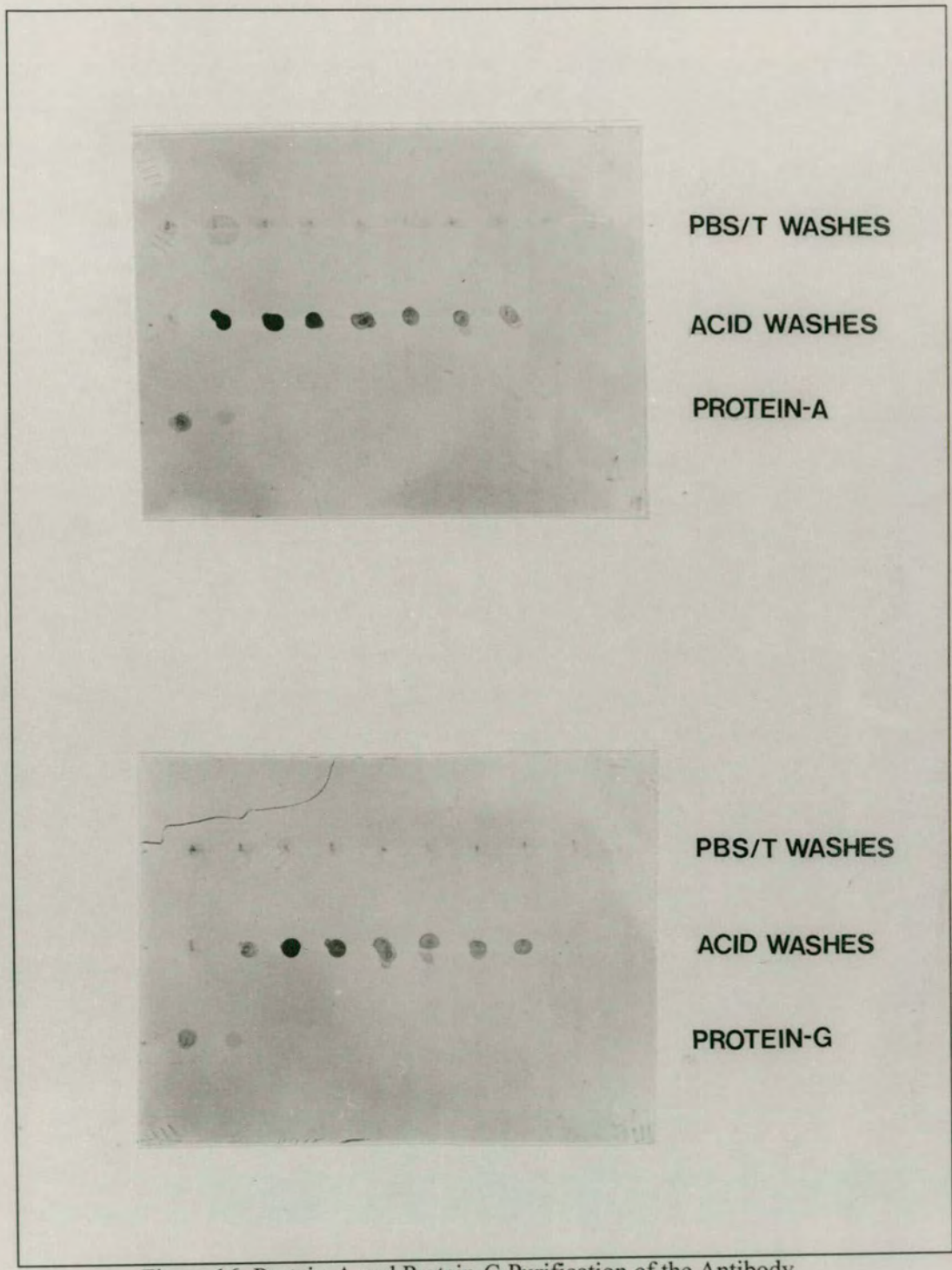

Figure 16: Protein-A and Protein-G Purification of the Antibody

membrane. The antibody-containing fractions were visualised by the addition of an anti-mouse antibody HRP conjugate and DAB substrate (figure 16).

All three monoclonal cell lines were frozen. The B5B9E4 cell line that showed the greatest promise in terms of affinity and Protein-A and Protein-G binding was maintained, recloned once more to ensure monoclonality and expanded into larger culture flasks. This cell line was cultured to provide enough antibody to evaluate its use in non-radioactive labelling methodology.

Application of Monoclonal Cell Line B5B9E4

A litre of antibody-containing medium was harvested from the cell culture and crudely purified by ammonium sulphate salt fractionation. The antibody was further purified by Protein-A affinity chromatography to yield 1750μg of anti-dansyl antibody. Antibody activity was ascertained by ELISA titration.

The application requires the antibody to recognise the dansyl group in the presence of large excesses of DNA. Therefore, it was important to establish no cross-reactivity of the antibody towards nucleosides. Competitive ELISA using a mixture of dA, dC, dG and T at $1mgml^{-1}$ of each revealed no detectable inhibition of anti-dansyl antibody binding.

3 dansyl labelled oligonucleotides had previously been synthesised using a dansyl phosphoramidite monomer compatible with automated oligonucleotide synthesis[54]. The labelled oligonucleotides bore 1, 3 and 5 dansyl groups at the 5' end. 5 fold dilutions from a 20μM solution of these dansyl labelled oligonucleotides were applied along with unlabelled, control oligonucleotide to nylon membrane and fixed by UV irradiation. A two step anti-dansyl antibody then anti-mouse antibody HRP conjugate dot blot assay revealed detection limits of 2 picomole, 80 femtomole and 400 femtomole for the oligonucleotides bearing 1, 3 and 5 dansyl groups respectively (figure 17).

A similar assay comparing the detection limits of the dansyl labelled oligonucleotides to identical oligonucleotides bearing 1, 3 and 5 terminal DNP groups was undertaken. 20 fold dilutions from a 160μM stock solution were applied and fixed to nylon membrane. This assay (figure 18) revealed detection limits of 80

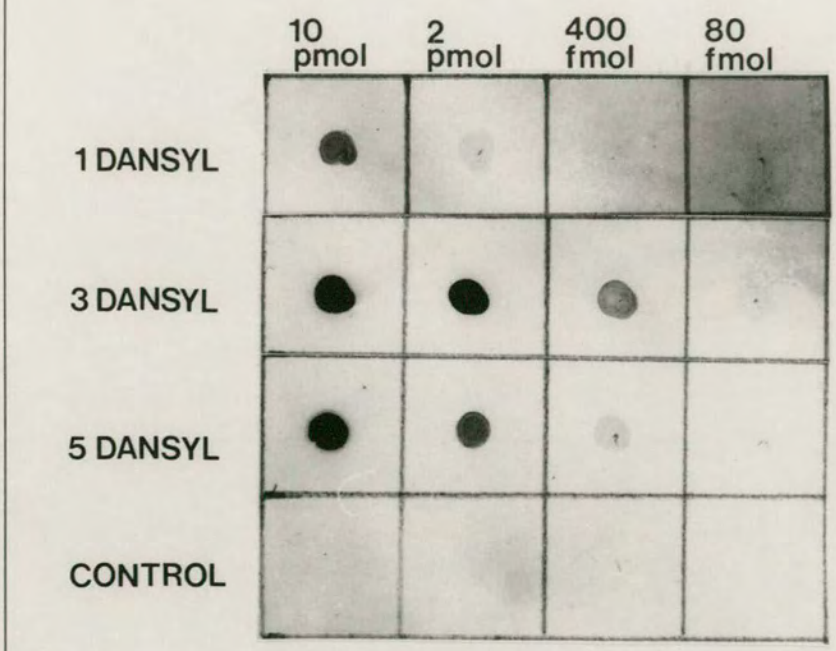

Figure 17: Dot Blot of Anti-dansyl Antibody

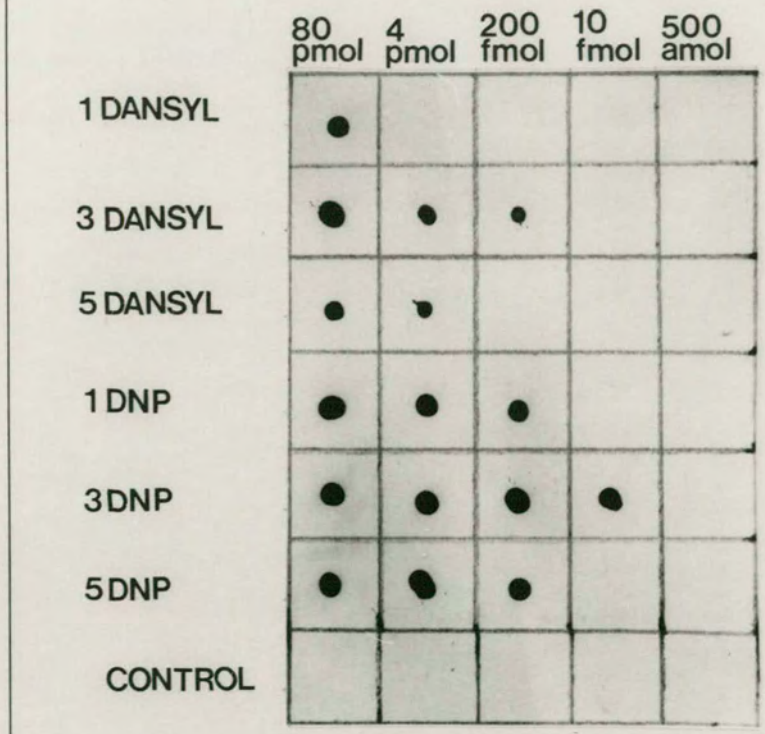

Figure 18: Dot Blot Comparison of Anti-dansyl and Anti-DNP Antibodies

picomole, 200 femtomole and 4 picomole for oligonucleotides bearing 1, 3 and 5 dansyl groups respectively. However, the DNP system exhibited far higher sensitivity with detection limits of 200 femtomole, 10 femtomole and 200 femtomole for oligonucleotides labelled with 1, 3 and 5 DNP groups respectively.

This was disappointing as it had been hoped that the anti-dansyl system would display as good if not better limits of detection than the anti-DNP system. The difference is undoubtably due to the relative affinities of the anti-dansyl and anti-DNP antibodies, the anti-DNP antibody being superior.

CONCLUSIONS AND FUTURE WORK

It is clear that a new, higher affinity anti-dansyl antibody is required to make this system of antibody mediated non-radioactive labelling viable. As antibodies of the IgG isotype tend to be of higher affinity a new immunogen that "selects" for an antibody of this class needs to be synthesised for further immunisations.

EXPERIMENTAL

Materials

All chemicals, buffer tablets, enzyme substrates and Adjuvants were obtained from Sigma. All cell culture media and hybridoma reagents were obtained from Gibco with the exception of polyethylene glycol (PEG) from Sera-Lab. Cell culture plasticware was obtained from Costar. Microtitre plates were obtained from Nunc. Sterile syringes were obtained from Becton Dickson and sterile needles from Sherwood Medicals. Secondary antibody horse radish peroxidase (HRP) conjugated rabbit anti-mouse immunoglobins were obtained from Dakopatts. Antibody isotyping kit was obtained from Sera-lab. Hibond nylon and nitrocellulose membranes were obtained from Amersham. Protein-A and Protein-G affinity chromatography columns plus buffers were obtained from Pierce. PD10 columns were obtained from Pharmacia. Pyrogen-free, reverse osmosis purified water was used throughout.

Buffers, Cell Culture Media and Substrates

N-morpholinoethanesulphonic acid (MES): 100mM *N*-morpholinoethanesulphonic acid buffered to pH=6.0.

Phosphate buffered saline pH=7.4 (PBS):100mM phosphate and 50mM sodium chloride tablets dissolved in water (1 tablet *per* 200ml).

RPMI: RPMI 1640 with glutamax.

RPMI/PS: RPMI with penicillin (200U/ml) and streptomycin (200μg/ml).

10% complete media: RPMI/PS with 10% (v/v) fetal calf serum, 2mM sodium pyruvate and amphotericin B deoxycholate (2.5μg/ml).

5% complete media: as 10% complete media with 5% (v/v) fetal calf serum.

10% complete media/HAT: 10% complete media with 100μM hypoxanthine, 40υM aminopterin and 16μM thymidine.

10% complete media/HT: 5% complete media with 100μM hypoxanthine and 16μM thymidine.

10% DMSO/myoclone: 10% DMSO (v/v) in myoclone.

Binding buffer: 100mM Tris at pH 8.5.

Eluting buffer: 100mM Glycine at pH 2.7.

Neutralising buffer: 1M Tris at pH 9.0.

Phosphate buffered saline/Tween 20 (PBS/T): PBS with 0.05% (w/v) Tween 20.

Coating buffer: 15mM sodium carbonate, 35mM sodium hydrogen carbonate buffered to pH 9.5.

PBS/azide: PBS with 0.02% (w/v) sodium azide.

Blocking buffer: PBS/T with 10% (w/v) skimmed milk.

Tetramethylbenzidine (TMB) substrate: 3,3',4,4'-tetramethylbenzidine liquid substrate system containing chromogen, buffer and hydrogen peroxide.

Diaminobenzidine (DAB) substrate: 3,3'-diaminobenzidine tetrahydrochloride tablet plus urea hydrogen peroxide tablet dissolved in water (15ml).

Instrumentation

^{1}H NMR specra were recorded on a Bruker WP-200 (200.130MHz) spectrometer. ^{13}C NMR spectra were recorded on a Bruker WP-200 (50.320MHz) spectrometer. Positive ion Fast Atom Bombardment mass spectra were recorded on a Kratos MS50 TC spectrometer using a 3-nitrobenzyl alcohol matrix (3-NOBA). UV spectra were recorded on a Perkin-Elmer Lambda 15 ultraviolet-visible spectrophotometer. IR spectra were recorded on a Bio Rad FTS-7 Fourier transform spectrometer controlled by a Bio Rad SPC 3200 microcomputer. ELISA plates were read on a Molecular Devices Vmax kinetic microplate reader incorporating the Softmax software package.

Preparation of Dansyl Immunogen

BSA (10mg) was dissolved in MES (2ml) and warmed to 37°C. Dansyl chloride (20mg) dissolved in DMSO (2ml), was added dropwise to the BSA solution and the mixture incubated at 37°C. After 72 h the product was purified on PD10 columns to the manufacturer's specifications, equilibrating and eluting with 50% ethanol. The conjugate was stored in 50% ethanol at -20°C until used.

Characterisation of Dansyl Immunogen

Dansyl immunogen (1ml of 750μg/ml in 50% ethanol) was warmed to 40°C. 4% sodium hydrogen carbonate (1ml) and 0.1% trinitrobenzene sulphonic acid (1ml) were added and the mixture incubated at 40°C. After 2 h 10% SDS (1ml) and 1M HCl (500μl) were added. BSA (1ml of 750μg/ml in 50% ethanol) was treated identically and the absorbance of both solutions read at 335nm against a blank of 50% ethanol treated as above.

Preparation of Dansyl Screen

As for the dansyl immunogen replacing BSA with CγG.

Ammonium 5-dimethylamino-1-napthalenesulphonate (ammonium dansylate)

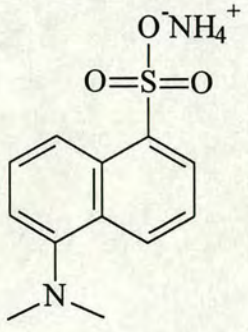

5-dimethylamino-1-napthalenesulphonyl chloride (525mg, 1.95mmol) was added to conc. NH_4OH (100ml) and stirred at room temperature for 96 h. The solution was concentrated *in vacuo* to yield the title compound as a pale yellow solid (481mg, 1.90mmol, 98%). Rf (solvent system DCM/ methanol 9/1), 0.15;

$\delta H([^2H_6]$-DMSO) 8.64-7.62 (6H, m, 4 napthalene H), 3.19 (6H, s, N-Me_2) and 2.50 (4H, s, NH_4^+); $\delta C([^2H_6]$-DMSO) 151 (C), 140 (C), 129 (C), 129 (CH), 128 (CH), 126 (CH), 124 (CH), 120 (CH), 115 (CH) and 45 (CH_3); υ_{max}(film)/cm^{-1} 3320 (NH_4^+), 1640 (NMe_2), 1140 and 1183 (SO_2-O); λ_{max}(water)/nm 214, 252 and 281; m/z (FAB) $C_{12}H_{13}NO_3S$ found: 251.06325 calculated: 251.06162.

Immunisation Protocol

Dansyl immunogen (100µl of 750µg/ml in 50% ethanol) was emulsified with Freund's Complete Adjuvant (400µl). 3 month old, female Balb/c mice (2) were immunised subcutaneously at the knape of the neck (200µl/mouse). After 21 d boosts were administered as above replacing Freund's Complete Adjuvant with Freund's Incomplete Adjuvant. Pre-fusion boosts were administered 3 d prior to fusion with dansyl immunogen (30µl of 750µg/ml in 50% ethanol) added to PBS (200µl), injecting 100µl *per* mouse *via* the peritoneum and mid-dorsal tail vein.

Pre-fusion Bleed

Mice under anaesthesia were bled via sterile pasteur pipette from the retro-orbital plescus. After sufficient blood (approx. 500µl) had been obtained the pipette was removed and the blood transfered to an eppendorf vial. The blood was spun (1500G, 30mins) separating serum from red blood cells. The serum was removed and stored at -20°C until analysed.

Splenocyte Preparation

3 d after administration of the pre-fusion boosts, mice were sacrificed by ether anaesthesia and cerebral dislocation. Mice were showered with 50% IPA and slit open along the abdomen towards the chest with sterile scissors to reveal the spleen. Sterile scissors and forceps were used for the splenectomy and the organ was placed into cold RPMI (10ml). The spleen was transfered to a laminar flow hood and placed on a sterile petri dish. Residual fatty tissue was trimmed away and a

superficial longitudinal incission made along the spleen. Splenocytes were ejected by injecting RPMI (2 x 10ml) into the spleen with 25 gauge needles, repeatedly puncturing the surface. The cell suspension was spun (500G, 5m) and the supernatant discarded. The pellets were resuspended in RPMI (20ml).

Myeloma Preparation

Sp2 myeloma cells maintained at 60-70% growth in 10% complete media (4 x 30ml) in a CO_2 incubator at 37°C was suspended and spun (500G, 5m). The supernatant was discarded and the pellets were resuspended in splenocyte suspension (20ml) prepared as above.

Splenocyte/Myeloma Cell Fusion

The day before cell fusion, the following were prepared in syringes and stored overnight in a CO_2 incubator at 37°C: RPMI/PS (2 x 10ml), RPMI/PS (1 x 20ml), PEG (6 x 300µl), RPMI/PS (6 x 10ml), 10% complete media (6 x 6ml) and 10% complete media/HAT (200ml). The splenocyte/myeloma suspension (20ml) prepared above was divided into 6 equal aliquots and spun (500G, 5m). The supernatant was discarded and the pellets drained. The pellets were agitated with 25 gauge needles before dropwise addition of PEG (300µl *per* pellet) over 30 s. RPMI (10ml *per* pellet) was immediately added dropwise over 60 s. The suspensions were spun (500G, 5m) and the supernatants discarded. The pellets were resuspended in 10% complete media (6ml *per* pellet) and transfered to the inner 60 wells of a 96 well cell culture plate (100µl *per* well). 10% complete media/HAT (100µl *per* well) was added and the plates placed in a CO_2 incubator at 37°C.

Thymocyte Preparation

On the day of cloning a greater than two month old, Balb/c mouse was sacrificed by ether anaesthesia. The mouse was opened from the abdomen, through the

ribcage to the neck with sterile scissors exposing the thymus lobes. The thymus was removed with sterile scalpel and forceps and placed into cold RPMI (10ml). The organs were transfered to a laminar flow hood and placed on a sterile petri dish. Residual fatty tissue was trimmed away and RPMI (10ml) added. Thymocytes were released by teasing the thymus lobes with sterile forceps. The thymocyte suspension was spun (500G, 5m) and the supernatant discarded. The pellet was resuspended in 10% complete media and thereafter the viable cells could stored in the CO_2 incubator at 37°C for a maximum of 5 d.

Cell Cloning

Hybridoma cells were resuspended from a 96 well culture plate well and added to a 4 times 1ml well culture plate. Sufficient suspension was removed for 200 cells *per* 100ml when added to the thymocyte suspension (4ml) prepared above. Thymocyte suspension (500µl) was added to the hybridoma suspension in the 4 well culture plate. Hybridoma/thymocyte suspension (2.4ml) was transfered (100µl *per* well) to rows A and B on a 96 well culture plate and thymuscyte suspension (2.4ml) added to the original hybridoma/thymuscyte sample. This procedure was repeated for rows C, D, E, and F. Thymuscyte suspension (800µl) was added to the original hybridoma/thymuscyte sample and the remaining (2.4ml) transfered (100µl *per* well) to rows G and H. 10% complete media (100µl *per* well) was added and the plates placed in a CO_2 incubator at 37°C. The plates were examined daily for the presence of clones taking care not to agitate the cells. After 8-14 d the number of clones *per* well was recorded and the plate screened.

Cell Culture

5% complete media was exchanged three times *per* week. The culture was examined for cell growth and at 70% confluency cells were suspended and removed with the old medium. The old medium was spun (500G, 5m) and the supernatant retained and stored at 4°C or frozen at -4°C. Fresh 5% complete

medium warmed to 37°C was added in equal volume and the cells returned to the CO_2 incubator at 37°C.

Fusion Culture Maintenance

At two to three day intervals 10% complete medium/HAT (100µl *per* well) was removed carefully from the top of the fusion wells, ensuring no cell agitation. Fresh 10% complete medium/HAT (100µl *per* well) was carefully replaced. This continued until after the primary screening where 10% complete media/HT was replaced.

Freezing Cell Lines

Cells were suspended into RPMI (5ml) and spun (500G, 5mins). The supernatant was discarded and the pellet drained before addition of 10% DMSO/fetal calf serum (3ml). The resuspensed cells were divided into cryotubes (4 x 1ml) and frozen to -70°C before transfer to cryofreeze at -180°C.

General ELISA Protocol

1) 96 well microtitre plates were coated with dansyl screen (100µl *per* well with 2mgml^{-1} in coating buffer) at room temperature overnight.

2) The plates were washed with PBS/T (5x), shaken and aspirated dry.

3) The plates were covered and stored at 4°C until used.

4) Primary antibody (100µl *per* well diluted in PBS/T) was applied to dansyl coated plates and incubated at room temperature overnight.

5) Repeated 2.

6) Secondary antibody/HRP (100µl *per* well at 1/1000 dilution in PBS/T) was applied and incubated at room temperature for 2 h.

7) Repeated 2.

8) TMB substrate (100µl *per* well) was applied and after 30 m incubation at room temperature the resultant blue colour was quantified spectrophotometrically at 690nm on an ELISA plate reader.

This ELISA protocol was modified for the following applications:

Bleeds

As above except 4) Serum was double diluted in PBS/T and applied (50µl *per* well) in triplicate.

Bleed Inhibition

As above except 4) Serum dilution that gave approx. 2OD at 690nm was applied (100µl *per* well) in triplicate at a range of concentrations of ammonium dansylate.

Primary Screening

As above except 4) 10-14 d post-fusion 10% complete medium/HAT (100µl *per* well) was transfered from fusion plates to dansyl coated plates and incubated at room temperature for 4 h.

Secondary Screening

As above except 4) The day after primary screening, positive wells from the primary screen were tested for inhibition by ammonium dansylate. 10% complete medium/HT (50µl *per* well) was tranfered to dansyl coated plates with ammonium dansylate (50µl *per* well of 100µM in PBS/T) and incubated at room temperature for 4 h.

Clone Plate Screening

As above except 4) 10% complete media (100µl *per* well) was transfered from clone plates to dansyl coated plates and incubated for 4 h.

Antibody Titre

As above except 4) Primary antibody (100µl *per* well double diluted in PBS/T) was applied in triplicate to dansyl coated plates and incubated at room temperature overnight.

Inhibition

As above except 4) Primary antibody dilution that gave approx. 2 OD at 690nm was applied (100µl *per* well) in triplicate with decreasing concentrations of inhibitor to dansyl coated plates and incubated at room temperature overnight.

Isotyping

As above except 6) Secondary antibody/HRP specific to the different mouse antibody isotypes (IgM, IgG1, IgG2a, IgG2b, IgG3 and κ and λ) was applied (100µl *per* well diluted 1/100 with PBS/T) and incubated at room temperature for 1 h.

Dot Blot Protocol

1) Oligonucleotide solutions (500nl) were spotted onto nylon membrane and allowed to dry.

2) The membrane was irradiated at 254nm for 5 m.

3) Blocking buffer (20ml) was applied and incubated at room temperature for 30 m.

4) The membrane was washed with PBS/T (5x).

5) Primary antibody (20ml diluted to 1/1000 with PBS/T from approx. 1mg/ml stock) was applied and incubated at room temperature for 3 h.

6) Repeated 4).

7) Secondary antibody/HRP (20ml diluted 1/1000 with PBS/T) was applied and incubated at room temperature for 1 h.

8) Repeated 4).

9) DAB substrate (10ml) was applied and incubated at room temperature for 30 m.

This dot blot protocol was modified for protein fixation by using nitrocellulose membrane. This only required drying, irradiation being unnecessary.

Ammonium Sulphate Precipitation

Saturated ammonium sulphate, cooled to 4°C was added slowly to an equal volume of hybridoma culture media whilst stirring on ice to give a 50% saturated ammonium sulphate solution. After 1 h the suspension was spun (8000G, 30m) and the supernatant discarded. The pellet was redissolved in a minimum quantity of water and dialysed (3x) against PBS/azide (3000ml).

Protein-A/Protein-G Affinity Chromatography Protocol

1) The affinity column was equilibrated with binding buffer (30ml).

2) Antibody was applied to the column as hybridoma culture media or post-ammonium sulphate precipitation.

3) The column was extensively washed with binding buffer (50ml).

4) Eluting buffer was applied (10ml) and fractions (2ml) collected with the addition of neutralising buffer (200µl).

5) The fractions collected were monitored spectrophotometrically at 280nm.

6) The peak fractions were pooled and dialysed (3x) against PBS/azide (1000ml).

7) The column was washed with binding buffer (30ml) then 20% ethanol (10ml) and stored in 20% ethanol at 4°C.

This protocol was used interchangibly for Protein-A and Protein-G affinity columns.

Antibody Storage

Purified antibody samples were stored for short periods of time (d or weeks) in PBS/azide at 4°C. For long periods of time (months) purified antibody samples were stored in PBS/azide at -20°C.

REFERENCES TO CHAPTER TWO

1. Harris M.R. (1991) Biotechnology Advances, 9, 185-196.

2. Wetmur J.G. (1991) Critical Reviews in Biochemistry and Molecular Biology, 26, 227-259.

3. Keller G.H. and Manak M.M. (1989) DNA Probes, Stockton Press, 105-148.

4. English U. and Gauss D.H. (1991) Angewandte Chemie, Int Ed Eng, 30, 613-722.

5. Schubert F., Ahlert K., Cech D. and Rosenthal A. (1990) Nucleic Acids Research, 18, 342-347.

6. Theisen P., McCollum C., Upadhyak K., Jacobsen K., Vu H. and Andrus A. (1992) Tetrahedron Letters, 33, 5033-5036.

7. Kaiser R.J., MacKellar S.L., Vinayak R.S., Sanders J.Z., Saavedra R.A. and Hood L.E. (1989) Nucleic Acids Research, 17, 6087-6102.

8. Smith L.M., Kaiser R.J., Sanders J.Z. and Hood L.E. (1987) Methods in Enzymology, 155, 260-301.

9. Murakami A., Nakaura M., Nakatsuji Y., Nagahara S., Tran-Cong Q. and Makino K. (1991) Nucleic Acids Research, 19, 4097-4102.

10. Smith L.M., Sanders J.Z., Kaiser R.J., Hughes P., Dodd C., Connell C.R., Heiner C., Kent S.B.H. and Hood L.E. (1986) Nature, 321, 674-679.

11. Ansorge W., Sproat B., Stegemann J., Schwager C. and Zenke M. (1987) Nucleic Acids Research, 15, 4593-4602.

12. Wong S.S. (1991) Chemistry of Protein Conjugation and Cross-linking, CRC Press.

13. Renz M. and Kurz C. (1984) Nucleic Acids Research, 12, 3435-3444.

14. Jablonski E., Moomaw E.W., Tullis R.H. and Ruth J.L. (1986) Nucleic Acids Research, 14, 6115-6128.

15. Urdea M.S., Warner B.D., Running J.A., Stempien M., Clyne J. and Horn T. (1988) Nucleic Acids Research, 16, 4937-4956.

16. Sigma Immunochemicals (1992) Product Data Sheet D-4293.

17. Sigma Immunochemicals (1992) Product Data Sheet B-5655.

18. Sigma Immunochemicals (1993) Product Data Sheet T-8540.

19. Sigma Immunochemicals (1992) Product Data Sheet N-1891.

20. Langer-Safer P.R., Levine M. and Ward D.C. (1982) Proceedings of the National Academy of Sciences USA, 79, 4313-4385.

21. Gebeyehu G., Rao P.Y., SooChan P., Simms D.A. and Klevan L. (1987) Nucleic Acids Research, 15, 4513-4534.

22. Cocuzza A.J. (1989) Tetrahedron Letters, 30, 6287-6290.

23. Pon R.T. (1991) Tetrahedron Letters, 32, 1715-1718.

24. Misiura K., Durrant I., Evans M.R. and Gait M.J. (1990) Nucleic Acids Research, 18, 4345-4354.

25. Pieles U., Sproat B.S. and Lamm G.M. (1990) Nucleic Acids Research, 18, 4355-4360.

26. Chollet A. and Kawashima E.H. (1985) Nucleic Acids Research, 13, 1529-1541.

27. Cook A.F., Vuocolo E. and Brakel C.L. (1988) Nucleic Acids Research, 16, 4077-4095.

28. Agrawal S., Christodoulou C. and Gait M.J. (1986) Nucleic Acids Research, 14, 6227-6245.

29. Forster A.C., McInnes J.L., Skingle D.C. and Symons R.H. (1985) Nucleic Acids Research, 13, 745-761.

30. Muhlerlegger K., Batz., Bohm S., Etz H.V.D., Holtke H.J. and Kessler C. (1989) Nucleosides and Nucleotides, 5, 1161-1163.

31. Hoetk H.J., Stebe R., Burg J, Muhlegger K. and Kessler C. (1990) Biological Chemistry, 371, 929-938.

32. Kessler C., Hoetke H.J., Stebe R., Burg J. and Muhlegger K. (1990) Biological Chemistry, 371, 917-927.

33. Vincent C., Tchen P., Cohen-Solal M. and Kourilsky P. (1982) Nucleic Acids Research, 10, 6787-6796.

34. Moriuchi T., Takehiko K., Nakane P.K., Yoshida M., Moriuchi J. and Arimori S. (1988) Nucleic Acids Research, 19, 79-90.

35. Keller G.H., Huang D.P. and Manak M.M. (1989) Analytical Biochemistry, 177, 392-395.

36. Will D.W., Prichard C.E. and Brown T. (1991) Carbohydrate Research, 216, 315-322.

37. Grzybowski J., Will D.W., Randall R.E., Smith C.A. and Brown T. (1993) Nucleic Acids Research, 21, 1705-1712.

38. Hood L.E., Weissman I.L., Wood W.B. and Wilson J.H. (1984) Imunology, second edition, Benjamin/Cummings Publishing Company Inc., 1.

39. Langman R.E. (1989) The Immune System, Academic Press Inc., 6-7.

40. Roitt I. (1988) Essential Immunology, Blackwell Scientific Publications, 1-14.

41. Roitt I., Brostaff J. and Male D.K. (1989) Immunology, second edition, Gower Medical Publishing, 1.1.

42. Owen M.J. and Lamb J.R. (1988) Immune Recognition, IRL Press, 1-14.

43. Owen M.J. and Lamb J.R. (1988) Immune Recognition, IRL Press, 17-28.

44. Roitt I., Brostaff J. and Male D.K. (1989) Immunology, second edition, Gower Medical Publishing, 9.1-9.13.

45. Roitt I., Brostaff J. and Male D.K. (1989) Immunology, second edition, Gower Medical Publishing, 8.5-8.11.

46. Roitt I., Brostaff J. and Male D.K. (1989) Immunology, second edition, Gower Medical Publishing, 2.8-2.9.

47. Roitt I. (1988) Essential Immunology, Blackwell Scientific Publications, 102-107.

48. Harrison W., Volk H., Defranoux N. and Wabl M. (1993) Annual Reviews in Immunology, 11, 361-384.

49. Kimball J.W. (1986) Introduction to Immunology, second edition, MacMillan Publishing Company, 359-380.

50. Zola H. (1987) Monoclonal Antibodies: A manual of Techniques, CRC Press, 1-3.

51. Goding J.W. (1986) Monoclonal Antibodies: Principals and Practice, second edition, Academic Press Inc., 1-48.

52. Lerharat W., Andersson J., Coutinho A. and Melchers F. (1978) Experimental Cell Research, 111, 309-316.

53. Goding J.W. (1986) Monoclonal Antibodies: Principals and Practice, second edition, Academic Press, 75.

54. Roget A., Bazin H. and Teoule R. (1989) Nucleic Acids Research, 17, 7643-7657.

55. Singh D., Kumar V. and Ganesh K.N. (1990) Nucleic Acids Research, 18, 3339-3345.

56. Grzybowski J. (1994) University of Edinburgh Ph.D. Thesis, 108-114.

57. Erlanger B.F. (1980) Methods in Enzymology, 70, 85-104.

58. Ellouz F., Adam A., Gorbaru R and Lederer E. (1974) Biochemical and Biophysical Research Communications, 59, 1317-1325.

59. Rang H.P. and Dale M.M. (1987) Pharmacology, Churchill Livingstone, 684.

60. Kohler G. and Milstein C. (1975) Nature, 256, 495-498.

61. Galfre G., Howe S.C., Milstein C., Butcher G.W. and Howared J.C. (1977) Nature, 266, 550-552.

62. Goding J.W. (1986) Monoclonal Antibodies: Principals and Practice, second edition, Academic Press, 35.

63. Rath S., Stanley C.M. and Steward M.W. (1988) Journal of Immunological Methods, 106, 245-249.

64. Hardy R.R (1984) Immunochemistry, Weir D.M. (editor), fourth edition, Blackwell Scientific Publications, 13.1-13.13.

65. Parham P. (1984) Immunochemistry, Weir D.M. (editor), fourth edition, Blackwell Scientific Publications, 14.1-14.23.

66. Lamoyi E. (1986) Methods in Enzymology, 121, 652-663.

67. Gorini G., Czuppon A., and Medgyesi G.A. (1972) Immunochemistry, 9,577-585.

68. Matthew W.D. and Reichardt L.F. (1982) Journal of Immunological Methods, 50, 239-253.

69. Goding J.W. (1986) Monoclonal Antibodies: Principals and Practice, second edition, Academic Press, p12.

70. Klaus G.G.B. and Cross A.M. (1974) Cellular Immunology, 14, 226-241.

71. Habeeb A.F.S.A. (1966) Analytical Biochemistry, 14, 328-336.

72. Kronval G. and Williams R.C. (1969) Journal of Immunology, 103, 828-833.

73. Pearson T.W. and Anderson N.L. (1985) Methods in Enzymology, 92, 210.

The Stability of Duplex DNA Containing 3,N^4-Etheno-2′-Deoxycytidine (εdC). A UV Melting and High Resolution ^{1}H NMR Study

Neil J. Gibson,[a] John A. Parkinson,[a] Thomas Barlow,[a] William P. Watson[b] and Tom Brown*[a]

[a] *Department of Chemistry, University of Edinburgh, King's Buildings, West Mains Road, Edinburgh, UK EH9 3JJ*
[b] *Shell Research Ltd., Sittingbourne Research Centre, Sittingbourne, Kent, UK ME9 8AG*

The mutagenic lesion 3,N^4-etheno-2′-deoxycytidine (εdC) greatly destabilises DNA when paired with each of the natural bases although the solution structure of a duplex containing a εC : A pair shows that the lesion does not greatly disrupt base pairing in the duplex.

Vinyl chloride, an established carcinogen in humans,[1] is epoxidised *in vivo* by cytochrome P-450 enzymes to chloroethylene oxide which rearranges to chloroacetaldehyde.[2] Both the haloxirane and the haloaldehyde alkylate DNA giving both mono and bifunctional adducts[3] including 3,N^4-etheno-2′-deoxycytidine (εdC) **1**. When single stranded DNA is treated with chloroacetaldehyde mutagenesis is almost exclusively at cytosines[4] and consists of 80% C-to-T transitions and 20% C-to-A transversions. Because the DNA polymerase is misreading the template at the εC site and there is ambiguity as to the inserted base, εC appears to form non-instructional lesions.[5] Such lesions are either devoid of template activity, as is the case with abasic sites, or have their template activity blocked by chemical adducts. When a base is incorporated opposite such a lesion it is usually found to be adenine with a lower incidence of thymine.[6] Non-instructional lesions block DNA replication and are lethal unless they are excised from the template or bypassed by the replication enzymes. According to the SOS hypothesis,[7] arrest of DNA synthesis by non-instructional lesions causes induction of the SOS regulon and the induced enzymes facilitate DNA synthesis beyond the lesion site by an unknown mechanism. However it has been observed that mutagenesis by εdC is SOS independent and highly efficient and that transfection of *Escherichia coli* with coliphage M13AB28 bearing a single εdC residue does not lead to a diminution of the survival of M13 DNA.[8] These are characteristics of a mispairing lesion. Such lesions contain template information which can be decoded by a DNA polymerase. However the information is incorrect and leads to the misincorporation of a base opposite the lesion without impairing DNA replication or cell survival.

In order to investigate whether εdC forms instructional or non-instructional lesions we have prepared the DNA duplexes d5′(GCTGεCGACG)3′/d5′(CGTCYCAGC)3′, where **Y** = A, G, T or C, which contain εdC paired with each of the four natural bases and examined their stability by UV melting. We have also examined the solution structure by high field ^{1}H NMR of one of these duplexes, d5′(GCTGεCGACG)3′/d5′(CGTCACAGC)3′, which contains an εdC : A pair.

The DNA synthesis monomer **2**, which was prepared from 2′-deoxycytidine,[9] coupled during DNA synthesis with 98.5% coupling efficiency. The crude oligonucleotide was purified by reverse phase HPLC and desalted on sephadex G10.

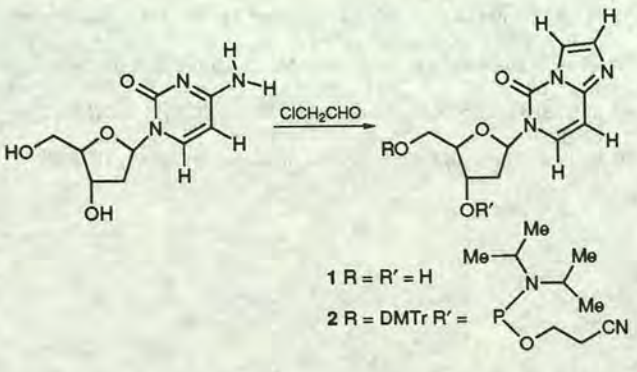

The thermal dissociation of duplex DNA into its constituent single strands leads to hyperchromicity. The point of maximum inflection of a plot of UV absorbency *versus* temperature is defined as the melting temperature T_{max} of the duplex. The thermodynamics of DNA duplex formation in the presence of a εdC lesion were determined according to the method of Gaffney and Jones.[10]

Table 1 shows that the incorporation of εdC into DNA leads to a large drop in the free energy of duplex formation. All four pairs to εdC are considerably less stable than the Watson–Crick C : G and A : T base pairs. These data also indicate that for the four εdC-containing duplexes, the pairing of A with εdC gives the duplex of greatest stability. However the εC : A pair is only very slightly more stable than the εC : G pair which in turn is slightly more stable than the εC : T pair while the differences in the stability of all four εC : Y pairs are not large. Consequently it would appear to be unlikely that the εdC lesion is instructional since it is observed that DNA polymerases pair εdC mainly with adenine but also with thymidine.

Analysis of the 600 MHz ^{1}H NOESY spectrum at 250 ms mixing time of the duplex d5′($G^1C^2T^3G^4\varepsilon C^5G^6A^7C^8G^9$)3′/d5′($C^{10}G^{11}T^{12}C^{13}A^{14}C^{15}A^{16}G^{17}C^{18}$)3′ in 99.99% D_2O buffer containing 10 mmol dm^{-3} phosphate and 100 mmol dm^{-3} sodium chloride at 25 °C reveals that the duplex adopts the B conformation. The pattern of cross-peaks between the sugar H(1)′ resonances and the base H(6) and H(8) resonances shows that every residue adopts the anti conformation (Fig. 1).

Fig. 2 shows the 600 MHz one-dimensional ^{1}H NMR spectrum of the imino protons in 90% H_2O/10% D_2O buffer containing 10 mmol dm^{-3} phosphate and 100 mmol dm^{-3} sodium chloride at 18 °C. The H_2O signal was supressed with presaturation and the imino proton spectrum demonstrates the different rates of exchange of these protons with the solvent. The resonances were assigned from analysis of the two-dimensional 600 MHz ^{1}H NOESY spectrum at 250 ms mixing time with presaturation of H_2O. The thymidine N(3)H

Table 1 The thermodynamic parameters of hybridisation for four εdC containing duplexes and the corresponding duplexes containing Watson–Crick base-pairs 5′GCT GXG ACG3′/3′CGA CYC TGC5′

X	Y	T_{max} (1 μmol)[a]/ °C	ΔH°/ kJ mol^{-1}	ΔS°/ kJ mol^{-1} K^{-1}	ΔG_{298}/ kJ mol^{-1}	r	$\Delta\Delta G_{298}$[b]
C	G	47.2	−264.77	−0.71	−53.19	0.9965	—
A	T	40.6	−290.70	−0.81	−49.32	0.9958	3.92
εC	A	24.6	−255.03	−0.74	−34.51	0.9971	18.67
εC	G	23.9	−218.79	−0.62	−34.03	0.9985	19.17
εC	T	22.3	−270.81	−0.80	−32.41	0.9992	21.56
εC	C	19.7	−236.19	−0.69	−30.57	0.9972	22.91

[a] For each duplex the T_{max} was determined in triplicate at six concentrations between the range 3 and 34 μmol dm^{-3}. r = correlation coefficient of straight line plot of $\ln C_T$ *vs* $1/T_{max}$. T_{max} (1 μmol) = the calculated melting temperature of the duplex at a concentration of 1 μmol dm^{-3}. [b] $\Delta\Delta G_{298}$ = the decrease in the free energy of duplex formation between the duplex 5′GCT GXG ACG3′/3′CGA CYC TGC5′ indicated and duplex 1.

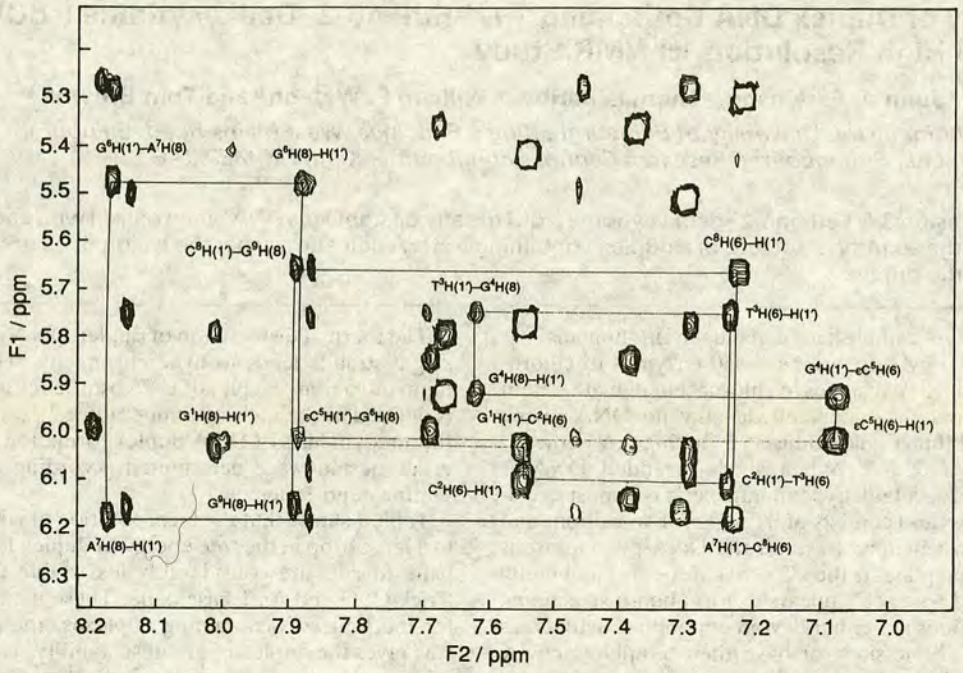

Fig. 1 Detail of the 600 MHz ^{1}H NOESY spectrum of the duplex 5′d(G^{1}C^{2}T^{3}G^{4}εC^{5}G^{6}A^{7}C^{8}G^9)3′/d5′(C^{10}G^{11}T^{12}C^{13}A^{14}G^{15}A^{16}G^{17}C^{18})3′ in 99.99% D_2O at 25 °C with 250 ms mixing time showing the connectivities between sugar H(1)′ and base H(6)/H(8) resonances and highlighting the connectivities from G^{1}H(8) to G^{9}H(1′)

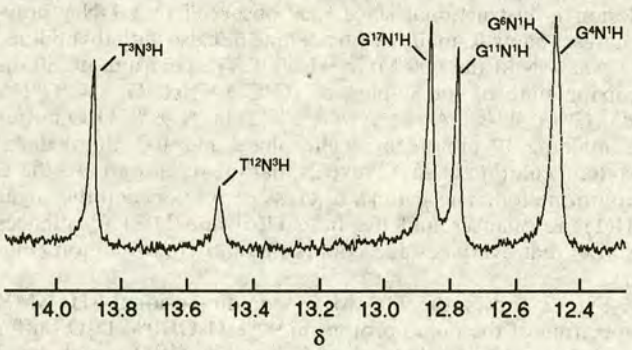

Fig. 2 Portion of the 600 MHz ^{1}H NMR spectrum of the duplex 5′d(G^{1}C^{2}T^{3}G^{4}εC^{5}G^{6}A^{7}C^{8}G^9)3′/d5′(C^{10}G^{11}T^{12}C^{13}A^{14}G^{15}A^{16}G^{17}C^{18})3′ in 90% H_2O at 18 °C showing the imino resonances

signals were assigned by observing an NOE to the corresponding cross-strand deoxyadenosine H(2) signals. The deoxyguanosine N(1)H signals were observed to give NOEs to both amino signals of the corresponding cross strand deoxycytidine, in turn these amino signals showed NOEs to the H(5) of the same base. Thus a chain of assignment could be traced from each deoxycytidine H(5) signal to the corresponding cross strand deoxyguanosine N(1)H. Of the six possible resonances potentially observable in this region (terminal imino protons are in fast exchange with the solvent) all are seen. It is noteworthy that T^{12}N(3)H, which is remote from the lesion site, is in faster exchange with the solvent than both the G^{6}N(1)H and G^{4}N(1)H which flank the lesion site and this suggests that the T^{12} : A^7 base pair is slightly melted out. The non-diminution of the G^{6}N(1)H and G^{4}N(1)H signals compared to G^{17}N(1)H and G^{11}N(1)H shows that the C : G base pairs on either side of the εC : A base pair are intact and that there is no melting of the central region of the duplex around the εC lesion. This shows that the instability of duplex DNA containing the εC lesion, as shown by UV melting, is not due to major disruption of base pairs flanking the lesion site.

We are grateful to the Royal Society of Edinburgh for a Caledonian Research Fellowship to T. Brown, to the SERC for an earmarked studentship to T. Barlow and for 600 MHz NMR time (Edinburgh University) and jointly to the SERC and to Shell Research Ltd. for a fellowship to N. J. G.

Received, 22nd June 1994; Com. 4/03801K

References

1 H. Bartsch, A. Barbin, M. J. Marion, J. Nair and Y. Guichard, *Drug Metab. Rev.*, 1994, **26**, 349.
2 F. P. Guengerich, W. M. Crawford and P. G. Watanabe, *Biochemistry*, 1979, **18**, 5177.
3 R. J. Laib, L. M. Gwinner and H. M. Bolt, *Chem. Biol. Interact.*, 1981, **37**, 219; E. Scherer, C. J. Van Der Laken, L. M. Gwinner, R. J. Laib and P. Emmelot, *Carcinogenesis*, 1981, **2**, 671.
4 J. S. Jacobsen, C. P. Perkins, J. T. Callahan, K. Sambamurti and M. Z. Humayun, *Genetics*, 1989, **121**, 213.
5 D. Simha, V. A. Palejwala and M. Z. Humayun, *Biochemistry*, 1991, **30**, 8727.
6 L. A. Loeb and B. D. Preston, *Annu. Rev. Genet.*, 1986, **20**, 201–230; S. D. Rabkin and B. S. Strauss, *J. Mol. Biol.*, 1984, **178**, 569.
7 V. A. Palejwala, R. W. Rzepka and M. Z. Humayun, *Biochemistry*, 1993, **32**, 4112.
8 V. A. Palejwala, D. Simha and M. Z. Humayun, *Biochemistry*, 1991, **30**, 8736.
9 S. C. Srivastava, S. K. Raza and R. Misra, *Nucl. Acids Res.*, 1994, **22**, 1296.
10 B. L. Gaffney and R. A. Jones, *Biochemistry*, 1989, **28**, 5881.